12-1-2014

Post Buckling of Non Sway Axially Restrained Columns Under Thermal(Fire) Loads

Bikash Khanal
Southern Illinois University Carbondale, khanalbikash@siu.edu

POST BUCKLING OF NON-SWAY AXIALLY RESTRAINED COLUMNS UNDER THERMAL (FIRE) LOADS

By

Bikash Khanal

BS in Civil Engineering

Tribhuwan University, 2009

A Thesis

Submitted in Partial Fulfillment of the Requirements for the

Masters of Science Degree

Department of Civil and Environmental Engineering

In the Graduate School

Southern Illinois University Carbondale

December, 2014

THESIS APPROVAL

POST BUCKLING OF NON-SWAY AXIALLY RESTRAINED COLUMNS UNDER THERMAL (FIRE) LOADS

By

Bikash Khanal

A Thesis Submitted in Partial

Fulfillment of the Requirements

for the Degree of

Masters of Science

in the field of Civil and Environmental Engineering

Approved by:

Dr. Aslam Kassimali, Chair

Dr. J. Kent Hsiao

Dr. Jale Tezcan

Graduate School

Southern Illinois University Carbondale

December,2014

AN ABSTRACT OF THE THESIS OF

Bikash Khanal, for the Master of Science degree in Civil Engineering, presented on September 19, 2014, at Southern Illinois University Carbondale.

TITLE: POST BUCKLING OF NON-SWAY AXIALLY RESTRAINED COLUMNS UNDERTHERMAL (FIRE) LOADS

MAJOR PROFESSOR: Dr. Aslam Kassimali, Ph.D.

The objective of this study was to numerically investigate the effects of slenderness ratios and end rotational restraints on the post-buckling behavior of non-sway columns.

To study the effect of end restraints, numerical solutions were generated for three different support conditions, namely, hinged-hinged, fixed-hinged and fixed-fixed. Furthermore, for each of these support conditions, the effects of slenderness ratios on the post-buckling response were analyzed by considering the slenderness ratios of 50,125 and 200.

Based on the numerical data presented in this thesis, the following conclusions can be made.

- The unrestrained columns under mechanical loads do not exhibit any significant post-buckling strength.
- Restrained Columns subjected to thermal loading undergo significantly smaller deformations in contrast to unrestrained columns, where deformations are relatively larger as the loads are increased only slightly above their critical levels.

- The mechanical post-buckling response does not seem to depend on the slenderness ratios of the columns ;whereas the thermal post-buckling response depends on the slenderness ratios of the columns with the relative deformation decreasing with slenderness ratio at a given temperature ratio.
- Post buckling behaviorof columns subjected to mechanical loadings does not seem to change when the rotational restraints are added whereas in case of columns subjected to thermal loading, the post-buckling response depends on the rotational restraints at the ends of the column.
    - For a constant slenderness ratio, the deflection ratio was found out to be the smallest for the hinged-hinged column and largest for the fixed-fixed column subjected to thermal loads at a given temperature ratio.

ACKNOWLEDGMENTS

I express my sincere gratitude to my academic advisor Dr. Aslam Kassimali for guiding and mentoring me during my research. It would not have been possible for me to conduct this research without his counseling and prepare this report without his critical reviewing. I highly appreciate his inexorable guidance and inspiration throughout the study.

I would like to extend my gratuity to my committee members Dr. J. Kent Hsiao and Dr. Jale Tezcan for providing additional assistance during the research and for reviewing this report.

Furthermore, I would like to be thankful to Civil and Environmental Engineering Department at Southern Illinois University Carbondale for giving me the opportunity to conduct this research with full financial assistantship and making the labs and computers available for me to pursue Masters in Civil Engineering.

This report wouldn't have been completed without the help of Marie Buring at Morris Library and I would like to express my thanks for her valuable suggestions and ideas.

Last but not the least; I would like to thank my family members, colleagues, friends and relatives who admired me to see as a graduate in Masters in Civil Engineering and continuously motivated for my research work. Without their encouragement and love, I would have been unable to conduct this research and pursue my Master's degree.

TABLE OF CONTENTS

Contents **Page No**

LIST OF TABLES

LIST OF FIGURES

CHAPTER 1

INTRODUCTION

1.1 General Introduction

Structures are the most important aspects of any civil engineering project that need to be designed, constructed and maintained with proper guidelines and safety precautions, that would serve well for the human benefit over a long term. The response of the structure subjected to applied load effects is called Structural Analysis. Today there are numerous analysis techniques and software that can be used to analyze the structures subjected to the combination of various loading effects. The basic principle used in analyzing the structure subjected to any loading condition is the stress strain relationship, popularly called as Hooke's law. The stress-strain relationship is based upon the fundamental principle that strain varies linearly with stress and the equilibrium condition of the structure is satisfied at undeformed state of the system. This approach of analysis of the structure is called the Linear Analysis of the Structures. In linear analysis, the deformations of the structure are so small that the strains produced in the members can be expressed as the linear functions of the joint displacements.

The linear analysis of the structure holds well when the structure is subjected to service(working) loads and the adequacy of the analysis is found to be deteriorating at ultimate or limiting loads. It is not necessarily important that the structures will be only subjected to service loads. In some cases such as cable systems, even the structure is acted upon service loads; the linear analysis is not quite effective as the load bearing capacity of the structure is governed by the geometrical non linearity. Hence, non-linear

analysis of the structures is required to know the ultimate load carrying capacity of the structures and to consider the equilibrium state of the structure at deformed configuration.

The advancement of science and technology has led to the formulations of the many incredible marvels which man dreamt of. The introduction of new design specifications that are based upon the ultimate load strength has increased the use of nonlinear analysis at a faster rate.

In nonlinear analysis, the limitations of linear analysis are removed by formulating the equations of equilibrium on the deformed geometry of the structure that were not known in advance in the linear analysis and considering the inelastic properties of the material. In non-linear analysis, the load-deformation relationships are found to be non-linear in as in contrary to the linear analysis and are calculated by using the iterative technique procedures. The purpose of this study is to perform a numerical investigation of the geometrically nonlinear response of axially restrained columns with three different boundary conditions suggested by AISC, under temperature changes.Beam-Column theory is utilized for generating the response. There are very few researches that have studied the post-buckling response under temperature variance with Beam-Column Theory. The benefit of Beam- Column approach over Elastica approach is that, it makes the problem solving and analysis much easier and less time consuming. The study focuses on the effects of temperature changes on displacement, axial force and end moments and their nature in the post buckling range for the column with the specified boundary condition and also studies the minimum number of elements or intermediate members required to generate an accurate and convergent result. Non-linear computer

software with capabilities to incorporate temperature changes is used to develop and analyze the model. Finally, a systematic comparison is made of the observed results with the response data available for the Elastica solution, which is also considered as the exact solution of the problem.

1.1.1 Pre-Buckling Response

When an axially unrestrained column as shown in Figure 1-1(a)is subjected to a uniform temperature increase T above an ambient temperature, the column can expand and hence its length elongates by an amount δ_a, which is given by

$$\delta_a = \alpha T L \qquad \text{Equation (1)}$$

in which, α= coefficient of thermal expansion, and L = undeformed length of the column. The column is statically determinate and therefore no any axial force develops in it.

However, if the same column is axially restrained as shown in Figure 1-1(b), the axial deformation is prevented by the support conditions, thereby inducing an axial force P in the column with

$$\delta_a = \frac{PL}{EA} \qquad \text{Equation (2)}$$

in which, E = Modulus of Elasticity, and A = cross-sectional area of the column.

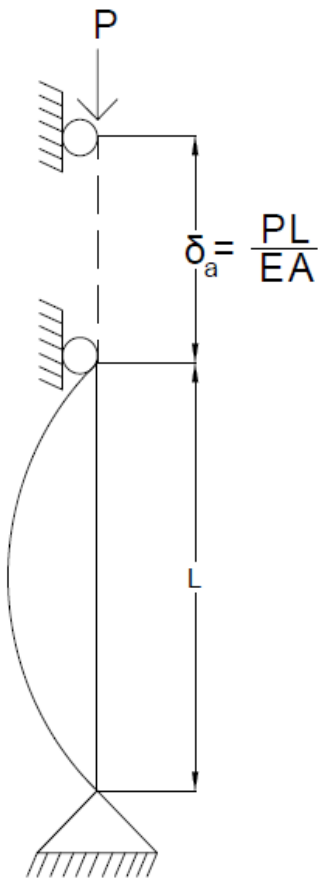

Fig.1-1(a) :Unrestrained Column

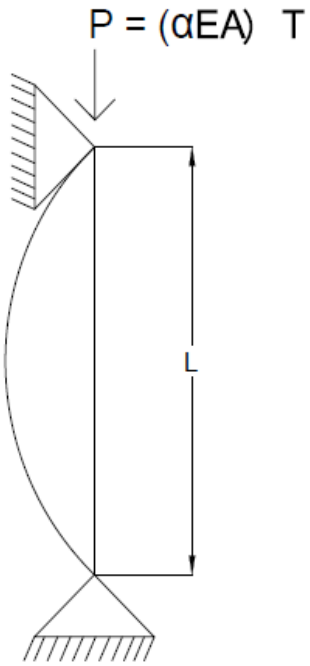

Fig.1-1(b):Restrained Column

Figure 1-1: Unrestrained & Restrained Columns

The relationship between the temperature increase,T, and the corresponding axial force, P,can be obtained by equating Eqs.(1) and (2), i.e.,

$$\delta_a = \alpha TL = \frac{PL}{EA}$$

from which,

$$T = \frac{P}{\alpha EA} \qquad \text{Equation (3)}$$

From the above equation, it is seen that as temperature T increases, the axial force P increases, until it reaches a critical value P_{cr}at which the column buckles in the lateral direction. The buckling load is given by AISC (2005) as

$$P_{cr} = \frac{\pi^2 EI}{(KL)^2} = P_{e1} \qquad \text{Equation (4)}$$

in which,

P_{e1} =Elastic Critical Buckling strength of the member in the plane of bending

I = moment of inertia, and K = effective length factor which depends on the support conditions of the column (AISC 2005). The buckling temperature,T_{cr}, can be obtained by substituting Eq. (4) into Eq.(3), that is,

$$T_{cr} = \frac{\pi^2 EI}{(KL)^2 \alpha EA} = \frac{\pi^2 I}{(KL)^2 \alpha A}$$

or

$$T_{cr} = \frac{\pi^2}{\alpha (K\lambda)^2} \qquad \text{Equation (5)}$$

in which the parameter λ is the slenderness ratio of the column and is given by

$$\lambda = \frac{L}{\sqrt{I/A}} \qquad \text{Equation (6)}$$

1.1.2 Post-Buckling Response

As discussed earlier, the axial force P is the function of temperature T and therefore we can say that at the temperature above the buckling temperatures (or at$\mathrm{P} > \mathrm{P_{cr}}$), the column undergoes large deflection in the lateral direction. These post-

buckling deflections cannot be determined by the linear analysis, and non-linear analysis is required to determine the post-buckling response of columns.

The post-buckling behavior of axially unrestrained columns subjected to external (mechanical) loads has been extensively studied over the last century, and it is well known that such columns undergo very large lateral deflections due to a slight increase in axial load above the buckling load (Timoshenko and Gere 1961; Chajes 1974).This small post-buckling stiffness is generally neglected in design, and the unrestrained columns are considered to have failed at the onset of buckling.

While very limited amount of research has been conducted on the post-buckling behavior of axially restrained columns under thermal loads, it has been clearly shown that such columns exhibit considerably more stiffness in the initial post-buckling stage than their unrestrained counterparts. However, no systematic study has been conducted to study the extent of this post-buckling stiffness, and how it is affected by various parameters, such as the column's slenderness ratio, and the rotational and lateral support conditions at the ends of the column.

1.2 Literature Review

The earliest research on the thermal post-buckling of axially restrained columns was apparently reported by Boley and Weiner (1960), who presented an approximate solution for the initial (small deformation) post-buckling response of a pinned-pinned column, by assuming that the column buckles in the first mode shape (consistent with the beam-column theory), and that its axial force remains constant at the critical value $\mathrm{P_{cr}}$ in the post-buckling range (i.e., at $T > T_{cr}$).Using a similar approach, Rao and Raju

(2002) developed an approximate solution for the initial post-buckling response of a fixed-fixed column. These approximate solutions indicated that the axially restrained columns undergo smaller lateral deflections in the post-buckling range, as compared to the unrestrained columns, and that their post-buckling stiffness is a function of the column slenderness ratio λ.

The problem of large-deformation thermal post-buckling of axially restrained columns was first examined by Coffin and Bloom (1999), who obtained solutions for pinned-pinned columns by numerically integrating the exact large-deformation moment –curvature differential equation of the column. The shapes of the column elastic curves obtained by solving the exact differential equations are called the *elastica* solutions. Coffin and Bloom (1999)'s solutions indicated that the column axial force doesn't remain constant at $\mathrm{P_{cr}}$ after buckling (as assumed in the approximate solutions), but decreases with increasing lateral deflections. Similar *elastica* solutions for the fixed-fixed and the pinned-fixed columns have been published by Li and Cheng (2000) and Li, Zhou and Zheng (2002), respectively.

The approach used by the foregoing researchers in obtaining the *elastica* solutions, where by the exact differential equations are solved by numerical techniques, is only feasible for isolated columns with simple end conditions and subjected to uniform temperature distributions. Because of the mathematical difficulties involved, this "exact" approach cannot be used as a general computational tool to study the effects of various parameters such as, non-uniform temperature distributions, degradation of material properties with rising temperatures, etc., on the post buckling response of columns.

In the present study, the numerical results for columns are generated using a finite element method, in which the element force-deformation relationships are based in the beam-column theory (Timoshenko and Gere 1961).This method was developed by Kassimali and Garcilazo (2010) for the analysis of plane frames. Local element force-deformation relations, used in this method, are based on the closed-form solution of the beam-column differential equation taking into consideration the effect of curvature due to temperature gradient across the element cross-section. The changes in element chord lengths due to thermal axial strain and bowing due to temperature gradient are also taken into account. This “beam-column “ approach yields more accurate element stiffness relations (involving stability and bowing functions) than those based on the polynomial shape functions commonly used in the finite element analysis, and therefore, requires significantly fewer elements per member(i.e., a column or a beam) for the analysis of framed structures.

Furthermore, this method employs an Eulerian (corotational) local coordinate system to separate an element’s chord rotations which may be arbitrarily large, from its end rotations with respect to the chord. Thus, large member end rotations (typically encountered in the post-buckling range) can be taken into account by dividing the natural member (i.e., a column or a beam) into two or more elements, thereby treating part(s) of member end rotations as element chord rotations as shown in Figure 1-2.

Extensive numerical studies have been conducted on a group of benchmark structures to demonstrate that the method is highly accurate in predicting large deformation responses of plane framed structures (Kassimali and Garcilazo 2010 and Baikuntha Silwal 2013).

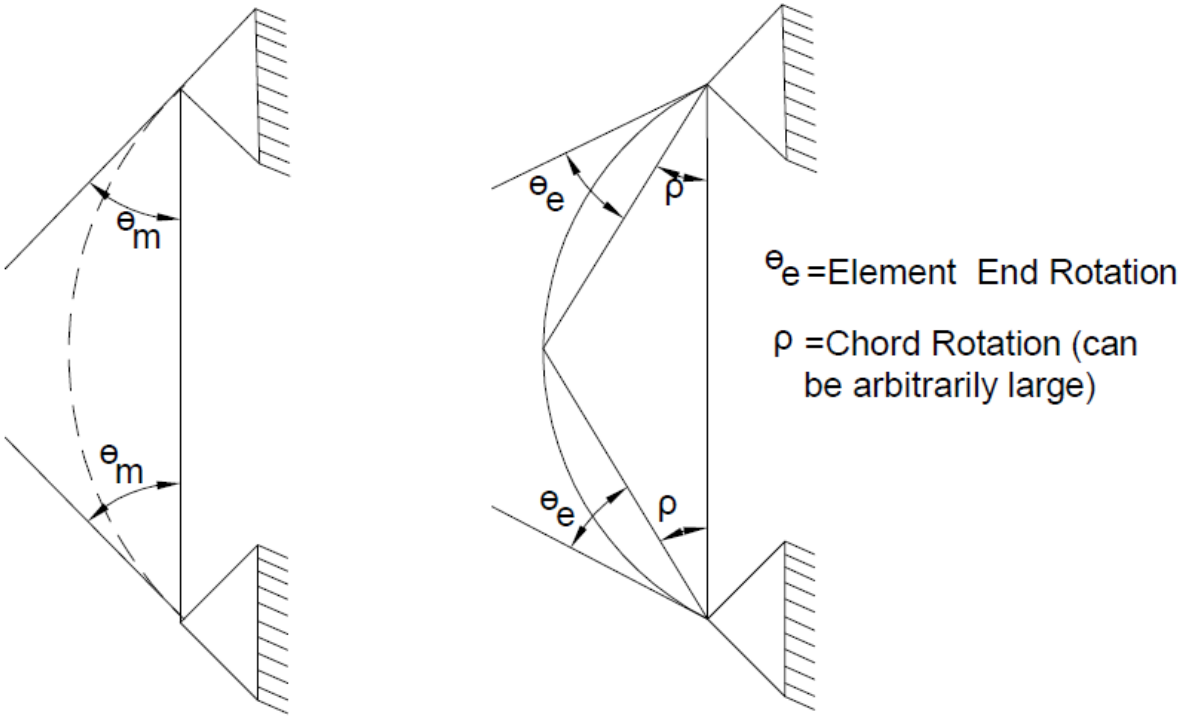

Fig.1-2 (a):Column End Rotations Fig.1-2(b):Element End Rotations

Figure 1-2: Column & Element End Rotations

1.3 Objective and Scope

The objective of this study is to numerically investigate the effects of slenderness ratios and end rotational restraints on the post-buckling behavior of non-sway columns.

The columns are assumed to be straight, prismatic, and composed of linearly elastic material. The temperature distribution is assumed to be uniform along the column's length, but may have a small linear gradient across its cross-sectional depth. This small temperature gradient serves as an imperfection that causes the column to buckle laterally. The effects of material nonlinearity (e.g. yielding) and degradation of material properties due to rising temperatures are not considered in this study.

CHAPTER 2

METHOD OF ANALYSIS

2.1 General

The geometrically non-linear method of analysis, used in this study, is reviewed in this chapter for the convenience of the reader.Further details of the method can be found in Kassimali and Garcilazo (2010).

2.2 Element Forces and Deformations in Local Co-ordinates

2.2.1 Evaluation of End Moments

Consider a prismatic element AB of a plane frame as shown in

Figure 2-1.The element is subjected to a linearly varying temperature increase over its depth$d$, fromT_b at the bottomto T_t at the top. The temperature is constant along the length of the element AB.

Here, θ_1 and $\theta_2$are the rotations at the beginning and end joints respectively with the centroidal axis of the element AB. As the rotation occurs on the two ends of the element, moments M_1 and M_2 develop at the beginning and end joints of the element respectively. Also, an axial force *Q* develops in the element AB. This axial force is assumed to be compressive as it shortens the element AB from its original length L to the final length$\bar{L}$. The change in length will be

$$\boldsymbol{u = L - \bar{L}} \qquad \text{Equation (1)}$$

Summing up the moments at end B, we get,

$$(+\circlearrowleft)\sum M_B = 0 \Rightarrow R_A = \frac{M_1 + M_2}{\bar{L}}$$ Equation (2)

The bending momentat any point at a distance x from the end A is given by

$$(+\circlearrowright)\sum M_x = R_A * x - M_1 - Q * y$$

$$M_x = -M_1 + \left(\frac{M_1+M_2}{\bar{L}}\right) * x - Q * y$$

We know that, moment at any section $=EI\frac{d_y^2}{d_x^2}$that is, $M_x = EI\frac{d_y^2}{d_x^2}$

By subtracting the temperature curvature from the bending curvature of beam due to loading, we get,

$$\frac{M_x}{EI} = y'' - Z$$

where, $Z = \alpha\frac{(T_b - T_t)}{d}$and α is the coefficient of linear expansion. Thus,

$$y'' = \frac{M_x}{EI} + Z$$

$$\frac{d_y^2}{d_x^2} = \frac{1}{EI}\left[-M_1 + \left(\frac{M_1 + M_2}{\bar{L}}\right) * x - Q * y\right] + Z$$

$$\frac{d_y^2}{d_x^2} + \frac{Q * y}{EI} = \frac{1}{EI}\left[-M_1 + \left(\frac{M_1 + M_2}{\bar{L}}\right) * x\right] + Z$$

Let $k^2 = \frac{Q}{EI}$

Therefore,

$$\frac{d_y^2}{d_x^2} + k^2 y = \frac{1}{EI}\left[-M_1 + \left(\frac{M_1 + M_2}{\bar{L}}\right) * x\right] + Z$$ Equation (3)

The above Equation (3) is a differential equation of second order and it has a general equation which consists of two parts: a complimentary solution and a particular solution.

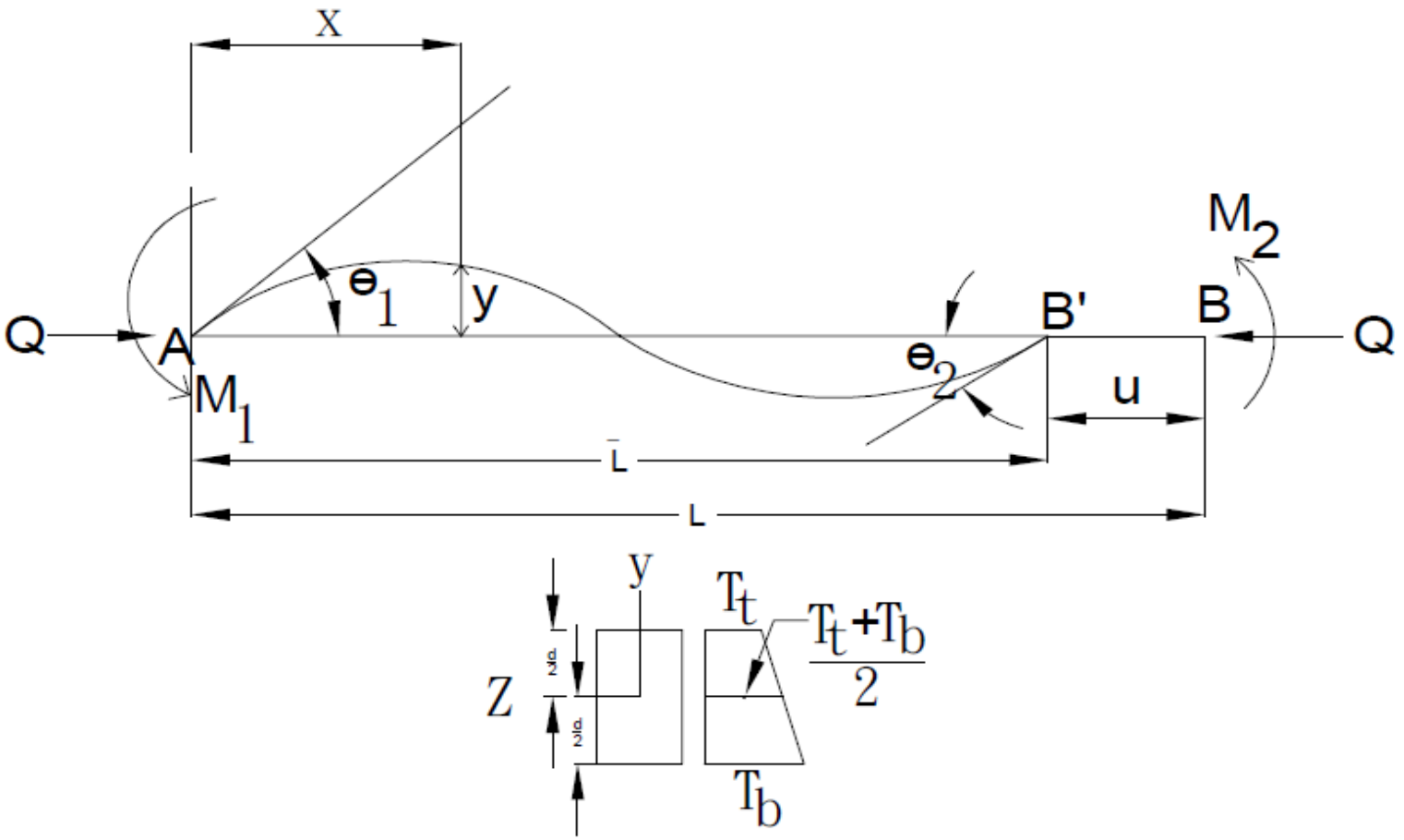

Figure 2-1: Element in Local (co-rotational) Co-ordinate System Subjected to Temperature Change

The complimentary solution for the above Equation (3) is

$$y_c = A \sin kx + B \cos kx$$

and the particular solution is

$y_p = Cx + D$

On differentiating the particular solution, we get, $y_p' = C$ and $y_p'' = 0$

Putting the values of y_p and y_p'' in Equation (3), we get,

$$0 + k^2(Cx + D) = \left(\frac{M_1 + M_2}{\bar{L}EI}\right) * x - \frac{M_1}{EI} + Z$$

By equating the linear and constant terms on the two sides,we get,

$$C(k^2)x = \left(\frac{M_1 + M_2}{\bar{L}EI}\right) * x$$

$$C = \frac{M_1 + M_2}{k^2\bar{L}EI}$$

and,

$$Dk^2 = \frac{-M_1}{EI} + Z$$

from which,

$$D = \frac{-M_1}{k^2EI} + \frac{Z}{k^2}$$

Thus, the particular solution becomes,

$$y_p = \left[\frac{M_1 + M_2}{k^2\bar{L}EI}\right]x - \frac{M_1}{k^2EI} + \frac{Z}{k^2}$$

The general solution for the above differential equation (3) is obtained by combining the two solutions called as complimentary solution and particular solution. Hence, the general solution is:-

$$y = A\sin kx + B\cos kx + \left[\frac{M_1 + M_2}{k^2\,\bar{L}EI}\right] x - \frac{M_1}{k^2 EI} + \frac{Z}{k^2}$$ Equation (4)

Differentiating the above Equation (4) with respect to x, we get,

$$y' = Ak\cos kx - Bk\sin kx + \left[\frac{M_1 + M_2}{k^2\,\bar{L}\,EI}\right]$$ Equation (5)

Using the boundary condition

$@x = 0, y = 0$, Equation (4) becomes

$$0 = 0 + B - \frac{M_1}{k^2 EI} + \frac{Z}{k^2}$$

$$B = \frac{M_1}{k^2 EI} - \frac{Z}{k^2}$$ Equation (6)

Again using the boundary condition$@x = \bar{L}, y = 0$, and putting the value of B from

Equation (6) to Equation (4), we get,

$$0 = A\sin k\bar{L} + \left[\frac{M_1}{k^2 EI} - \frac{Z}{k^2}\right]\cos k\bar{L} + \left[\frac{M_1 + M_2}{k^2\,EI}\right] - \left[\frac{M_1}{k^2 EI} - \frac{Z}{k^2}\right]$$

$$A\sin k\bar{L} = \left[\frac{M_1}{k^2 EI} - \frac{Z}{k^2}\right](1 - \cos k\bar{L}) - \left[\frac{M_1 + M_2}{k^2\,EI}\right]$$

Letting, $k\bar{L} = \phi$, the above Equationbecomes,

$$A\sin\phi = \left[\frac{M_1}{k^2 EI} - \frac{Z}{k^2}\right](1 - \cos\phi) - \left[\frac{M_1 + M_2}{k^2\,EI}\right]$$

$$A = \left[\frac{M_1}{k^2 EI} - \frac{Z}{k^2}\right]\frac{(1 - \cos\phi\,)}{\sin\phi} - \left[\frac{M_1 + M_2}{k^2\,EI\ \sin\phi}\right]$$ Equation (7)

Now, using the boundary condition

$$@x = 0, y' = \frac{dy}{dx} = \theta_1$$

$$\theta_1 = Ak + \left[\frac{M_1 + M_2}{k^2\,\bar{L}EI}\right]$$

Now, putting the value of A from Equation (7) to above equation, we get,

$$\theta_1 = \left[\frac{M_1}{kEI} - \frac{Z}{k}\right]\left(\frac{1 - cos\,\phi}{sin\,\phi}\right) - \left[\frac{M_1 + M_2}{k^2\,EI\ sin\,\phi}\right] + \left[\frac{M_1 + M_2}{k^2\,\bar{L}EI}\right] \qquad \text{Equation (8)}$$

Again, using the boundary condition,

$@x = L, y' = \frac{dy}{dx} = \theta_2$, we get,

$$\theta_2 = Ak\,cos\,\phi - Bk\,sin\,\phi + \left[\frac{M_1 + M_2}{k^2\,\bar{L}EI}\right]$$

Substituting the values of A and B from Equations (7) and (6) respectively into the above equation, we get,

$$\theta_2 = \left[\frac{M_1}{kEI} - \frac{Z}{k}\right]\left(\frac{1 - cos\,\phi}{tan\,\phi}\right) - \left(\frac{M_1 + M_2}{kEI\,tan\,\phi}\right) - \left[\frac{M_1}{kEI} - \frac{Z}{k}\right] sin\,\phi + \left[\frac{M_1 + M_2}{k^2\,\bar{L}EI}\right]$$

By solving the two equations of $\theta_1$andθ_2 for the moments M_1 and M_2, we come up to the following equations

$$\boldsymbol{M_1 = \frac{EI}{\bar{L}}(c_1\theta_1 + c_2\theta_2) + EI\alpha\frac{(T_b - T_t)}{d}} \qquad \text{Equation (9)}$$

$$\boldsymbol{M_2 = \frac{EI}{\bar{L}}(c_2\theta_1 + c_1\theta_2) - EI\alpha\frac{(T_b - T_t)}{d}} \qquad \text{Equation (10)}$$

The above Equations (9) and (10) can be used to evaluate the end moments at the beginning and end joints of the element respectively for given material and cross sectional properties, temperature changes, and the end rotations. The constants $c_1\ and\ c_2$ in the above relations are called the Stability Functions(Livesley and Chandler, 1956)and are given by the following equations:-

$$c_1 = \frac{\phi \sin\phi - \phi^2 \cos\phi}{2 - 2\cos\phi - \phi \sin\phi} \qquad c_2 = \frac{\phi^2 - \phi \sin\phi}{2 - 2\cos\phi - \phi \sin\phi}$$

with$\phi^2 = K^2\bar{L}^2$

and $K = \sqrt{\frac{Q}{EI}}$

$$\phi^2 = \frac{Q\bar{L}^2}{EI}$$ Equation (11)

Letting, $q = \frac{Q}{Q_{Euler}} = \frac{Q}{\left(\frac{\pi^2 EI}{L^2}\right)} = \frac{QL^2}{\pi^2 EI}$ Equation (12)

in which ,q is a dimensionless parameter that is used to describe if thecolumn undergoes buckling or not and is the ratio of an axial load to the Euler's load. The limits for the value of$q$are$1.0 \leq q \leq 4.0$;with $q = 1$ for the simply supported column case and $q = 4$ for the column with both ends fixed case.

Hence, we can write,

$$\phi^2 = \pi^2 q \left(\frac{\bar{L}}{L}\right)^2$$ Equation (13)

2.2.2 Evaluation of Element Axial Force

The total axial deformation u of an element is given by

$$u = u_a - u_t + u_b$$ Equation (14)

in which,

$$u_a = \frac{QL}{EA}$$ Equation (15)

is the axial shortening caused by the axial force *Q*,

$$u_t = \alpha L\left(\frac{T_b + T_t}{2}\right)$$ Equation (16)

is the axial elongation due to the uniform temperature increase $\left(\frac{T_b+T_t}{2}\right)$, and $u_b$is the axial shortening due to the bending (bowing) of the element.The bowing deformation is expressed as

$$u_b = LC_b$$ Equation (17)

in which C_b is the axial strain due to flexural bowing. Substitution of Equations (15),(16) and (17) into Equation(14) yields

$$u = \frac{QL}{EA} - \alpha L\left(\frac{T_b + T_t}{2}\right) + LC_b$$ Equation (18)

from which the expression for member axial force is obtained as

$$Q = EA\left[\frac{u}{L} + \alpha\frac{(T_b + T_t)}{2} - C_b\right]$$ Equation (19)

The axial strain due to bowing can be written in terms of the element axial force and end rotations as (Saafan 1963, and Oran 1973)

$$C_b = b_1(\theta_1 + \theta_2)^2 + b_2(\theta_1 - \theta_2)^2$$ Equation (20)

$$b_1 = \frac{(c_1 + c_2)(c_2 - 2)}{8\pi^2 q}$$ Equation (21)

$$b_2 = \frac{c_2}{8(c_1 + c_2)}$$ Equation (22)

Therefore, for any assigned (given) values of deformations $(\theta_1, \theta_2 \; and \; u)$, we can calculate the member end moments and axial force considering the thermal effect by the following relations:

$$\mathrm{M}_1 = \frac{EI}{\bar{L}}(c_1\theta_1 + c_2\theta_2) + EI\alpha\frac{(T_b - T_t)}{d} \qquad \text{Equation (23)}$$

$$\mathrm{M}_2 = \frac{EI}{\bar{L}}(c_2\theta_1 + c_1\theta_2) - EI\alpha\frac{(T_b - T_t)}{d} \qquad \text{Equation (24)}$$

$$\mathrm{Q} = EA\left[\frac{u}{L} + \alpha\frac{(T_b + T_t)}{2} - C_b\right] \qquad \text{Equation (25)}$$

2.3 Member Forces and Deformations in Global Co-ordinates

The global element-forces$\mathbf{F}$ in Figure 2-2 can be related to an element's local forces $\mathbf{Q}$ as stated by the following relationship, (Oran, 1973)

$$\mathbf{F} = \mathbf{B} * \mathbf{Q} \qquad \text{Equation (26)}$$

Here,$\mathbf{B}$ is called the Transformation Matrix and is given as

$$\mathbf{B} = \frac{1}{\bar{\mathrm{L}}}\begin{bmatrix} -C_Y & -C_Y & C_X\bar{\mathrm{L}} \\ C_X & C_X & C_Y\bar{\mathrm{L}} \\ \bar{\mathrm{L}} & 0 & 0 \\ C_Y & C_Y & -C_X\bar{\mathrm{L}} \\ -C_X & -C_X & -C_Y\bar{\mathrm{L}} \\ 0 & \bar{\mathrm{L}} & 0 \end{bmatrix} \qquad \text{Equation (27)}$$

in which, $C_X = Cos\;\bar{\theta}$and $C_Y = Sin\;\bar{\theta}$ and

$$\mathbf{Q} = \begin{bmatrix} M_1 \\ M_1 \\ Q \end{bmatrix} \text{ and } \mathbf{u} = \begin{bmatrix} \theta_1 \\ \theta_2 \\ u \end{bmatrix} \qquad \text{Equation (28)}$$

The terms$\bar{L} \; and \; \bar{\theta}$in the above Equations (26) and (27) represent the length and the

orientation of the chord of the element in its deformed configuration respectively as shown in Figure 2-2.The method to obtain $\bar{L}, m, n,$ **u**from the element's global end-displacements, **v** has been previously published by **(Kassimali, 1983)**.

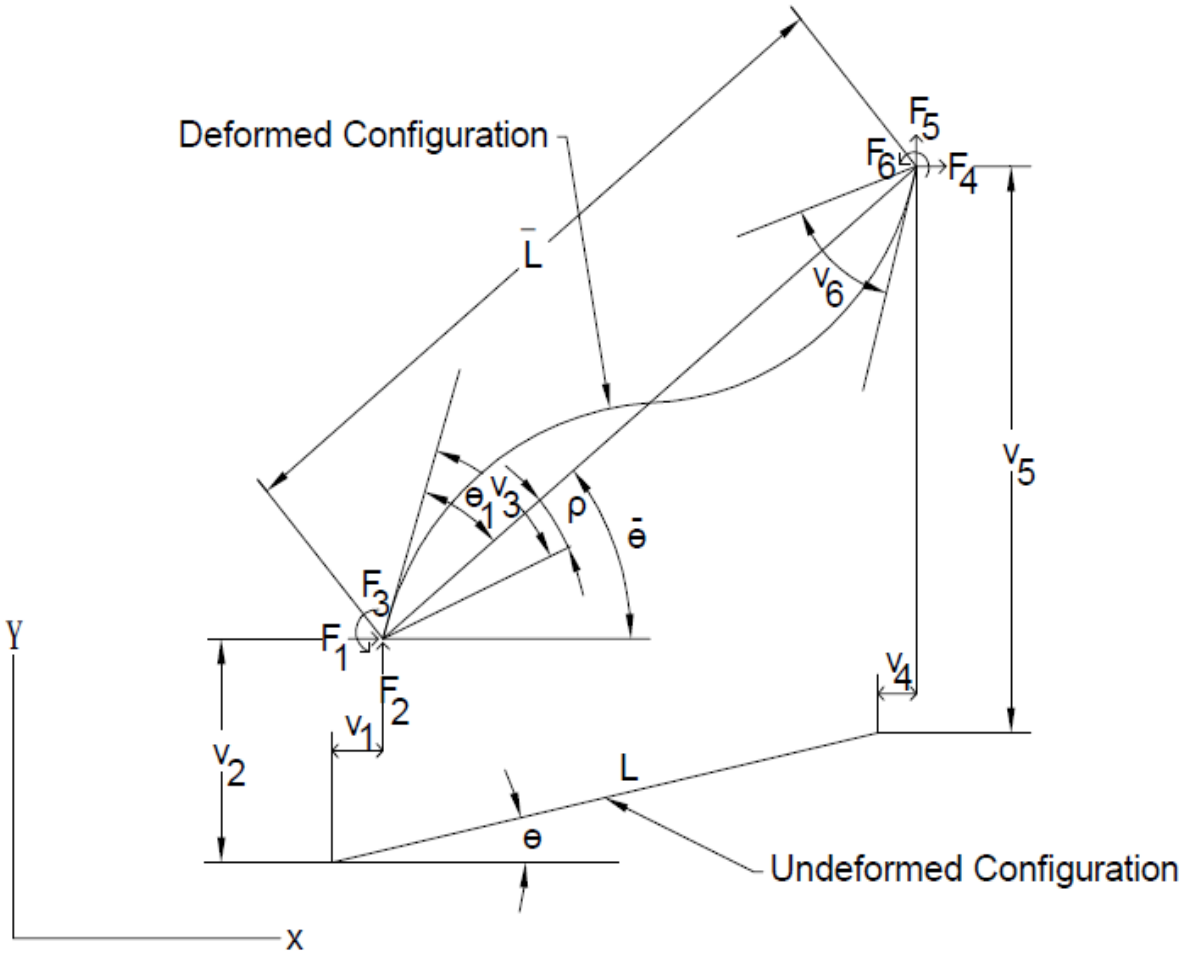

Figure 2-2: Element Forces and Displacements in Global Co-ordinate System

2.4 Elemental Tangent Stiffness Relations

By differentiating the element force-deformation relations [Equations (22)-(24)], the tangent stiffness relationships can be established in local co-ordinates. Thus,

$$\Delta \boldsymbol{Q} = \boldsymbol{k}\Delta \boldsymbol{u} + \Delta \boldsymbol{Q_t} \quad \text{Equation (29)}$$

where, $\boldsymbol{k}$ =element tangent stiffness matrix in local coordinates (Oran,1973);and

$\Delta \boldsymbol{Q_t}$ =Element fixed end forces due to temperature increments $\Delta T_b \; and \; \Delta T_t$, with

$$\Delta Q_t = EI\alpha \begin{bmatrix} \frac{G_1}{2LH}(\Delta T_b + \Delta T_t) + \frac{1}{d}(\Delta T_b - \Delta T_t) \\ \frac{G_2}{2LH}(\Delta T_b + \Delta T_t) - \frac{1}{d}(\Delta T_b - \Delta T_t) \\ \frac{\pi^2}{2L^2H}(\Delta T_b + \Delta T_t) \end{bmatrix} \quad \text{Equation (30)}$$

in which,

$$G_1 = c_1{}'u_1 + c_2{}'u_2 \quad \text{Equation (31)}$$

$$G_2 = c_2{}'u_1 + c_1{}'u_2 \quad \text{Equation (32)}$$

$$H = \frac{\pi^2}{\lambda^2} + b_1'(u_1 + u_2)^2 + b_2'(u_1 - u_2)^2 \quad \text{Equation (33)}$$

and,

$$\lambda = \text{Slenderness Ratio} = \frac{L}{\sqrt{\frac{I}{A}}} \quad \text{Equation (34)}$$

The prime superscript used in above Equations shows a differentiation with respect to q(See ***Kassimali and Garcilazo 2010***).

The element tangent-stiffness relationship between global end-forces and end-displacements can be expressed as

$$\Delta \mathbf{F} = \mathbf{K}\,\Delta \mathbf{v} + \Delta \mathbf{F_t} \quad \text{Equation (35)}$$

in which the element global tangent stiffness, $\mathbf{K_t}$, is given by **(Oran, 1973).**

$$\mathbf{K_t} = \boldsymbol{BkB^T} + \sum_{\boldsymbol{j=1}}^{\boldsymbol{3}} \boldsymbol{Q_j g^{(j)}} \qquad \text{Equation (36)}$$

in which, $\boldsymbol{g^{(j)}}$ =geometric matrices;and

$$\Delta\mathbf{F_T} = \mathbf{B}\,\Delta\mathbf{Q_T} \qquad \text{Equation (37)}$$

2.5 Structure Equilibrium Equations

For any plane frame that is in equilibrium and subjected to an external joint loads **P** and temperature changes **T**, the nonlinear equations of equilibrium can be expressed as

$$\mathbf{f}(\mathbf{d}, \mathbf{T}) = \mathbf{P} \qquad \text{Equation (38)}$$

in which $\mathbf{f}(\mathbf{d}, \mathbf{T})$ represents resultant internal forces;**d**denotes translations and rotations of the joints; and **P**refers to the applied external joint forces.

We already know that the member force deformation relationships are non-linear resulting to non-linear relationships between **f**and **d**. Hence, to perform the calculations, the differential form of the equation can be expressed as

$$\Delta\mathbf{P} - \Delta\mathbf{P_T} = \mathbf{S}\Delta\mathbf{d} \qquad \text{Equation (39)}$$

in which

$\Delta\mathbf{P}$ and$\Delta\mathbf{d}$refer to the increments of external joint loads and joint displacements, respectively; Srepresents the structural tangent-stiffness matrix; and the vector $\Delta\mathbf{P_T}$denotes the structural fixed-joint forces due to the effect of temperature increment. These matrices **S**and $\Delta\mathbf{P_T}$can be expediently assembled from their element tangent-

stiffness matrix $\mathbf{K}$and global end-forces $\Delta\mathbf{F_t}$respectively, with the aid of the element code number technique (Kassimali, 1999).

2.6 Computational Procedure

The pre - and post buckling response of columns was determined by applying the total temperature increase (or load) in several increments. At the end of each increment, a Newton –Raphson iteration was performed to satisfy the joint equilibrium equations. A block diagram showing the steps of the Newton-Raphson iteration is given in Figure 2-3.

2.7 Computer Programs

The software used in analyzing the performance of the columns in this research was developed by Kassimali for the geometrically nonlinear thermal analysis of plane framed-structures. This program was developed to implement the general method of geometrically nonlinear thermal analysis based on the Beam-Column formulation described in **Kassimali and Garcilazo (2010**).The input into the program consists of the total temperature loadings, the number of temperature increments, the convergence tolerance ,and the maximum number of iteration cycles to be performed at any given temperature level.

The program uses a convergence criteria based on a comparison of the changes in joint displacement,$\Delta_{\mathbf{d}}$ to their cumulative displacement$\mathbf{d}$. In applying this criteria, translations and rotations of the joints are treated as separate groups, and convergence criteria is assumed to have occurred when the following inequality is satisfied independently for each group.

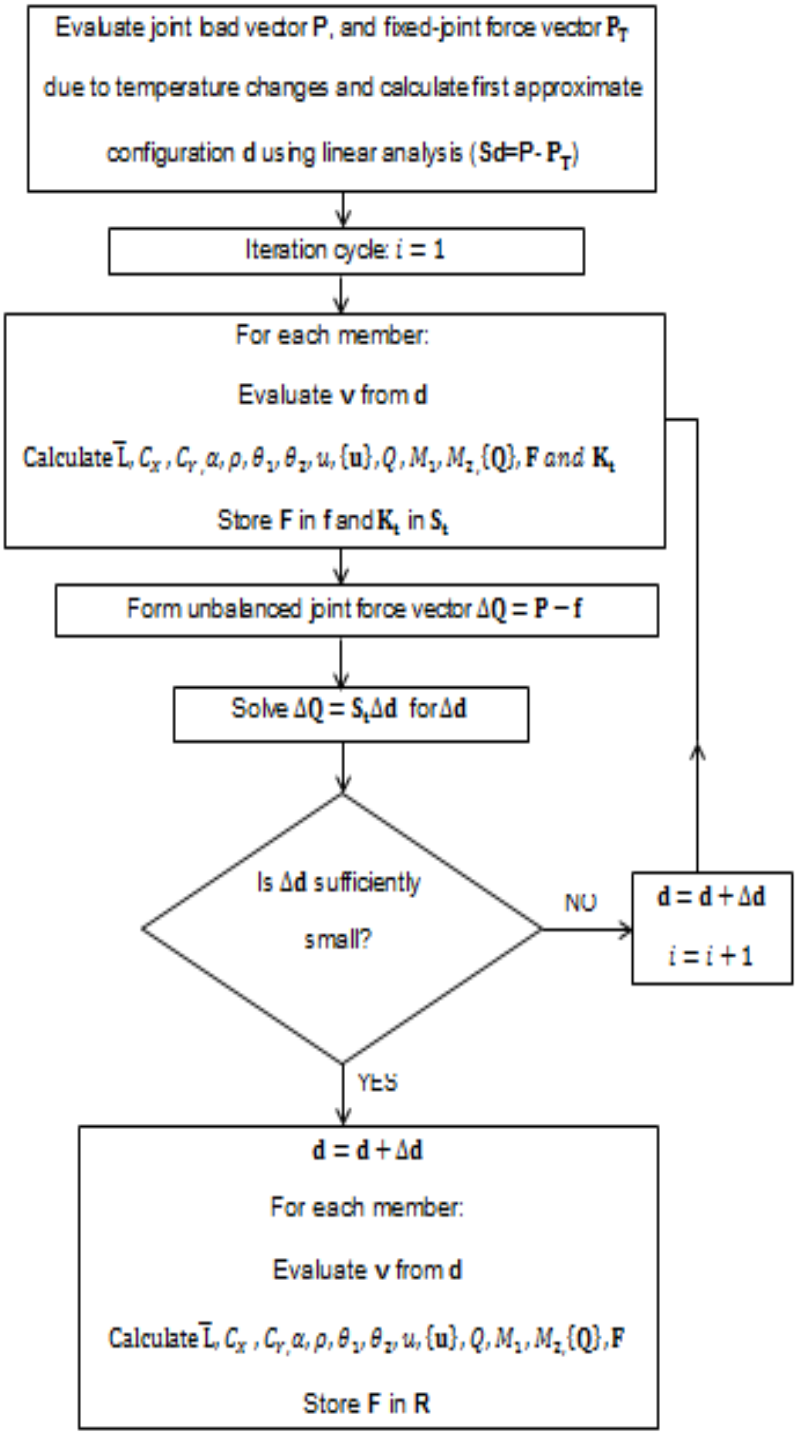

Figure 2-3: Block Diagram for Newton-Raphson Iteration

$$\sqrt{\frac{\sum_{j=1}^{j=NDOF}(\Delta \mathbf{d})^2}{\sum_{j=1}^{j=NDOF}(\mathbf{d})^2}} \leq \boldsymbol{e}$$ Equation (39)

in which the dimensional parameter $\mathbf{e}$ denotes the desired tolerance limit adopted for the analysis. For the consistency purpose, a standard value of 0.001 for $\mathbf{e}$has been used in the analysis of the columns in this research.

Sole aim is taken in validating the results of this program to the Elastica solutions and on that process, a program made in spreadsheet is also taken in consideration (see appendix A).In addition to the Kassimali's software, several small spreadsheet programs were also written to check and to develop an understanding of, the various features of the Kassimali's software, as well as to process its output data and to plot the graphs presented in this thesis (see appendix A).

CHAPTER 3

NUMERICAL RESULTS FOR HINGED-HINGED COLUMN

3.1 General

To study effect of end restraints on the thermal post-buckling behavior of non-sway column, numerical solutions were generated for three different support conditions namely, hinged-hinged, fixed-hinged and fixed-fixed. The results for the hinged-hinged columns (Figure 3-1) are presented in this chapter, and those for the fixed-hinged and fixed-fixed columns are given in Chapters 4 and 5, respectively.

The cross-sectional and material properties of the columns were kept constant throughout the study. These properties are listed Table 3-1.As shown in this table, the columns are assumed to be composed of structural steel with a W200X46 **(Canadian Steel Code CSA S-16)**cross section. The length of the column was varied to examine the effect of slenderness ratio on the post-buckling response.

Table 3-1:Cross-Sectional and Material Properties of Column Used for Numerical Study

d	=	203	mm
A	=	5860	mm^2
I	=	4.54×10^7	mm^4
E	=	210	KN/mm^2
α	=	1.20×10^{-5}	/°C

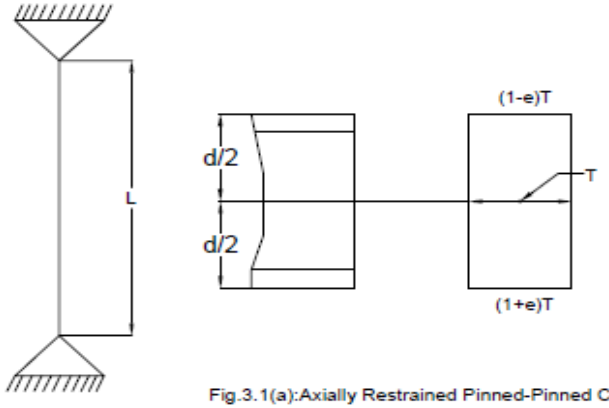

Fig.3.1(a):Axially Restrained Pinned-Pinned Column

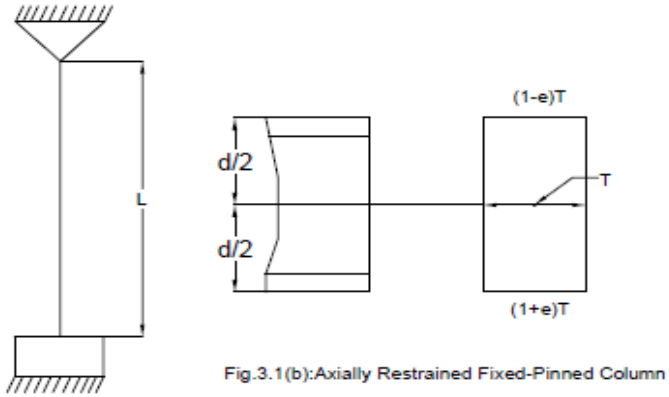

Fig.3.1(b):Axially Restrained Fixed-Pinned Column

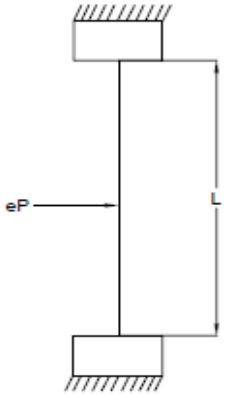

Fig.3.1(c):Axially Restrained Fixed-Fixed Column

Figure 3-1: Axially Restrained Columns Used in Research

The column was subjected to a uniform temperature increase T, with a small gradient e to account for the imperfections in the temperature distribution. Therefore, the temperature varies linearly from $(1-e)T$ at the top to $(1+e)T$ at the bottom of the column cross section as shown in Figure 3-1(a).It was tried to make the imperfection as small as possible and the least value was considered in the study. For this case, (Hinged-Hinged Column), the least value of $e$was found to be 0.001.

3.2 Analytical Models

Two analytical models of the column were constructed by dividing the column length into 2 and 10 finite elements. The column was subjected to a uniform temperature increase T, with a small gradient e to account for the imperfections in the temperature distribution. Therefore, the temperature varies linearly from $(1-e)T$ at the top to $(1+e)T$ at the bottom of the column cross section as shown in Figure 3-1(a).It was tried to make the imperfection as small as possible and the least value was considered in the study. For this case, (Hinged-Hinged Column), the least value of e was found to be 0.001.

The temperature-deformation curves obtained for the column of the slenderness ratio of 125 when subjected to a total temperature increase of 160℃ applied in 60 equal increments are depicted in Figure 3-2and Figure 3-3.Of these, Figure 3-2shows the horizontal mid-span deflection of the column and Figure 3-3reflects the rotation of the top hinged support. The numerical data used to plot Figure 3-2and Figure 3-3are tabulated in Table B- 1of Appendix B.

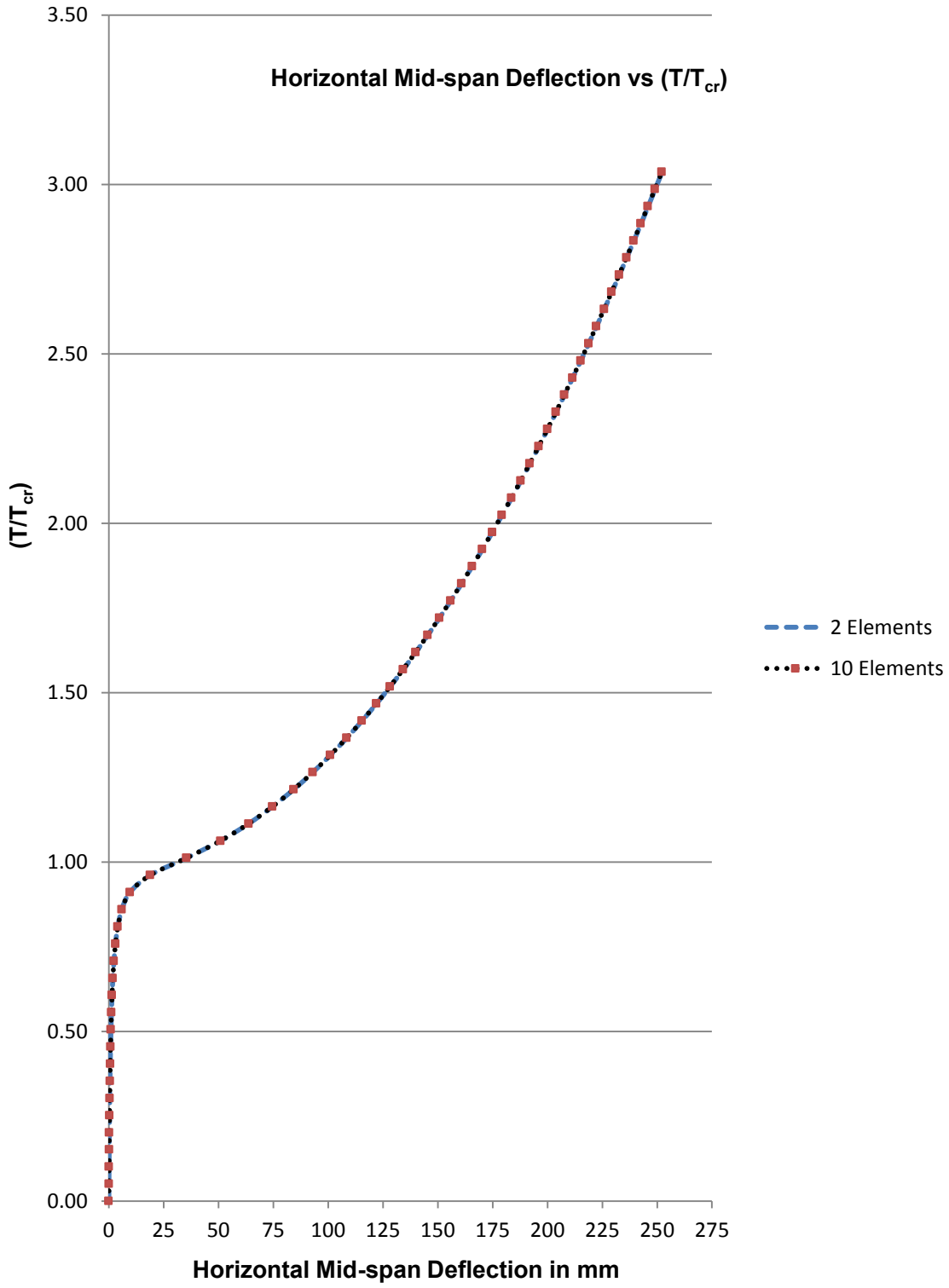

Figure 3-2:Horizontal Mid-Span Deflections vs. (T/T_{cr}) for Hinged-Hinged Column for 2 & 10 Elements for Slenderness Ratio of 125

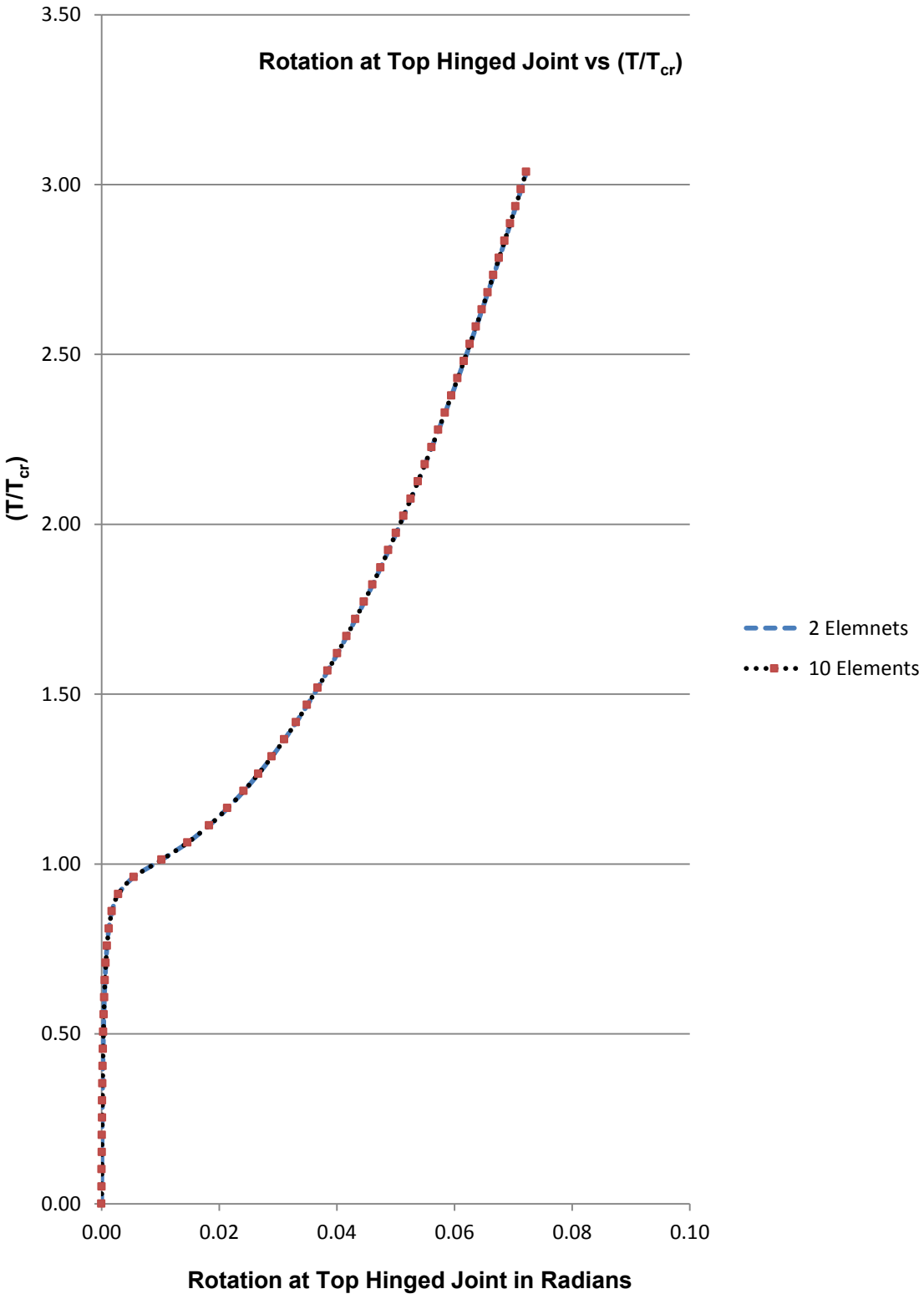

Figure 3-3: Rotation at Top Hinged Joint vs. (T/T_{cr}) for Hinged-Hinged Column for 2 & 10 Elements for Slenderness Ratio of 125

The results shown in Figure 3-2 and Figure 3-3indicate that even when the deformations are very large, the 2-element model yields highly accurate results which are in close agreement with 10 elements model.

Therefore, it is concluded that 2 elements are sufficient for accurately modeling the column and hence for the further analysis of the columns is carried out with 2-element models.

3.3 Validation of Analytical Models Using Benchmark Structures

In order to validate the adequacy of the 2-element model for accurately predicting the post buckling response of hinged-hinged columns, numerical results were determined for two benchmark structures for which the exact (elastica) solutions were available in the literature.

The first benchmark structure is an axially unrestrained hinged-hinged column subjected to an axial mechanical load. The exact post-buckling solution for this structure, as published by Chajes (1974), is given in Table 3-2.

Table 3-2: Numerical Data from Chajes (1974) for Hinged-Hinged Column Subjected to Mechanical Loading

Mid-Span Deflection per Original Length	Ratio of P/P_{cr}
0	1
0.11	1.015
0.211	1.063
0.2966	1.152

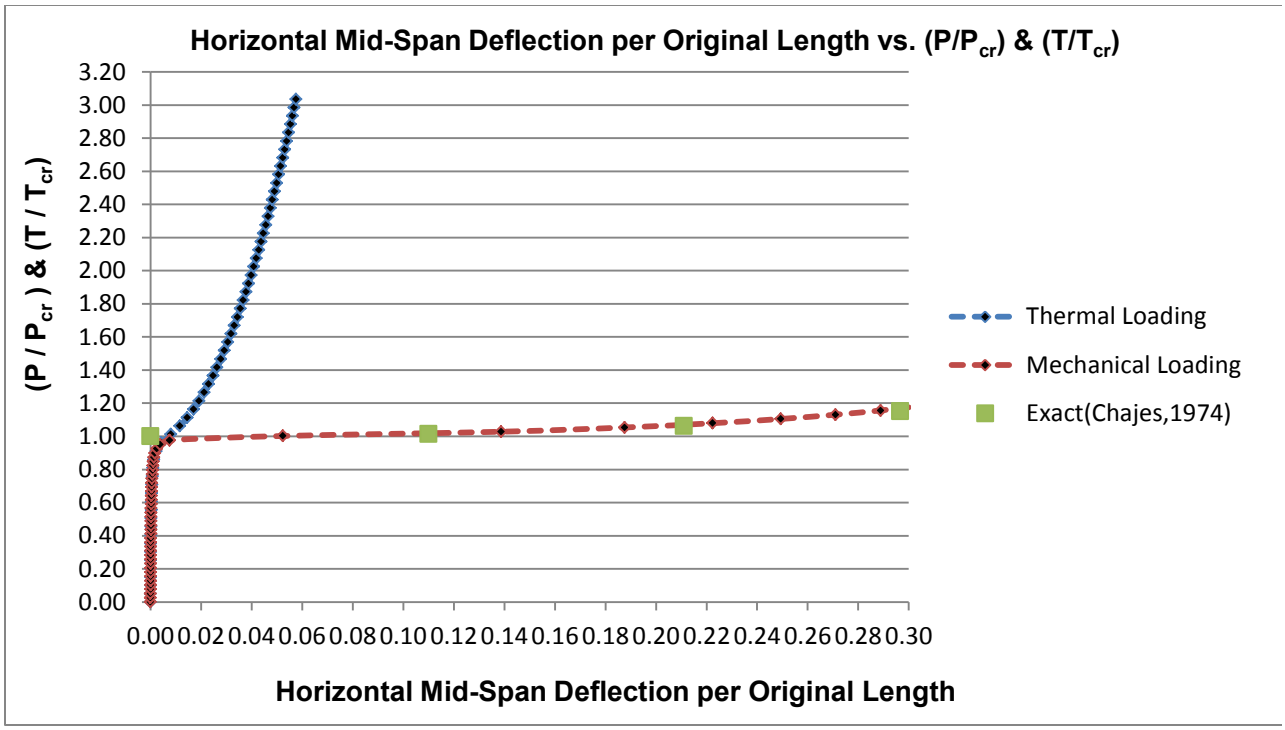

Figure 3-4: Horizontal Mid-Span Deflection per Original Length vs. (T/T_{cr}) & (P/P_{cr}) for Hinged-Hinged Column of Slenderness Ratio 50

It can be seen from Figure 3-4, the solution obtained in the present study by using the 2-element model is in excellent agreement with the exact solution even when the column's mid-span deflection is substantial. The present solution was obtained by applying a small lateral load (equal to 0.01% of the axial load) at the column mid-span to simulate a condition of imperfection.

Also shown in Figure 3-4, for comparison purposes, is the thermal post-buckling solution determined for the corresponding axially restrained column with a slenderness ratio of 50.It can be clearly seen that the axially restrained column exhibits considerably more stiffness in the post-buckling range than its unrestrained counterpart. Figure 3-5depicts similar graphs for the rotation of the column's hinged end in the post-buckling

range. The numerical data used to plot Figure 3-4and Figure 3-5 is given in Table B- 2thru Table B- 4 of Appendix B.

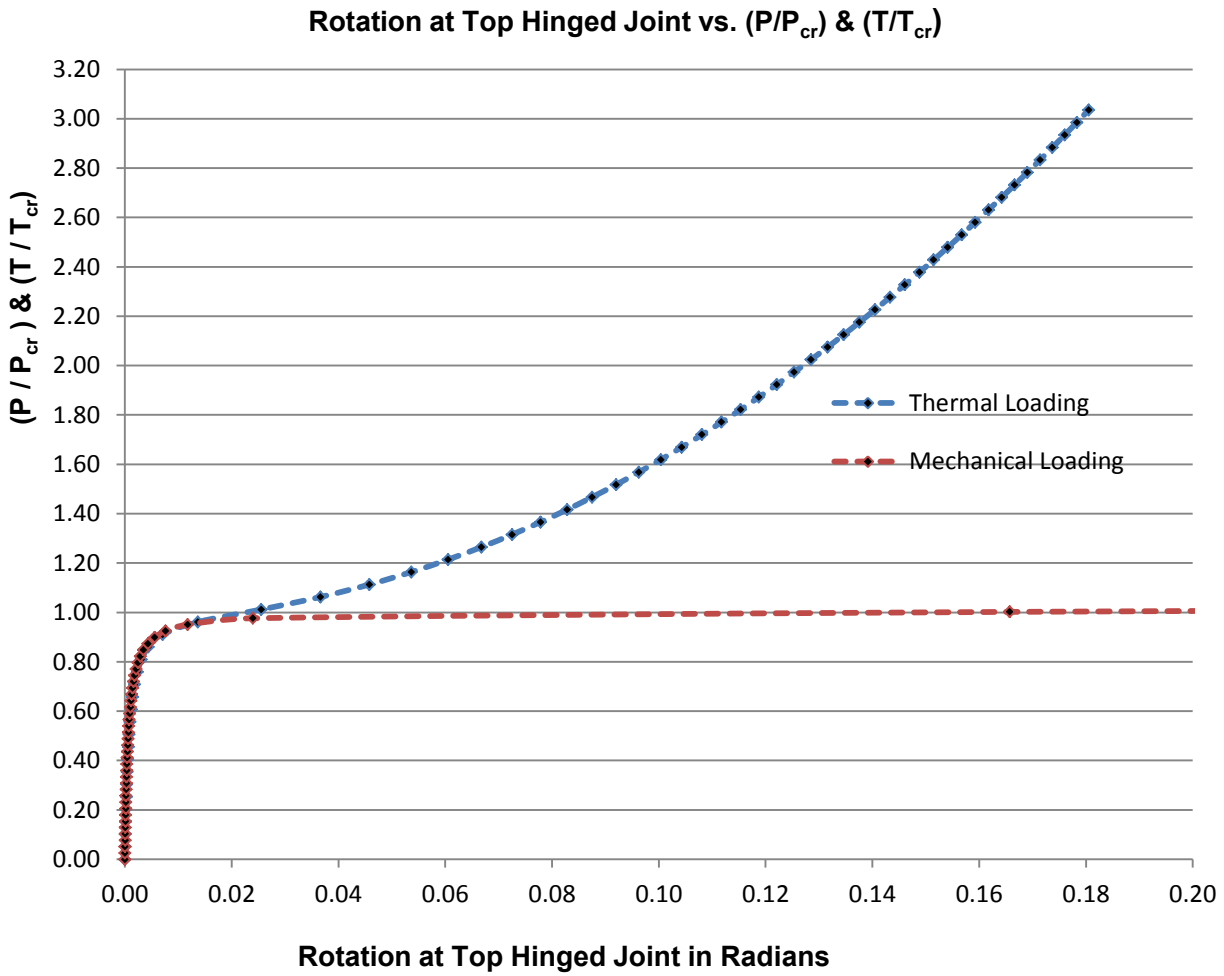

Figure 3-5: Rotation at Top Hinged Joint vs. (T/T_{cr}) & (P/P_{cr}) for Hinged-Hinged Column of Slenderness Ratio 50

The second benchmark structure considered is an axially restrained hinged-hinged column of slenderness ratio of 20, subjected to a uniform temperature increase. The exact post-buckling solution for this case has been published by Coffin and Bloom (1999), and it indicates that at the temperature ratio (T/Tcr) of 2.933, the column's mid-span deflection ratio to be 1/7.The present analysis, using the 2 –element model,

predicted the mid-span deflection of 1/6.993 at the same temperature ratio. Note that, the results of the present study are within 0.1 percent of the exact solution.

The temperature (load) versus deflection and the temperature (load) versus rotation, curves for this column generated in the present study are depicted in Figure 3-6 and Figure 3-7 respectively. The corresponding numerical data used to plot these figures is listed in Table B- 5 and Table B- 6 of the Appendix B.

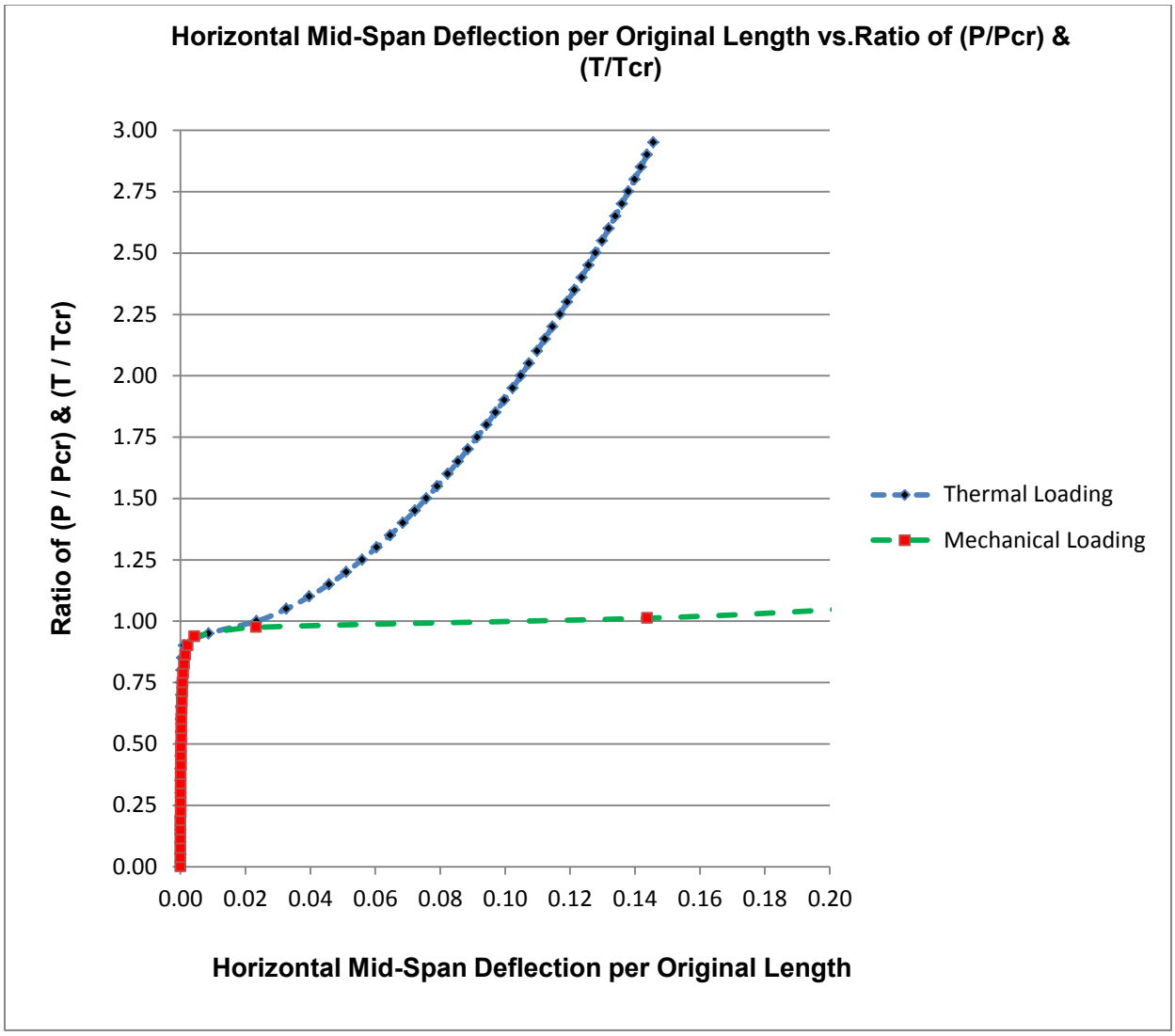

Figure 3-6: Horizontal Deflection at Mid-Span per Original Length vs. (T/T_{cr}) & (P/P_{cr}) for Hinged-Hinged Column of Slenderness Ratio 20 (Validation to Elastica)

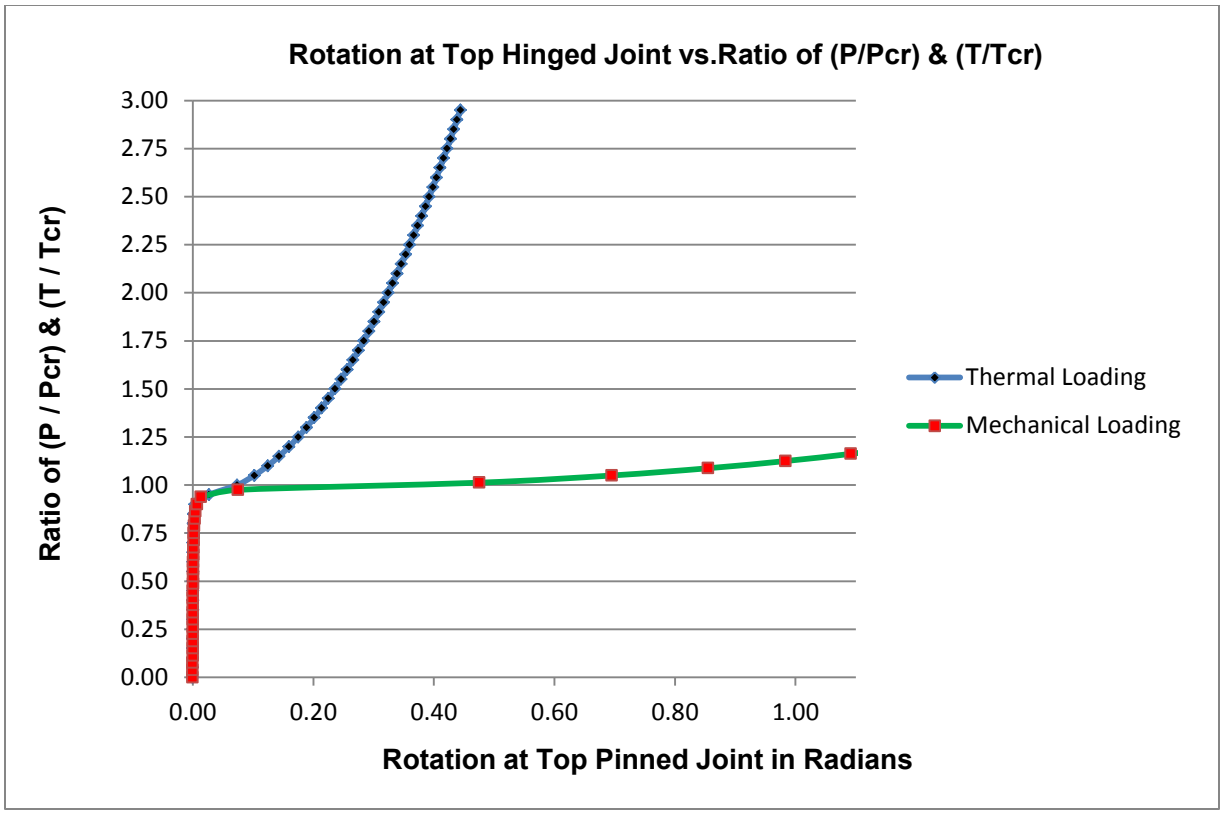

Figure 3-7: Rotation at Top Hinged Joint vs. (T/T_{cr}) & (P/P_{cr}) for Hinged-Hinged Column of Slenderness Ratio 20 (Validation to Elastica Solution)

3.4 Effect of Slenderness Ratios on Post –Buckling Response

To study the effect of slenderness ratios on the thermal post-buckling response of hinged-hinged columns, three different columns with slenderness ratios of 50,125 and 200 were analyzed up to a temperature$T \cong 3T_{cr}$. The material properties and other data for the three different columns are given in Table 3-3.

For comparison purposes, the corresponding unrestrained columns subjected to axial (mechanical) loads were also analyzed. Numerical data thus generated is tabulated in Table B- 7 thru Table B- 12 of Appendix B, and is used to plot the non-dimensional temperature (load) versus deflection (rotation) curves depicted in Figure 3-8 and Figure 3-9.

Table 3-3: Summary of the Analysis for Hinged-Hinged Column of Different Slenderness Ratios

S.No.	Properties	Slenderness Ratio		
		50	125	200
1	Length of Column (L) in mm	4400	11000	17600
2	Radius of Gyration (r) in mm	88	88	88
3	Cross Sectional Area (A) in mm^2	5860	5860	5860
4	Moment of Inertia (I) in mm^4	$4.54*10^7$	$4.54*10^7$	$4.54*10^7$
5	Modulus of Elasticity (E) in KN/mm^2	210	210	210
6	Critical (Buckling) Temperature in ℃	329.4	52.7	20.59
7	Critical (Buckling) Load in KN	4864.29	778.29	304.02
8	Elevated Temperature for Analysis in ℃	1000	160	65
9	Elevated Mechanical Load for Analysis in KN	7500	1750	650
10	Load Increments for Temperature	60	60	60
11	Load Increments for Mechanical Load	60	40	60
12	Eccentricity for imperfection for Thermal Analysis	0.001	0.001	0.001
13	Eccentricity for imperfection for Mechanical Analysis	0.001	0.001	0.001

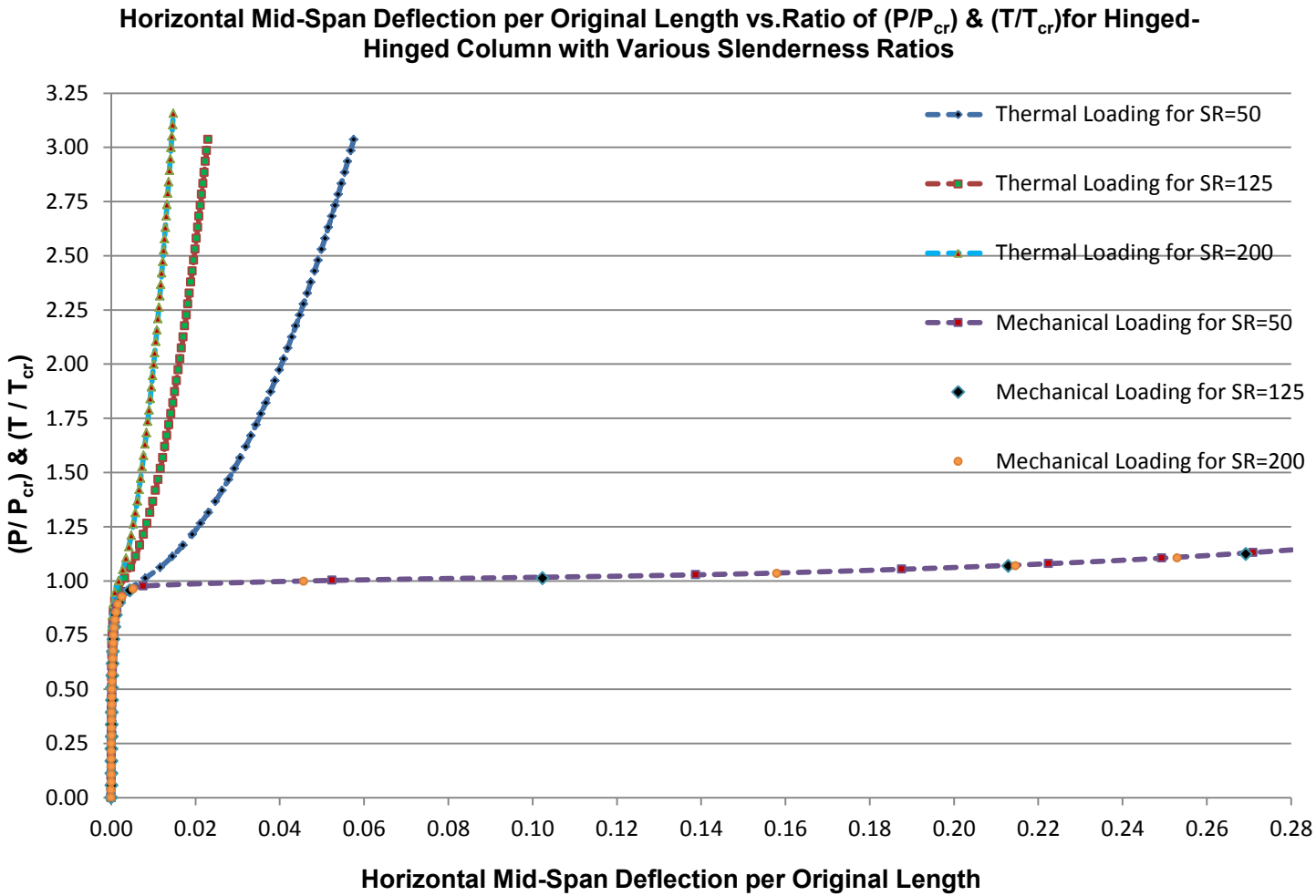

Figure 3-8: Horizontal Mid-Span Deflection per Original Length vs. Ratio of (P/P_{cr}) & (T/T_{cr}) for Hinged-Hinged Column with Various Slenderness Ratios

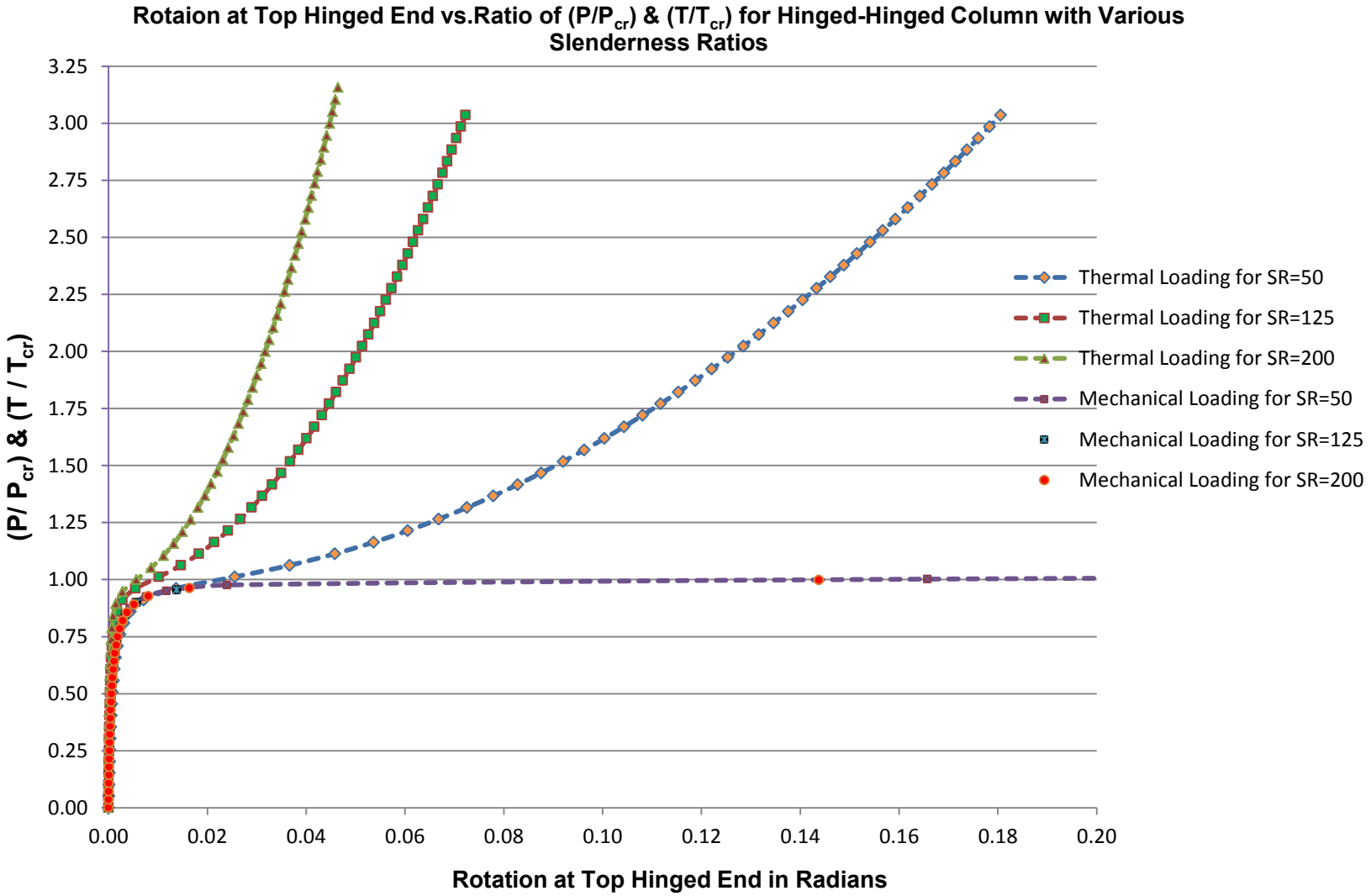

Figure 3-9: Rotation at Top Hinged Joint vs. (T/T_{cr}) & (P/P_{cr}) for Hinged-Hinged Column with Various Slenderness Ratio

From Figure 3-8 and Figure 3-9, it can be observed that the unrestrained columns under mechanical loads do not exhibit any significant post-buckling strength; i.e.; they undergo very large deformations as the loads are increased only slightly above their critical levels. Furthermore, this mechanical post-buckling response does not seem to depend on the slenderness ratios of the columns.

On the other hand, the restrained columns subjected to thermal loading do exhibit significant post-buckling strength, in that they undergo significantly smaller deformations than the unrestrained columns. Furthermore, this thermal post-buckling response depends on the slenderness ratios of the columns with the relative deformation and end rotation decreasing with increasing slenderness ratio at a given temperature ratio $\left(T/T_{cr}\right)$.

Figure 3-10 and Figure 3-11, & Table 3-4 and Table 3-5 shows the variation of the column mid-span deflection ratios and end rotations as functions of the slenderness ratio, for four different temperature ratios.

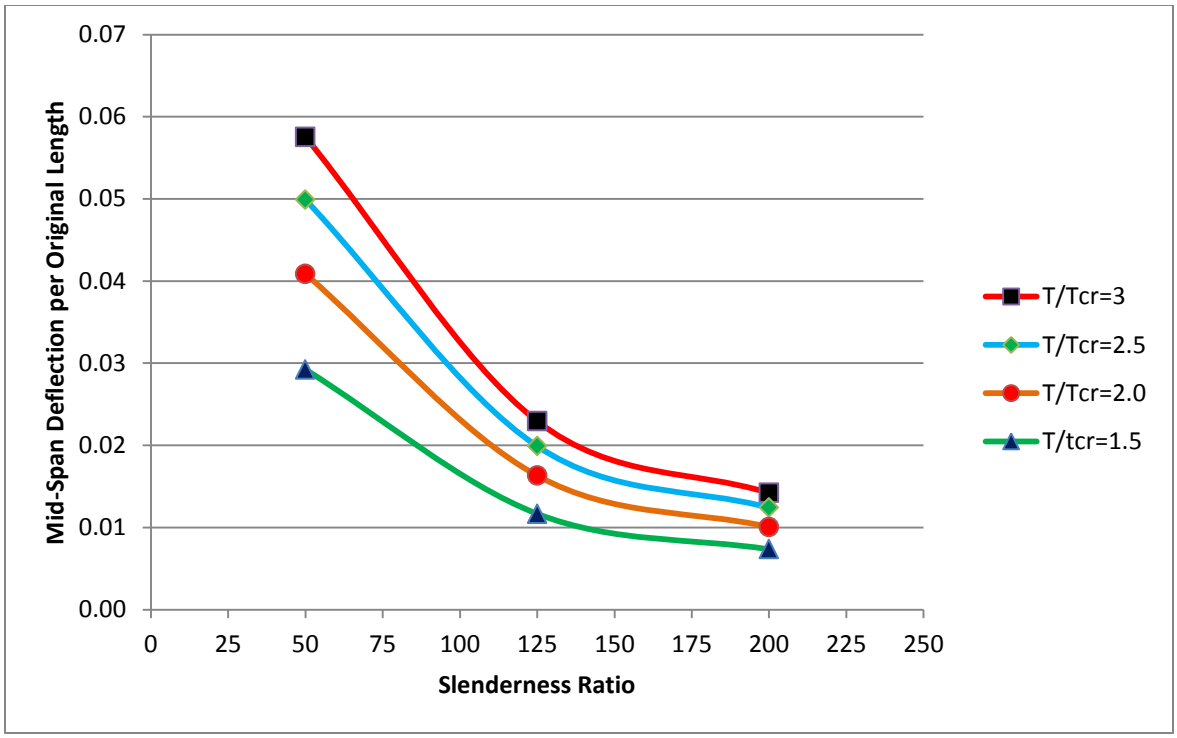

Figure 3-10:Mid-Span Deflection vs. Slenderness Ratio at Various Temperature Ratios for Hinged-Hinged Column

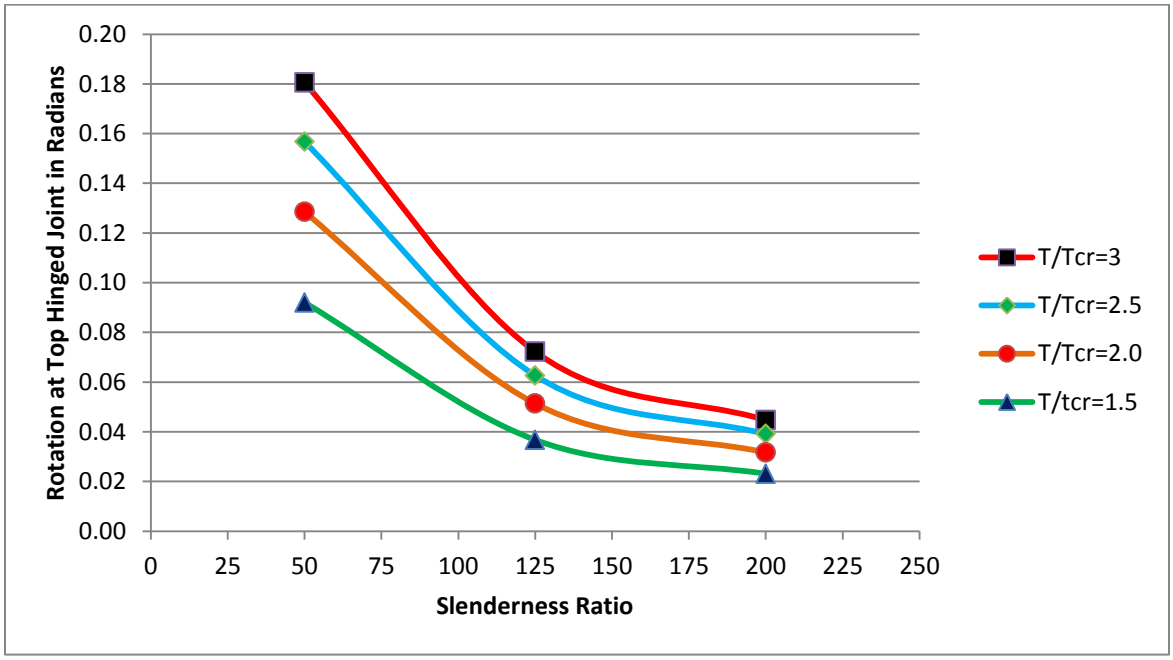

Figure 3-11: Rotation vs. Slenderness Ratio at Various Temperature Ratios for Hinged-Hinged Column

Table 3-4:Mid-Span Deflection at Various Temperature Ratios for Hinged-Hinged Column for Different Slenderness Ratios

T/T_{cr}	Slenderness Ratio , λ			% Difference w.r .to λ=200	
	50	125	200	λ=50	λ=125
1.5	0.02923118274082	0.01166579551703	0.00734446435450	298.00	58.84
2	0.04087769192731	0.01630587256363	0.01006770787999	306.03	61.96
2.5	0.04990542965402	0.01989750340624	0.01241491560943	301.98	60.27
3	0.05755167648720	0.02293521512308	0.01420019037461	305.29	61.51

Table 3-5: Rotation at Various Temperature Ratios for Hinged-Hinged Column for Different Slenderness Ratios

T/T_{cr}	Slenderness Ratio , λ			% Difference w.r .to λ=200	
	50	125	200	λ=50	λ=125
1.5	0.09201779986938	0.03676206705792	0.02314702715097	297.54	58.82
2	0.12850733697774	0.05136668618557	0.03172291163023	305.09	61.92
2.5	0.15671244473752	0.06267384484602	0.03911880275594	300.61	60.21
3	0.18053114133475	0.07223784530349	0.04474645999200	303.45	61.44

CHAPTER 4

NUMERICAL RESULTS FOR FIXED-HINGED COLUMN

4.1 General

The results for the fixed-hinged columns Figure 3-1(b) are presented in this chapter. The cross-sectional and material properties of the columns were kept constant throughout the study. These properties are listed in Table 4-1. As shown in this table, the columns are assumed to be composed of structural steel with a W200X46 cross section. The lengths of the columns were varied to examine the effect of slenderness ratio on the post-buckling response.

Table 4-1:Cross-Sectional and Material Properties of Column Used for Numerical Study

d	=	203	mm
A	=	5860	mm^2
I	=	4.54×10^7	mm^4
E	=	210	KN/mm^2
α	=	1.20×10^{-5}	/°C

4.2 Analytical Models

Two analytical models of the column were constructed by dividing the column length into 2 and 10 finite elements. The column was subjected to a uniform temperature increase T, with a small gradient e to account for the imperfections in the temperature distribution. Therefore, the temperature varies linearly from $(1-e)T$ at the top to $(1+e)T$ at the bottom of the column cross section as shown in Figure 3-1 (b). It

was tried to make the imperfection as small as possible and the least value was considered in the study. For this case, (Fixed-Hinged Column), the least value of e was found to be 0.001.

The temperature-deformation curves obtained for the column of the slenderness ratio of 125 when subjected to a total temperature increase of 325℃ applied in 60 equal increments are depicted in Figure 4-1and Figure 4-2. Of these, Figure 4-1shows the horizontal mid-span deflection of the column and Figure 4-2reflects the rotation of the top hinged support. The numerical data used to plot Figure 4-1and Figure 4-2are tabulated in Table C- 1 of Appendix C.

The results shown in Figure 4-1 and Figure 4-2 indicate that even when the deformations are very large, the 2-element model yields highly accurate results which are in close agreement with the 10 elements model.

Therefore, it is concluded that 2 elements are sufficient for accurately modeling the column, and hence for the further analysis of the columns is carried out with 2-element models.

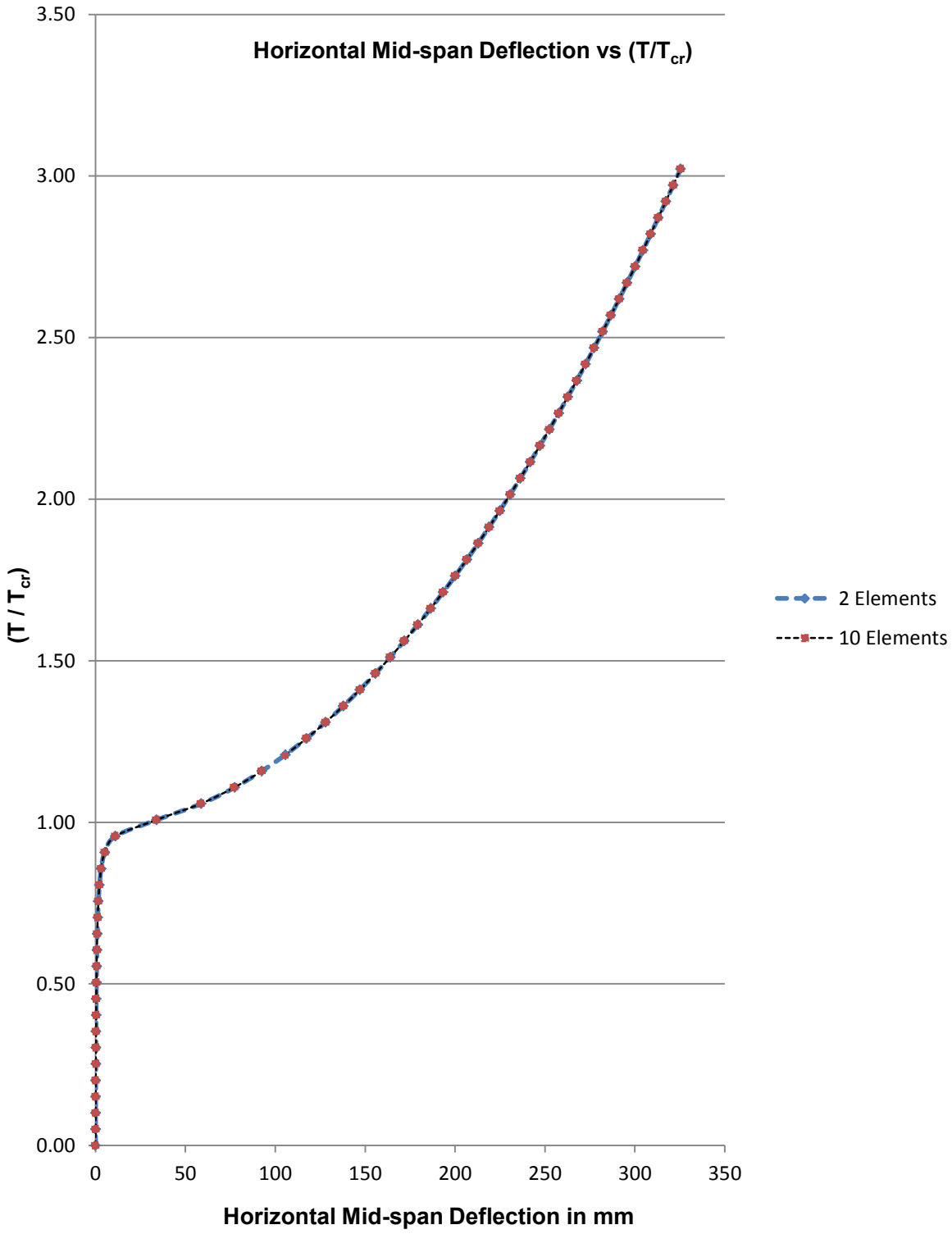

Figure 4-1: Horizontal Mid-Span Deflections vs. (T/T$_{cr}$) for Fixed-Hinged Column for 2 & 10 Elements for Slenderness Ratio of 125

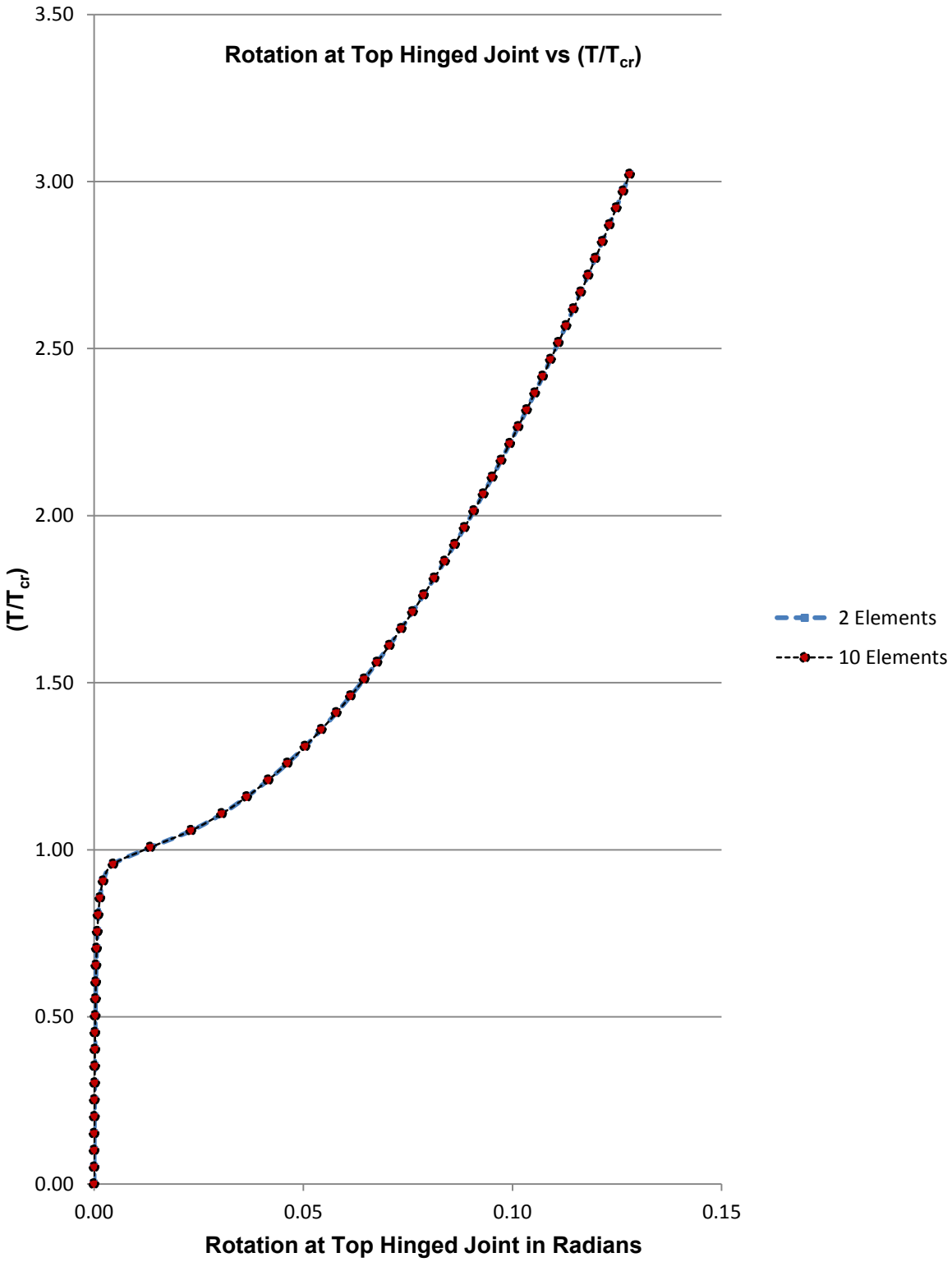

Figure 4-2: Rotation at Top Pinned Joint vs. (T/T_{cr}) for Fixed-Hinged Column for 2 & 10 Elements for Slenderness Ratio of 125

4.3 Effect of Slenderness Ratio on Post-buckling Response

To study the effect of slenderness ratios on the thermal post-buckling response of hinged-hinged columns, three different columns with slenderness ratios of 50,125 and 200 were analyzed up to a temperature$T \cong 3T_{cr}$. The material properties and other data for the three different columns are given in Table 4-2.

For comparison purposes, the corresponding unrestrained columns subjected to axial (mechanical) loads were also analyzed. Numerical data thus generated is tabulated in Table C- 2 thru Table C- 7 of Appendix C, and is used to plot the non-dimensional temperature (load) versus deflection (rotation) curves depicted in Figure 4-3 and Figure 4-4**.**

From Figure 4-3and Figure 4-4, it can be observed that the unrestrained columns under mechanical loads do not exhibit any significant post-buckling strength; i.e.; they undergo very large deformations as the loads are increased only slightly above their critical levels. Furthermore, this mechanical post-buckling response does not seem to depend on the slenderness ratios of the columns.

On the other hand, the restrained columns subjected to thermal loading do exhibit significant post-buckling strength, in that they undergo significantly smaller deformations than the unrestrained columns. Furthermore, this thermal post-buckling response depends on the slenderness ratios of the columns with the relative deformation decreasing with increasing slenderness ratio at a given temperature ratio$\left(T/T_{cr}\right)$.

Table 4-2: Summary of the Analysis for Fixed-Hinged Column of Different Slenderness Ratios

S.No.	Properties	Slenderness Ratio		
		50	125	200
1	Length of Column (L) in mm	4400	11000	17600
2	Radius of Gyration (r) in mm	88	88	88
3	Cross Sectional Area (A) in mm^2	5860	5860	5860
4	Moment of Inertia (I) in mm^4	$4.54*10^7$	$4.54*10^7$	$4.54*10^7$
5	Modulus of Elasticity (E) in KN/mm^2	210	210	210
6	Critical (Buckling) Temperature in ℃	672.24	107.56	42.02
7	Critical (Buckling) Load in KN	9927.11	1588.34	620.44
8	Elevated Temperature for Analysis in ℃	2014	325	126
9	Elevated Mechanical Load for Analysis in KN	29750	4760	1850
10	Load Increments for Temperature	80	80	80
11	Load Increments for Mechanical Load	80	80	80
12	Eccentricity for imperfection for Thermal Analysis	0.001	0.001	0.001
13	Eccentricity for imperfection for Mechanical Analysis	0.001	0.001	0.001

Figure 4-5 and Figure 4-6, & Table 4-3 and Table 4-4shows the variation of the column mid-span deflection ratios and end rotations as functions of the slenderness ratio, for four different temperature ratios.

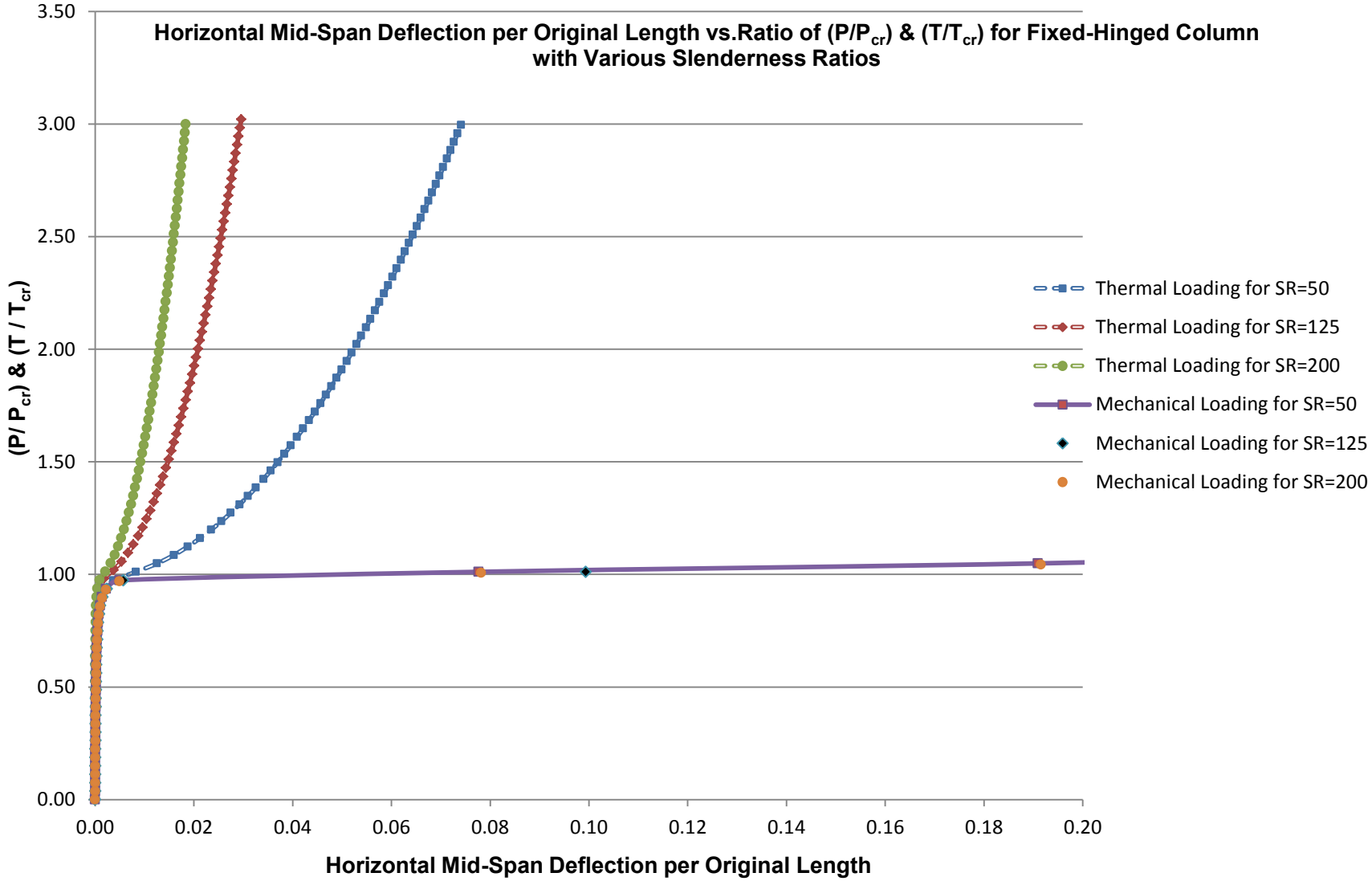

Figure 4-3: Horizontal Mid-Span Deflection per Original Length vs. Ratio of (P/P_{cr}) & (T/T_{cr}) for Fixed-Hinged Column with Various Slenderness Ratios

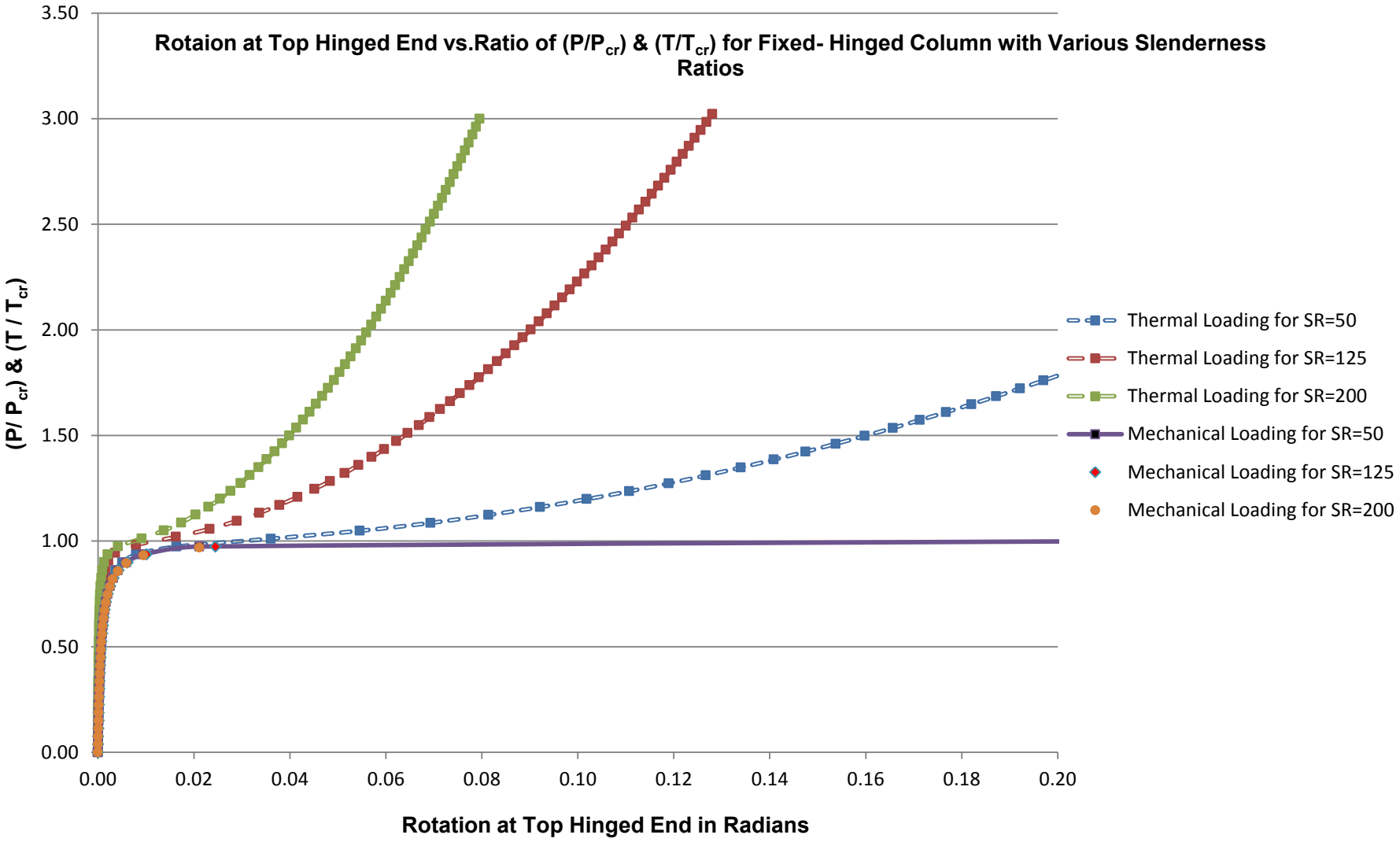

Figure 4-4: Rotation at Top Hinged Joint vs. (T/T_{cr}) & (P/P_{cr}) for Fixed-Hinged Column with Various Slenderness Ratios

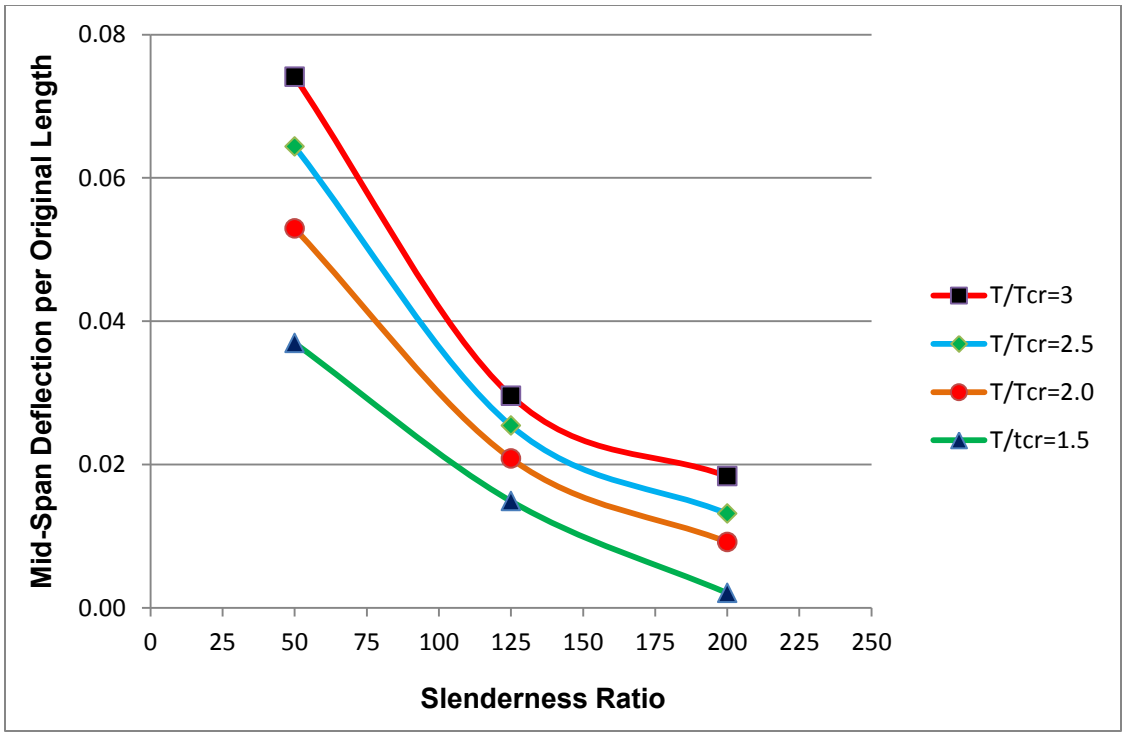

Figure 4-5:Mid-Span Deflection vs. Slenderness Ratio at Various Temperature Ratios for Fixed-Hinged Column

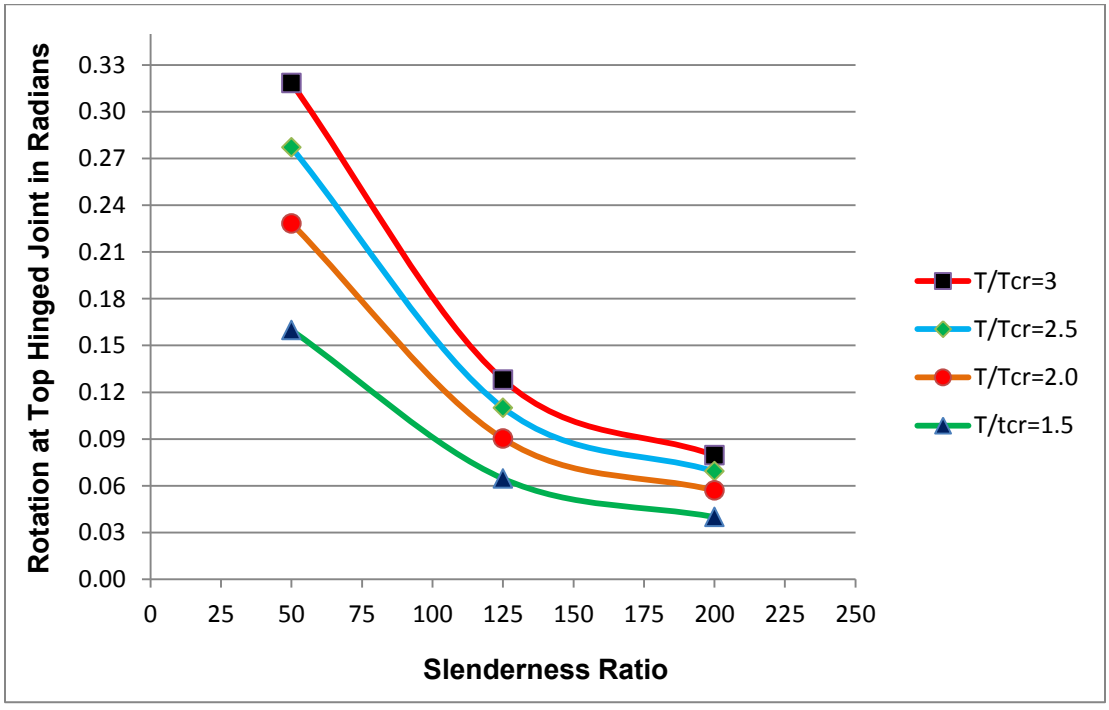

Figure 4-6: Rotation vs. Slenderness Ratio at Various Temperature Ratios for Fixed-Hinged Column

Table 4-3:Mid-Span Deflection at Various Temperature Ratios for Fixed-Hinged Column for Different Slenderness Ratios

T/T_{cr}	Slenderness Ratio ,λ			% Difference w.r.to λ=200	
	50	125	200	λ=50	λ=125
1.5	0.03695855153912	0.01490259756243	0.00920603367933	301.46	61.88
2	0.05293557370784	0.02083892828034	0.01291783417747	309.79	61.32
2.5	0.06435460438965	0.02542218244471	0.01597528368373	302.84	59.13
3	0.07409639593932	0.02930542762020	0.01836780601357	303.40	59.55

Table 4-4: Rotation at Various Temperature Ratios for Fixed-Hinged Column for Different Slenderness Ratios

T/T_{cr}	Slenderness Ratio ,λ			% Difference w.r.to λ=200	
	50	125	200	λ=50	λ=125
1.5	0.15981189761855	0.06455543961020	0.03988829295036	300.65	61.84
2	0.22832554692568	0.09021818935340	0.05699822614422	300.58	58.28
2.5	0.27703094472669	0.11003421553460	0.06918846469924	300.40	59.04
3	0.31836202610922	0.12802261646349	0.07955419611273	300.18	60.93

CHAPTER 5

NUMERICAL RESULTS FOR FIXED-FIXED COLUMN

5.1 General

The results for the fixed-fixed columns Figure 3-1(c) are presented in this chapter. The cross sectional and material properties of the columns were kept constant throughout the study. These properties are listed in Table 5-1.As shown in this table, the columns are assumed to be composed of steel with a W200X46 cross section. The lengths of the columns were varied to examine the effect of slenderness ratio on the post-buckling response.

Table 5-1:Cross-Sectional and Material Properties of Column Used for Numerical Study

d	=	203	mm
A	=	5860	mm^2
I	=	4.54×10^7	mm^4
E	=	210	KN/mm^2
α	=	1.20×10^{-5}	/°C

5.2 Analytical Models

Two analytical models of the column were constructed by dividing the column length into 2 and 10 finite elements. The column was subjected to a small lateral load at its mid-height to simulate a condition of imperfection. It was tried to make the imperfection as small as possible and the least value was considered in the study. For

this case, (Fixed-Fixed Column), the least value of $e$was found to be 0.009.The temperature-deformation curves obtained for the column of the slenderness ratio of 125 when subjected to a total temperature increase of 630℃ applied in 60 equal increments isdepicted in Figure 5-1.The Figure 5-1shows the horizontal mid-span deflection of the column and the numerical data used to plot Figure 5-1is tabulated in Table D- 1of Appendix D.

The result shown in Figure 5-1indicate that even when the deformations are very large, the 2-element model yields highly accurate results which are in close agreement with the 10 elements model.

Therefore, it is concluded that 2 elements are sufficient for accurately modeling the column, and hence for the further analysis of the column is carried out with 2-element models.

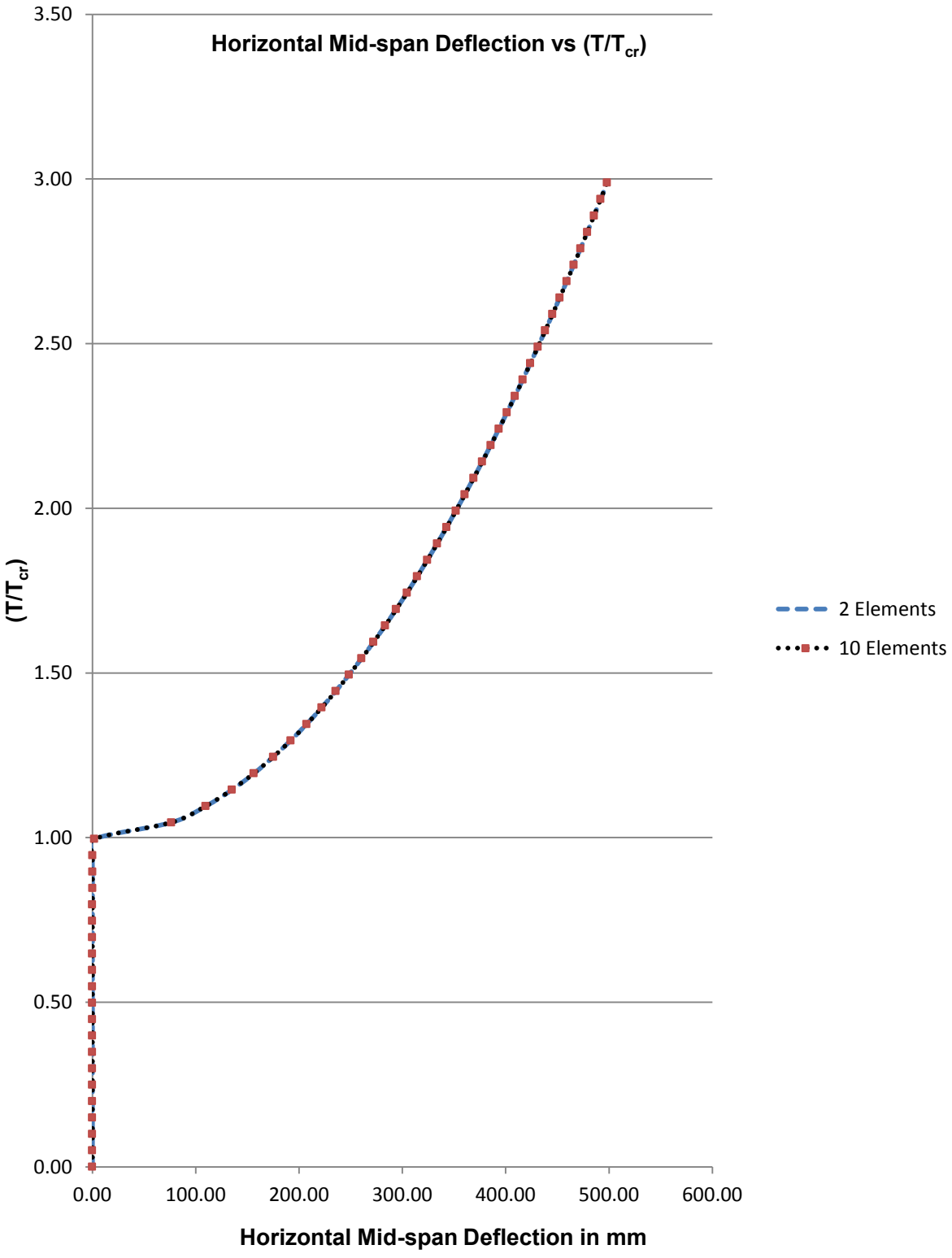

Figure 5-1: Horizontal Mid-Span Deflections vs. (T/T_{cr}) for Fixed-Fixed Column for 2 & 10 Elements

5.3 Validation of Analytical Models Using a Benchmark Structure

In order to validate the adequacy of the 2-element model for accurately predicting the post-buckling response of fixed-fixed columns, numerical results were determined for one benchmark structure for which the exact (elastica) solution is available in the literature.

The benchmark structure is an axially restrained fixed-fixed elastic rod subjected to thermal increase by Li Shirong and Cheng Changjun entitled as “Analysis of Thermal Post-Buckling of Heated Elastic Rods (2000)”.The exact post-buckling solution for this structure, as published by the authors is given in Table 5-2. It can be seen from Figure 5-2and Figure 5-3, the solution obtained in the present study by using the 2-element model is in excellent agreement with the exact solution even when the column’s mid-span deflections and the end rotationsare substantial. The present solution was obtained by applying a small lateral load (equal to 0.01% of the axial load) at the column mid-span to simulate a condition of imperfection.

Table 5-2: Numerical Data from Li & Cheng for Fixed-Fixed Column Subjected to Thermal Loading

m	0.2	0.4	0.6	0.8
$f \times 10^{-2}$	1.0126	2.0275	3.0471	4.0737
T/T_{cr}	1.1638	1.6563	2.4816	3.6464
P/P_{cr}	0.9996	0.9985	0.9965	0.9939

The benchmark structure, as taken as a reference elastica solution is an axially restrained fixed-fixed column of slenderness ratio of 160, subjected to a uniform temperature increase. From the elastica solution of the authors as mentioned above, it

indicates that at the temperature ratio $\left({}^{T}/_{T_{cr}}\right)$ of 1.6563, the column's end moment ratio was 0.4. The present analysis, using the 2-element model, predicted the end moment ratio of 0.400552 at the same temperature ratio. Similarly, for the same temperature ratio, the elastica solution had the column's mid-span deflection ratio to be 0.020275 and the present analysis predicted the ratio to be0.02029671.Note that, the results of the present study are within 0.11 percent of the exact solution.

The temperature (load) versus deflection and the temperature (load) versus rotation curves for this column generated in the present study are depicted in Figure 5-2 and Figure 5-3, respectively. The corresponding numerical data used to plot these figures is listed in Table D- 3thru Table D- 6.

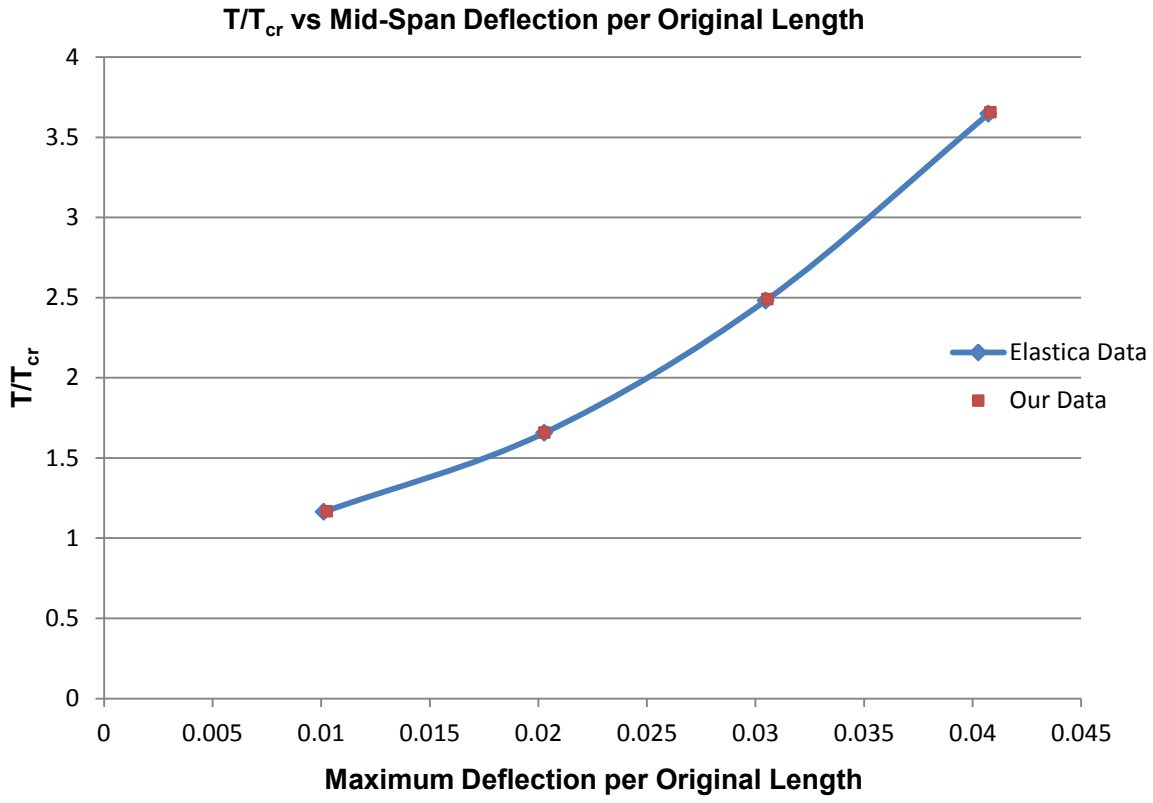

Figure 5-2: Horizontal Deflection at Mid-Span per Original Length vs. (T/T_{cr}) for Fixed-Fixed Column of Slenderness Ratio 160 (Validation to Elastica)

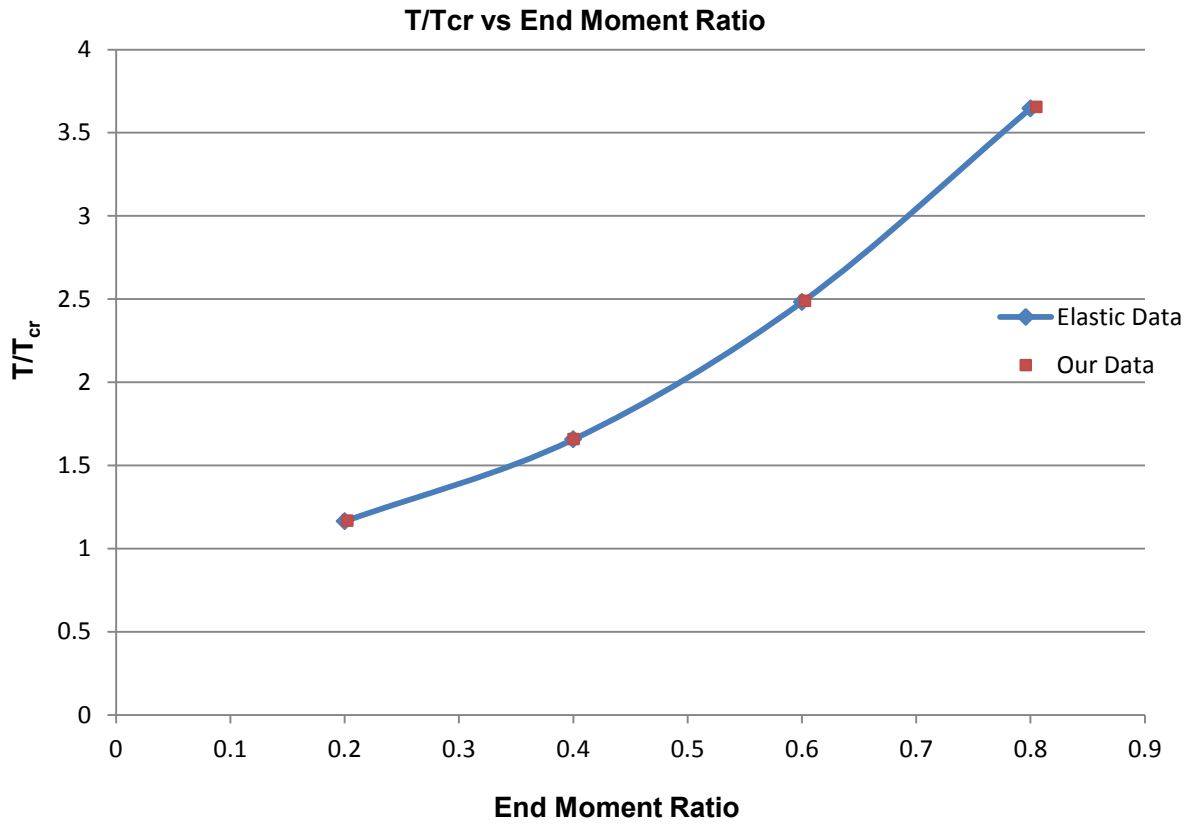

Figure 5-3: End Moment Ratio vs. (T/T_{cr}) for Fixed-Fixed Column of Slenderness Ratio 160 (Validation to Elastica)

5.4 Effect of Slenderness Ratio on Post-buckling Response

To study the effect of slenderness ratios on the thermal post-buckling response of fixed-fixed columns, three different columns with slenderness ratios of 50,125 and 200 were analyzed up to a temperature$T \cong 3T_{cr}$. The material properties and other data for the three different columns are given in Table 5-3.

For comparison purposes, the corresponding unrestrained columns subjected to axial (mechanical) loads were also analyzed. Numerical data thus generated is

tabulated in Table D- 7thru Table D- 9of Appendix D, and is used to plot the non-dimensional temperature (load) versus deflection curves depicted in Figure 5-4.

From Figure 5-4, it can be observed that the unrestrained columns under mechanical loads do not exhibit any significant post-buckling strength; i.e.; they undergo very large deformations as the loads are increased only slightly above their critical levels. Furthermore, this mechanical post-buckling response does not seem to depend on the slenderness ratios of the columns.

On the other hand, the restrained columns subjected to thermal loading do exhibit significant post-buckling strength, in that they undergo significantly smaller deformations than the unrestrained columns. Furthermore, this thermal post-buckling response depends on the slenderness ratios of the columns with the relative deformation decreasing with increasing slenderness ratio at a given temperature ratio$\left(T/T_{cr}\right)$.

Figure 5-5 and Table 5-4 shows the variation of the column mid-span deflection ratios on functions of the slenderness ratio, for four different temperature ratios.

Table 5-3: Summary of the Analysis for Fixed-Fixed Column of Different Slenderness Ratios

S.No.	Properties	Slenderness Ratio		
		50	125	200
1	Length of Column (L) in mm	4400	11000	17600
2	Radius of Gyration (r) in mm	88	88	88
3	Cross Sectional Area (A) in mm^2	5860	5860	5860
4	Moment of Inertia (I) in mm^4	$4.54*10^7$	$4.54*10^7$	$4.54*10^7$
5	Modulus of Elasticity (E) in KN/mm^2	210	210	210
6	Critical (Buckling) Temperature in ℃	1317.59	210.81	82.35
7	Critical (Buckling) Load in KN	19457.14	3113.14	1216.07
8	Elevated Temperature for Analysis in ℃	3950	630	245
9	Elevated Mechanical Load for Analysis in KN	37000	4750	2250
10	Load Increments for Temperature	60	60	60
11	Load Increments for Mechanical Load	60	60	60
12	Eccentricity for imperfection for Thermal Analysis	0.001	0.001	0.001
13	Eccentricity for imperfection for Mechanical Analysis	0.001	0.001	0.001

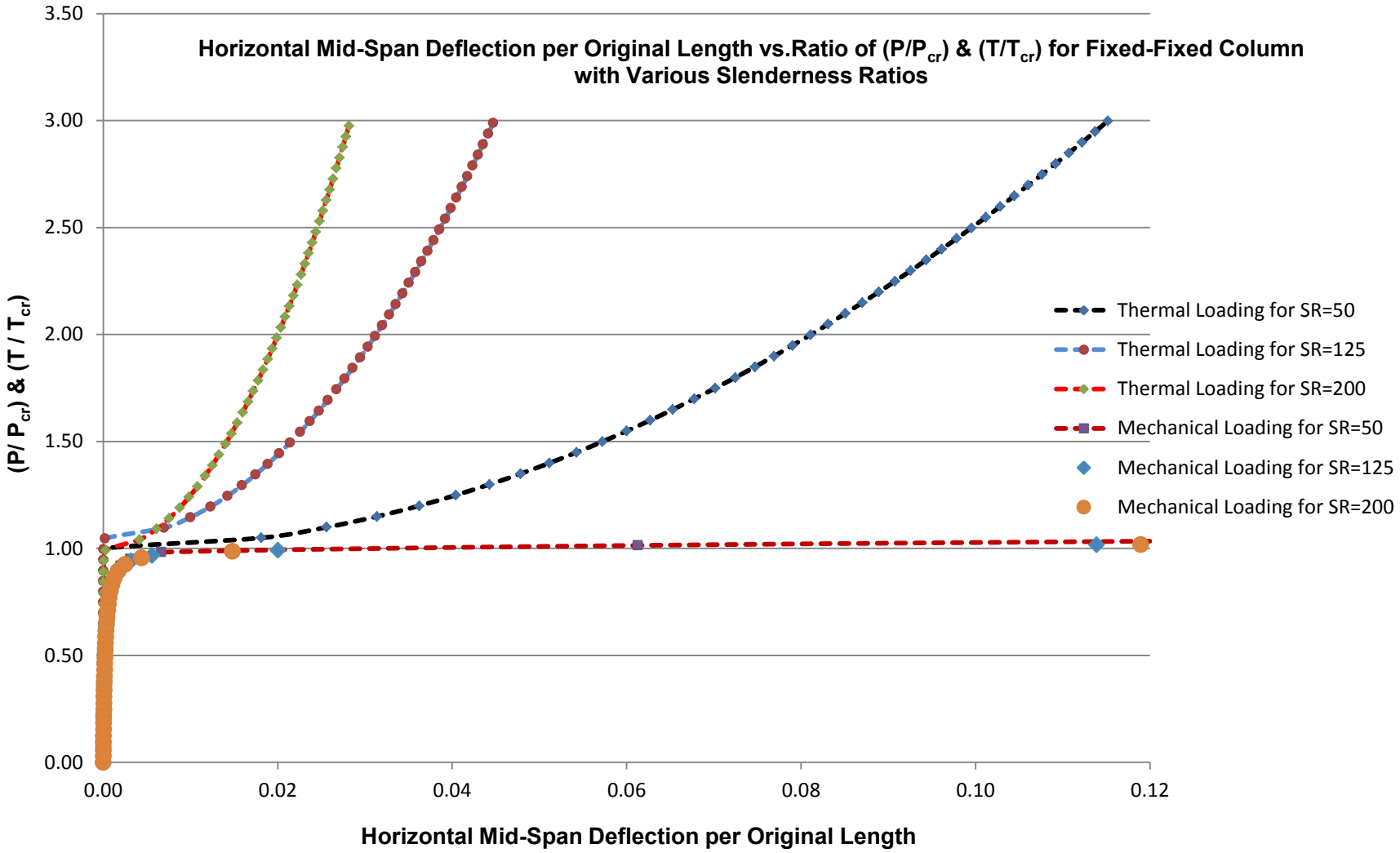

Figure 5-4: Horizontal Mid-Span Deflection per Original Length vs. Ratio of (P/P_{cr}) & (T/T_{cr}) for Fixed-Fixed Column with Various Slenderness Ratios

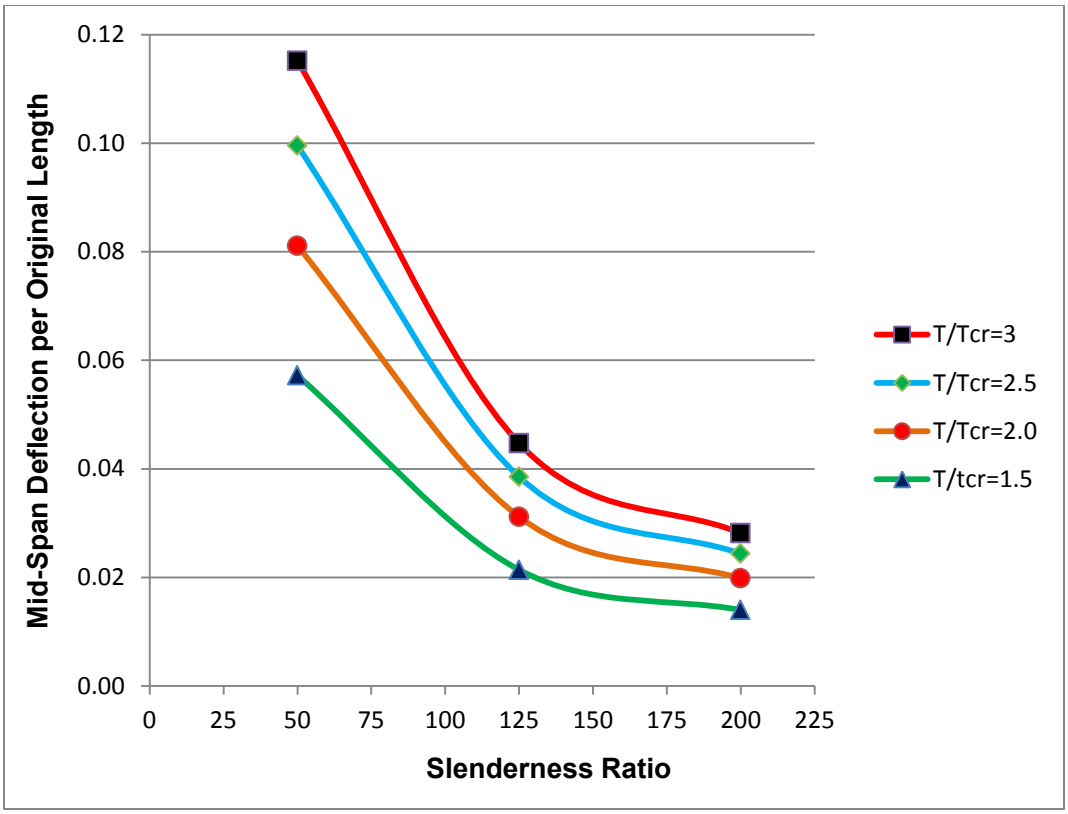

Figure 5-5:Mid-Span Deflection vs. Slenderness Ratio at Various Temperature Ratios for Fixed-Fixed Column

Table 5-4:Mid-Span Deflection at Various Temperature Ratios for Fixed-Fixed Column for Different Slenderness Ratios

T/T_{cr}	Slenderness Ratio , λ			% Difference w. r.to λ=200	
	50	125	200	λ=50	λ=125
1.5	0.05721380776898	0.02140197132916	0.01399694930610	308.76	52.90
2	0.08108920702875	0.03116305146128	0.01987126828504	308.07	56.82
2.5	0.09953300171938	0.03853525867385	0.02437088664847	308.41	58.12
3	0.11518478710471	0.04471613898813	0.02816250937437	309.00	58.78

CHAPTER 6

EFFECTS OF END ROTATIONAL RESTRAINTS ON THERMAL POST-BUCKLING

6.1 General

In this chapter, the numerical results previously presented in Chapters 3 thru 5, for three different end rotational restraints (hinged-hinged, fixed-hinged and fixed-fixed), are combined and analyzed to examine the effect of such restraints on the thermal post-buckling response of non-sway columns.

6.2 Numerical Results

Figure 6-1shows the non-dimensional temperature (load) versus mid-span deflection curves for the three different support conditions for the column slenderness ratio of 50.Similar graphs for the columns of slenderness ratios of 125 and 200 are given in Figure 6-2and Figure 6-3, respectively.

It can be seen from these figures that, regardless of the rotational end restraints, the columns under mechanical loads do not exhibit any significant post-buckling strength, and they experience very large deformation as the loads are increased even slightly above the critical levels.

However, the columns under temperature increase do show significant post-buckling strength as they experience significantly less deformations. It should also be noted that the thermal post-buckling response depends on the rotational restraints at the ends of the column, with the hinged-hinged column having the smallest deflection ratio and the fixed-fixed column the largest, at a given temperature ratio $\left({}^{T}/_{T_{cr}}\right)$.

Figure 6-4thru Figure 6-6&Table 6-1thru Table 6-3, show the variation of the column mid-span deflection ratios as functions of the column ends fixed against rotation, for four different temperature ratios. It can be seen that as the temperature ratio increases, the differences in the deflection ratio widens.

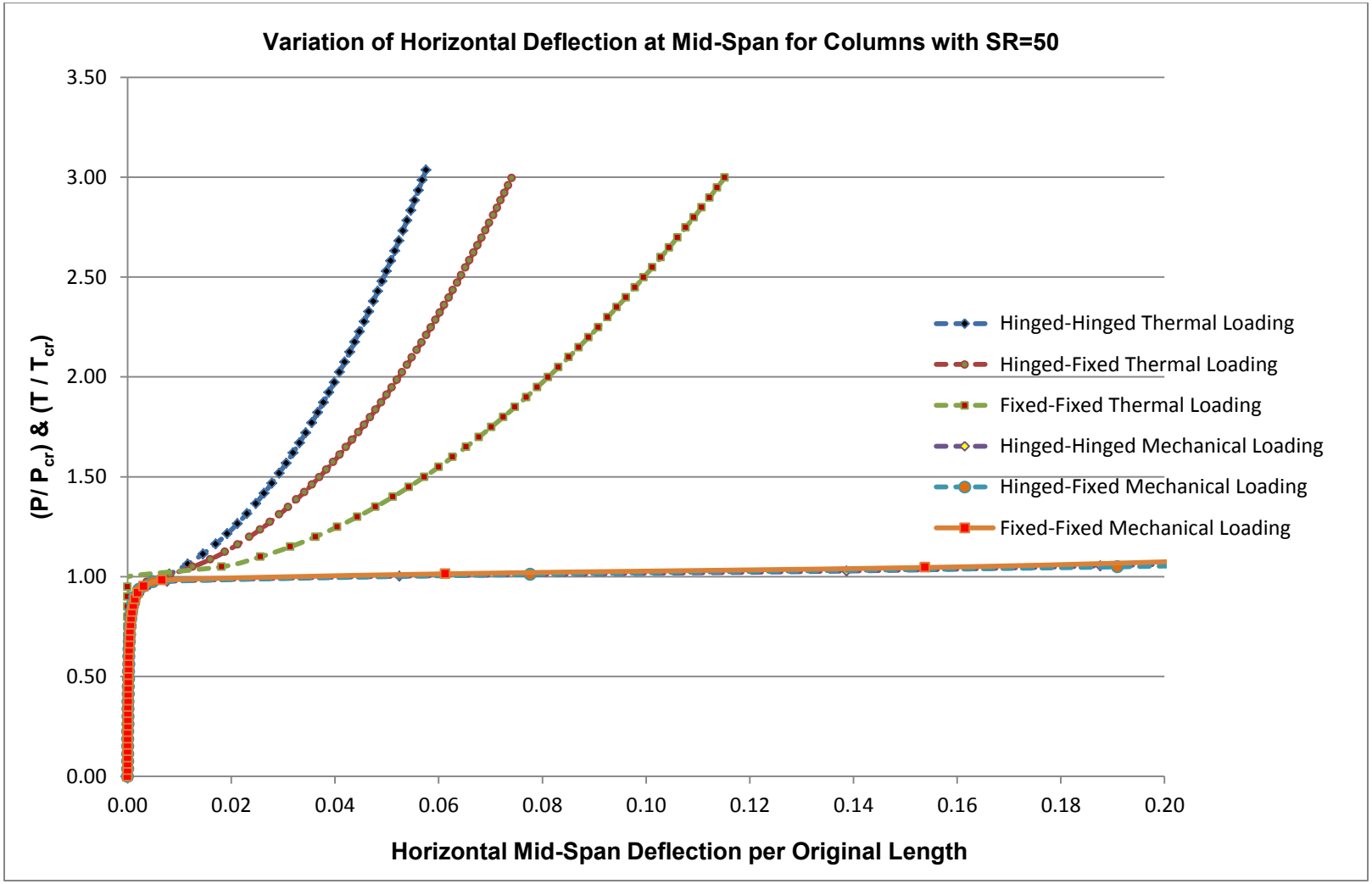

Figure 6-1: Comparison of Mid-Span Deflection per Original Length for 3 Columns for a Given Slenderness Ratio of 50

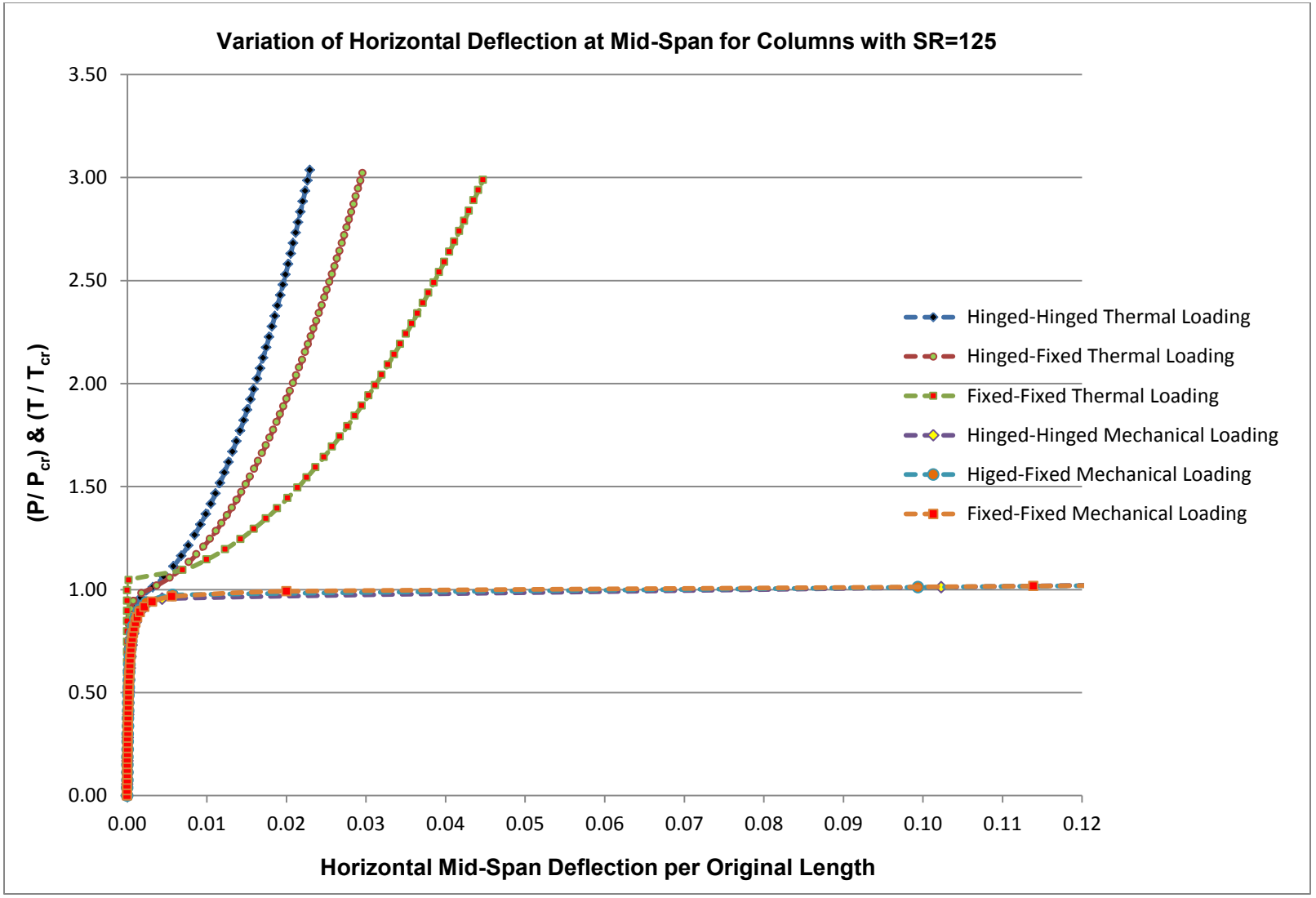

Figure 6-2: Comparison of Mid-Span Deflection per Original Length for 3 Columns for a Given Slenderness Ratio of 125

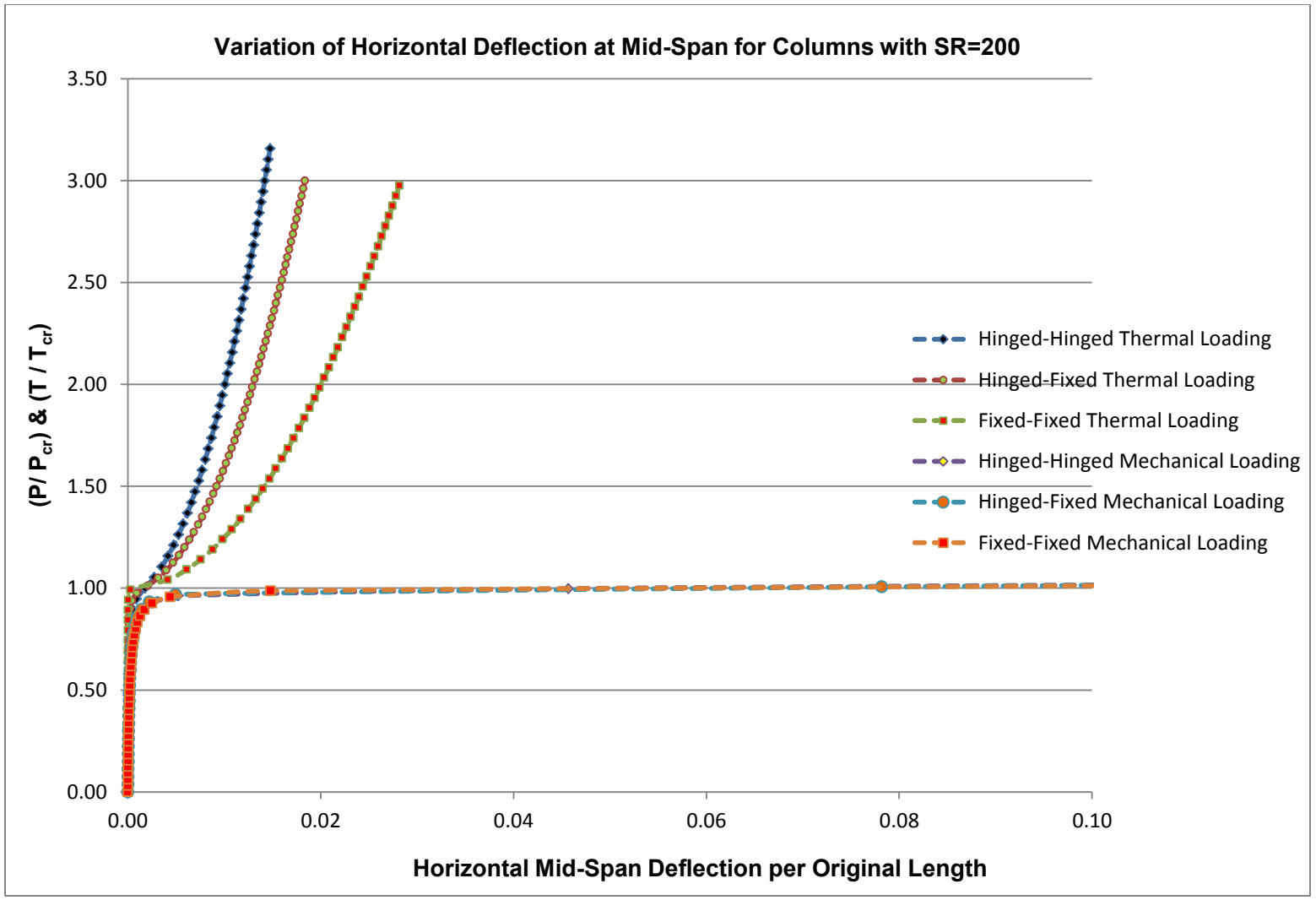

Figure 6-3: Comparison of Mid-Span Deflection per Original Length for 3 Columns for a Given Slenderness Ratio of 200

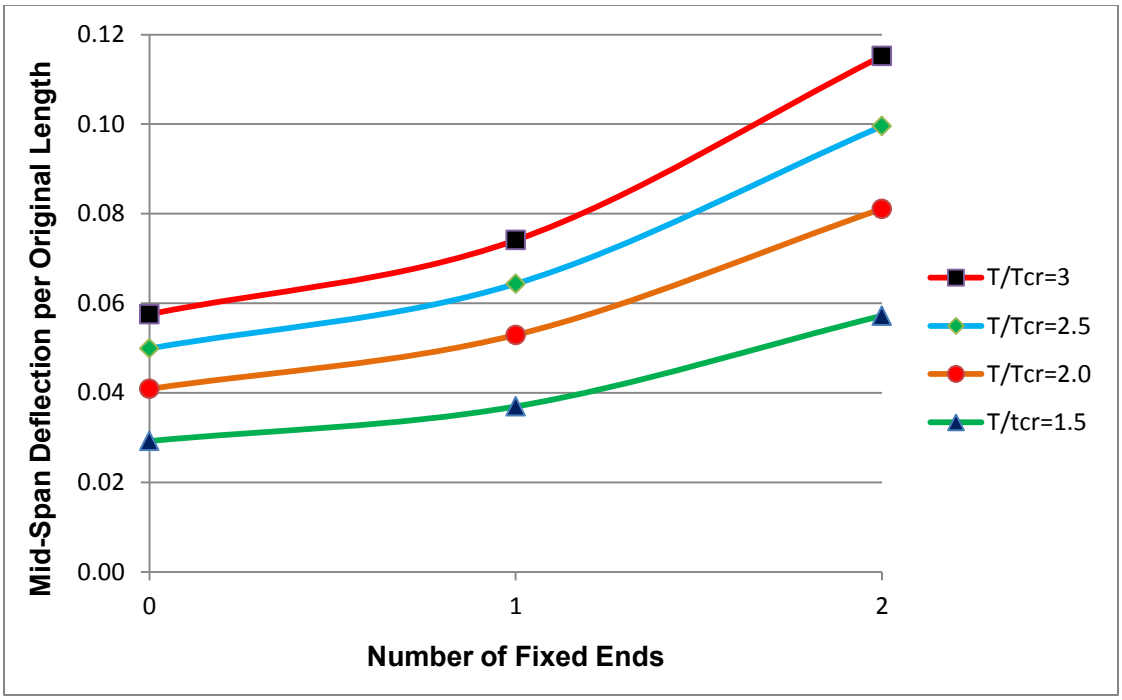

Figure 6-4:Mid-Span Deflection at Various Temperature Ratios for SR=50

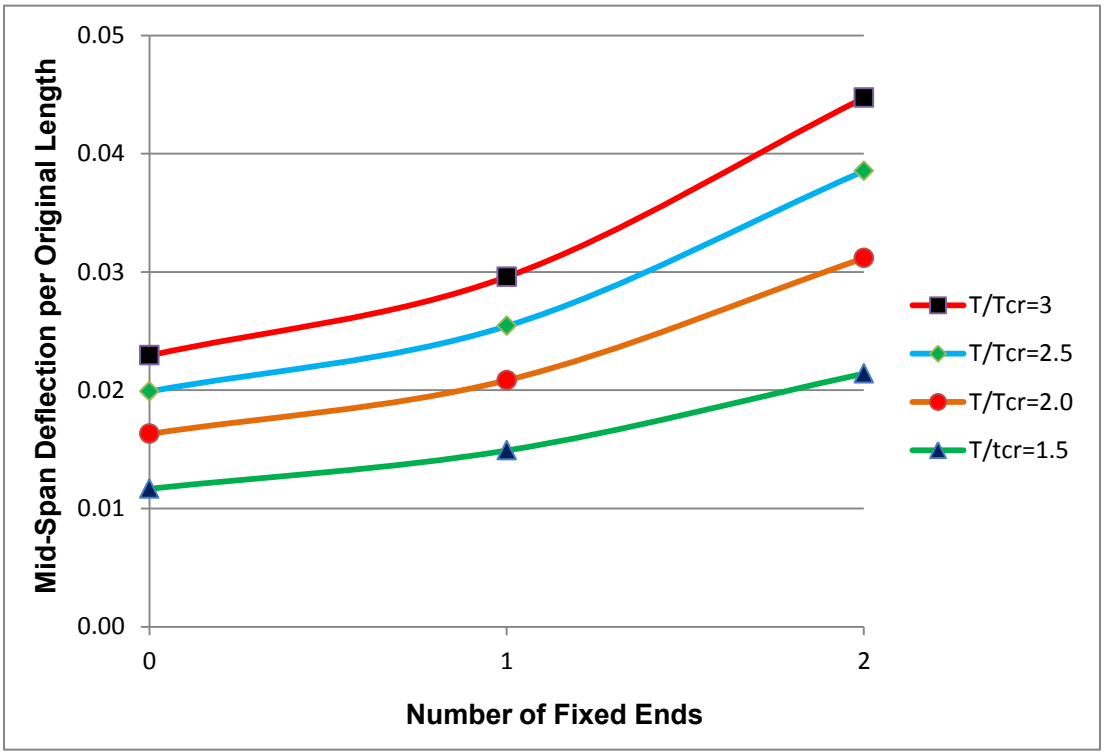

Figure 6-5: Mid-Span Deflection at Various Temperature Ratios for SR=125

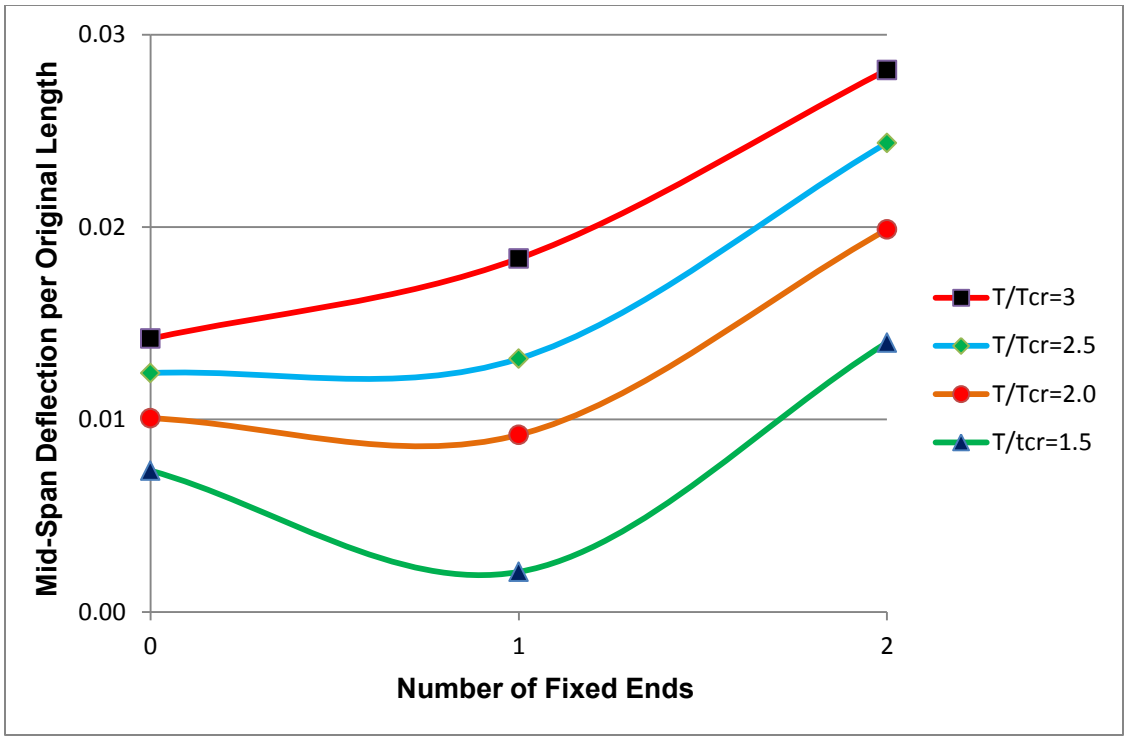

Figure 6-6:Mid-Span Deflection at Various Temperature Ratios for SR=200

Table 6-1:Mid-Span Deflection at Various Temperature Ratios for SR=50

T/T_{cr}	Rotational Restraints			% Difference w.r.to Fixed-Fixed Case	
	Hinged-Hinged	Fixed-Hinged	Fixed-Fixed	Hinged-Hinged	Fixed -Hinged
1.5	0.02923118274082	0.03695855153912	0.05721380776898	48.91	35.40
2	0.04087769192731	0.05293557370784	0.08108920702875	49.59	34.72
2.5	0.04990542965402	0.06435460438965	0.09953300171938	49.86	35.34
3	0.05755167648720	0.07409639593932	0.11518478710471	50.04	35.67

Table 6-2:Mid-Span Deflection at Various Temperature Ratios for SR=125

T/T_{cr}	Rotational Restraints			% Difference w.r.to Fixed-Fixed Case	
	Hinged-Hinged	Fixed-Hinged	Fixed-Fixed	Hinged-Hinged	Fixed -Hinged
1.5	0.01166579551703	0.01490259756243	0.02140197132916	45.49	30.37
2	0.01630587256363	0.02083892828034	0.03116305146128	47.68	33.13
2.5	0.01989750340624	0.02542218244471	0.03853525867385	48.37	34.03
3	0.02293521512308	0.02958315166119	0.04471613898813	48.71	33.84

Table 6-3:Mid-Span Deflection at Various Temperature Ratios for SR=200

T/T_{cr}	Rotational Restraints			% Difference w.r.to Fixed-Fixed Case	
	Hinged-Hinged	Fixed-Hinged	Fixed-Fixed	Hinged-Hinged	Fixed -Hinged
1.5	0.00734446435450	0.00208438953847	0.01399694930610	47.53	85.11
2	0.01006770787999	0.00920603367933	0.01987126828504	49.34	53.67
2.5	0.01241491560943	0.01316022679516	0.02437088664847	49.06	46.00
3	0.01420019037461	0.01836780601357	0.02816250937437	49.58	34.78

CHAPTER 7

SUMMARY & CONCLUSIONS

The objective of this study was to numerically investigate the effects of slenderness ratios and end rotational restraints on the post-buckling behavior of non-sway columns.

The columns were assumed to be straight, prismatic, and composed of linearly elastic material. The temperature distribution was assumed to be uniform along the column's length, but might have a small linear gradient across its cross-sectional depth. This small temperature gradient served as an imperfection that caused the column to buckle laterally. The effects of material nonlinearity (e.g. yielding) and degradation of material properties due to rising temperatures were not considered in this study.

To study the effect of end restraints, numerical solutions were generated for three different support conditions, namely, hinged-hinged, fixed-hinged and fixed-fixed. Furthermore, for each of these support conditions, the effects of slenderness ratios on the post-buckling response were analyzed by considering the slenderness ratios of 50,125 and 200.

The first important conclusion that can be made from this study is about the number of elements required in analysis of the given column case. For all three columns with varying slenderness ratios of 50,125 and 200;it was found that in contrast to other finite element analysis methods, the beam column analysis requires a very minimum number of elements .In present study, analysis were carried out for 2 and 10 elements

and it was concluded that the minimum of 2 elements were more than sufficient to get the results within the permissible tolerance limit.

Based on the numerical data presented in this thesis, the following additional conclusions can be made.

- The unrestrained columns under mechanical loads do not exhibit any significant post-buckling strength.
- Restrained Columns subjected to thermal loading undergo significantly smaller deformations in contrast to unrestrained columns, where deformations are relatively larger as the loads are increased only slightly above their critical levels.
- The mechanical post-buckling response does not seem to depend on the slenderness ratios of the columns ;whereas the thermal post-buckling response depends on the slenderness ratios of the columns with the relative deformation decreasing with slenderness ratio at a given temperature ratio.
- Post buckling behavior of columns subjected to mechanical loadings does not seem to change when the rotational restraints are added whereas in case of columns subjected to thermal loading, the post-buckling response depends on the rotational restraints at the ends of the column.
    - For a constant slenderness ratio, the deflection ratio was found out to be the smallest for the hinged-hinged column and largest for the fixed-fixed column subjected to thermal loads at a given temperature ratio.

REFERENCES

AISC, A. (2005). "360-Specification for Structural Steel Buildings; American Institute of Steel Construction." Inc.

Boley, B. A., and Weiner, J. H. (2012). *Theory of thermal stresses*, Courier Dover Publications.

Chajes, A. (1974). *Principles of structural stability theory*, Prentice-Hall Englewood Cliffs, NJ.

Coffin, D. W., and Bloom, F. (1999). "Elastica solution for the hygrothermal buckling of a beam." *International Journal of Non-Linear Mechanics*, 34(5), 935-947.

Kassimali, A., and Garcilazo, J. J. (2010). "Geometrically nonlinear analysis of plane frames subjected to temperature changes." *Journal of structural engineering*, 136(11), 1342-1349.

Li, S., Zhou, Y.-H., and Zheng, X. (2002). "Thermal post-buckling of a heated elastic rod with pinned-fixed ends." *Journal of Thermal Stresses*, 25(1), 45-56.

Rao, G. V., and Raju, K. K. (2002). "Thermal postbuckling of uniform columns: a simple intuitive method." *AIAA journal*, 40(10), 2138-2140.

Shirong, L., and Changjun, C. (2000). "Analysis of thermal post-buckling of heated elastic rods." *Applied Mathematics and Mechanics*, 21(2), 133-140.

Silwal, Baikuntha, "An Investigation of the Beam-Column and the Finite-Element Formulations for Analyzing Geometrically Nonlinear Thermal Response of Plane Frames" (2013). Theses.Paper 1160.

Timoshenko, S. P., Gere, J. M. (1961). "Theory of elastic stability." 2nd ed., McGraw-Hill, New York

APPENDICES

APPENDIX A

Program Sample 1:

This Program is used for calculating the Member End Moments(M1 & M2 at the beginning and end of the members respectively) and Axial Force(Q) for a given set of following data:-
•Member End Rotations for the beginning and end members denoted as θ1 and θ2 respectively.
•Lateral Shift for the end member denoted as u .
•Material Properties such as E,I,Land A. — **Written By:BIKASH KHANAL**
•Temperature Increase for the top and bottom fibres.

INPUT DATA:-	
► Please Enter the value of **θ1 in radians**:	**0.06743**
► Please Enter the value of **θ2 in radians**:	**0.171748**
► Please Enter the value of **u in inches**:	**0.675139**
► Please Enter the value of **E(Modulus of Elasticity) in ksi** :	**30000**
► Please Enter the value of **I(Moment of Inertia)in in^4**:	**310.1**
► Please Enter the value of **A(Area) in in^2**:	**11.77**
► Please Enter the value of **L(Length of the Beam) in inches**:	**102.6**
► Please Enter the value of **d(Depth of the Beam) in inches**:	**4**
► Please Enter the value of **T_b(Temperature Increase in Bottom Fibre) in degree Celsius**:	**0**
► Please Enter the value of **T_t(Temperature Increase in Top Fibre) in degree Celsius:**	**0**
► Please Enter the value of **α(Coefficient of Thermal Expansivity) in per degree celsius:**	**0**
► Please enter the **tolerance limit(Ɛs)of your calculations:**	**0.001**

S.No.	q	J(q)	J'(q)	$\Delta q = -\frac{J(q)}{J'(q)}$	Tolerance of Δq	$\phi = \frac{}{\pi\sqrt{q}}$	$\psi = \frac{}{\pi\sqrt{q}}$	c_1	c_2	b_1	b_2	b'_1	b'_2	c'_1	c'_2	c_b	c'_b
1	0	-0.00470	0.02503	0.18766	CONTINUE ITERATION	N.A	N.A	4.00000	2.00000	0.02500	0.04167	0.00352	0.01369	-1.31461	0.32865	0.00188	0.00035
2	0.18766	0.00000	0.02506	-0.00013	STOP ITERATION	1.36025	N.A	3.74707	2.06540	0.02568	0.04442	0.00375	0.01569	-1.38230	0.36945	0.00195	0.00039
3	0.18754	0.00000	0.02506	0.00000	STOP ITERATION	1.35980	N.A	3.74725	2.06536	0.02568	0.04442	0.00375	0.01568	-1.38225	0.36942	0.00195	0.00039
4	0.18754	0.00000	0.02506	0.00000	STOP ITERATION	1.35980	N.A	3.74725	2.06536	0.02568	0.04442	0.00375	0.01568	-1.38225	0.36942	0.00195	0.00039
5	0.18754	0.00000	0.02506	0.00000	STOP ITERATION	1.35980	N.A	3.74725	2.06536	0.02568	0.04442	0.00375	0.01568	-1.38225	0.36942	0.00195	0.00039
108	0.18754	0.00000	0.02506	0.00000	STOP ITERATION	1.35980	N.A	3.74725	2.06536	0.02568	0.04442	0.00375	0.01568	-1.38225	0.36942	0.00195	0.00039
109	0.18754	0.00000	0.02506	0.00000	STOP ITERATION	1.35980	N.A	3.74725	2.06536	0.02568	0.04442	0.00375	0.01568	-1.38225	0.36942	0.00195	0.00039
110	0.18754	0.00000	0.02506	0.00000	STOP ITERATION	1.35980	N.A	3.74725	2.06536	0.02568	0.04442	0.00375	0.01568	-1.38225	0.36942	0.00195	0.00039
111	0.18754	0.00000	0.02506	0.00000	STOP ITERATION	1.35980	N.A	3.74725	2.06536	0.02568	0.04442	0.00375	0.01568	-1.38225	0.36942	0.00195	0.00039
112	0.18754	0.00000	0.02506	0.00000	STOP ITERATION	1.35980	N.A	3.74725	2.06536	0.02568	0.04442	0.00375	0.01568	-1.38225	0.36942	0.00195	0.00039

Slenderness Ratio Calculation:

$$J(q) = \frac{\pi^2}{\lambda^2} q + c_b \frac{u}{L} - \alpha \frac{(Tb - Tt)}{2}$$

$$\lambda = \frac{L}{\sqrt{I/A}} = \quad 19.98870732$$

OUTPUT DATA:-

Final Constant Values for the value of q=	0.187537327

b_1=	0.02568	c_1=	3.7472465	b'_1=	0.00374834	c'_1=	-1.382253136	c_b=	0.00195247
b_2=	0.04442	c_2=	2.0653558	b'_2=	0.0156837	c'_2=	0.369422	c'_b=	0.00038510

FINAL VALUES OF MOMENTS AND AXIAL FORCE:-

$M_1 = \frac{EI}{L}(c_1\Theta_1+c_2\Theta_2)+EI\alpha\left(\frac{Tb-Tt}{d}\right)=$	55,074.26	Kips Inches=	4,589.52	Kips Feet
$M_2 = \frac{EI}{L}(c_2\Theta_1+c_1\Theta_2)-EI\alpha\left(\frac{Tb-Tt}{d}\right)=$	70,982.89	Kips Inches=	5,915.24	Kips Feet
$Q = EA\left[\frac{u}{L} - Cb + \alpha\left(\frac{Tb-Tt}{2}\right)\right] =$	1634.0875	Kips		

Program Sample 2:

Given:-	**ø1=0.06743 radians**		**ø2=0.171748 radians**	
	u=0.675139 inches			
	E=30,000ksi		**I=310.1 in^4**	
	A=11.77in^2		**L=102.6 inches**	
	Tolerance Limit=0.001		ε_s =	0.001
	Temperature Difference is assumed to be none			
Calculate:-	**M1,M2 and Q**			
Solution:-				
For q=0(Initial Case),				
c1=4	c2=2	b1=1/40	b2=1/24	
b1'=π^2/2800				
b2'=π^2/720				
$c_{b=b1(ø1+ø2)^2+b2(ø1-ø2)^2}$		=	0.001884	
$c'_{b=b'1(ø1+ø2)^2+b'2(ø1-ø2)^2}$		=	0.000350	
For q=0.187664(2nd Iteration)				

$c1=4-\frac{2}{15}\pi^2 q-\frac{11}{6300}\pi^4 q^2-\frac{1}{27000}\pi^6 q^3=$ 3.747082

$c2=2+\frac{1}{30}\pi^2 q+\frac{13}{12600}\pi^4 q^2+\frac{11}{378000}\pi^6 q^3=$ 2.065393

$b1=\frac{1}{40}+\frac{1}{2800}\pi^2 q+\frac{1}{168000}\pi^4 q^2+\frac{37}{388080000}\pi^6 q^3=$ 0.0256818

$b2=\frac{1}{24}+\frac{1}{720}\pi^2 q+\frac{1}{20160}\pi^4 q^2+\frac{1}{604800}\pi^6 q^3=$ 0.0443232

$b'1=\frac{1}{2800}\pi^2+\frac{1}{84000}\pi^4 q+\frac{37}{129360000}\pi^6 q^2=$ 0.00374812

$b'2=\frac{1}{720}\pi^2+\frac{1}{10080}\pi^4 q+\frac{1}{201600}\pi^6 q^2=$ 0.015671158

$c_{b=b1(ø1+ø2)^2+b2(ø1-ø2)^2}$ = 0.00195

$c'_{b=b'1(ø1+ø2)^2+b'2(ø1-ø2)^2}$ = 0.00038

FINAL CONSTANTS(for q=0.187578)

$c1=4-\frac{2}{15}\pi^2 q-\frac{11}{6300}\pi^4 q^2-\frac{1}{27000}\pi^6 q^3=$ 3.747201

$c2=2+\frac{1}{30}\pi^2 q+\frac{13}{12600}\pi^4 q^2+\frac{11}{378000}\pi^6 q^3=$ 2.065361

$b1=\frac{1}{40}+\frac{1}{2800}\pi^2 q+\frac{1}{168000}\pi^4 q^2+\frac{37}{388080000}\pi^6 q^3=$ 0.025681

$b2=\frac{1}{24}+\frac{1}{720}\pi^2 q+\frac{1}{20160}\pi^4 q^2+\frac{1}{604800}\pi^6 q^3=$ 0.044322

$c_{b=b1(ø1+ø2)^2+b2(ø1-ø2)^2}$ = 0.0019515

No.of iterations	q	J(q)	J'(q)	Δq=-J(q)/J'(q)	New q=q+Δq
1	0	-0.004697	0.025027	0.187664	0.18766383
2	0.18766	0.000002	0.025062	-0.000086	Stop
3	0.187578				

$J(q)=\frac{\pi^2}{\lambda^2}q+c_b\frac{u}{L}\cdot\alpha\frac{(Tb-Tt)}{2}$ $\quad J'(q)=\frac{\pi^2}{\lambda^2}+c'_b$

$\lambda=\frac{L}{\sqrt{I/A}}=\frac{102.60}{\sqrt{310.1/11.77}}=$ 19.988707

FINAL VALUES

$M1=\frac{EI}{L}(c1ø1+c2ø2)\frac{30000*310.1}{102.6}*((3.747201*0.06743)+(2.065361*0.171748))=$ 55074.1 K

$M2=\frac{EI}{L}(c2ø1+c1ø2)\frac{30000*310.1}{102.6}*((2.065361*0.06743)+(3.747201*0.171748))=$ 70982.2 K

$Q=EA(\frac{u}{L}-cb)=30000*11.77*(\frac{0.675139}{102.6}-0.0019515)=$ 1634.44 Kips

APPENDIX B: Numerical Data for Hinged-Hinged Columns

Table B- 1: Numerical Results for Hinged-Hinged Column Subjected to 160℃ with 60 Load-Steps and Eccentricity (e=0.001& convergence tolerance=0.001) for 2 & 10 Elements for Slenderness Ratio of 125

Temperature Increment (T)	Horizontal Deflection at Mid-span due to Temperature Increment for 2 Elements	Horizontal Deflection at Mid-span due to Temperature Increment for 10 Elements	Rotation at Top Hinged Joint due to Temperature Increment for 2 Elements	Rotation at Top Hinged Joint due to Temperature Increment for 10 Elements	Ratio of T/T_{cr}
0	0.00000000000000	0.00000000000000	0.00000000000000	0.00000000000000	0.00000000000000
2.666666667	0.05030006830024	0.04768472906661	0.00001810009053	0.00001733990148	0.05061983471074
5.333333333	0.10642216900018	0.10642216900156	0.00003788972674	0.00003788972674	0.10123966942149
8	0.16941225527972	0.16941225527943	0.00005966805499	0.00005966805499	0.15185950413223
10.66666667	0.24058198262118	0.24058198261270	0.00008381011542	0.00008381011542	0.20247933884298
13.33333333	0.32159875438505	0.32159875432242	0.00011079255915	0.00011079255913	0.25309917355372
16	0.41461503482299	0.41461503456632	0.00014123058011	0.00014123058003	0.30371900826446
18.66666667	0.52245846237017	0.52245846151437	0.00017593221141	0.00017593221116	0.35433884297521
21.33333333	0.64891892658265	0.64891892407799	0.00021598031430	0.00021598031358	0.40495867768595
24	0.79919561123135	0.79919560444659	0.00026286025313	0.00026286025119	0.45557851239669
26.66666667	0.98061850936884	0.98061849178555	0.00031866595887	0.00031866595385	0.50619834710744
29.33333333	1.20386307164242	1.20386302696517	0.00038644683020	0.00038644681744	0.55681818181818
32	1.48510071983989	1.48510060602601	0.00047082191501	0.00047082188251	0.60743801652893
34.66666667	1.85004704190341	1.85004674437450	0.00057913606351	0.00057913597856	0.65805785123967
37.33333333	2.34218546951621	2.34218464897066	0.00072380858345	0.00072380834922	0.70867768595041
40	3.04117583370159	3.04117335406057	0.00092759065143	0.00092758994371	0.75929752066116
42.66666667	4.10964638050749	4.10963767471986	0.00123692888646	0.00123692640188	0.80991735537190
45.33333333	5.93410739010823	5.93406811438806	0.00176220938657	0.00176219817729	0.86053719008265
48	9.64693061952886	9.64665839780493	0.00282683009507	0.00282675239403	0.91115702479339
50.66666667	18.89109377408960	18.88811276127990	0.00547117350175	0.00547032257528	0.96177685950413
53.33333333	35.43273846677640	35.41908025571440	0.01019945954211	0.01019556219755	1.01239669421488

Temperature Increment (T)	Horizontal Deflection at Mid-span due to Temperature Increment for 2 Elements	Horizontal Deflection at Mid-span due to Temperature Increment for 10 Elements	Rotation at Top Hinged Joint due to Temperature Increment for 2 Elements	Rotation at Top Hinged Joint due to Temperature Increment for 10 Elements	Ratio of T/T_{cr}
56	50.93642111519450	50.91248131546310	0.01463104939318	0.01462422277865	1.06301652892562
58.66666667	63.74470553043790	63.71280571216780	0.01829267440849	0.01828358487572	1.11363636363636
61.33333333	74.68671094994120	74.64819420306640	0.02142117586225	0.02141020946946	1.16425619834711
64	84.34410706734330	84.29980102956340	0.02418270003160	0.02417009533492	1.21487603305785
66.66666667	93.06581492918420	93.01627213665210	0.02667691141675	0.02666282811300	1.26549586776859
69.33333333	101.07200469288200	101.01762538671900	0.02896669914660	0.02895125324616	1.31611570247934
72	108.51008562212200	108.45117450792500	0.03109416955650	0.03107744964344	1.36673553719008
74.66666667	115.48380270692500	115.42060016485600	0.03308895705078	0.03307103322708	1.41735537190083
77.33333333	122.06917431798900	122.00187515584400	0.03497277636378	0.03495370562609	1.46797520661157
80	128.32375068734700	128.25251613030200	0.03676206705792	0.03674189673687	1.51859504132231
82.66666667	134.29242438159800	134.21724784096600	0.03846965305845	0.03844838260470	1.56921487603306
85.33333333	140.01043245762400	139.93182938676200	0.04010560065082	0.04008338131381	1.61983471074380
88	145.50681583584100	145.42462186894400	0.04167820582821	0.04165498824662	1.67045454545455
90.66666667	150.80529465827000	150.71959840442000	0.04319424486556	0.04317005554680	1.72107438016529
93.33333333	155.92566543497600	155.83654475350300	0.04465937325281	0.04463423556717	1.77169421487603
96	160.88464910363900	160.79217247356600	0.04607836793372	0.04605230251325	1.82231404958678
98.66666667	165.69651785127700	165.60074595828800	0.04745530635204	0.04742833155479	1.87293388429752
101.3333333	170.37356735376700	170.27455431486400	0.04879370134354	0.04876583361119	1.92355371900827
104	174.92647844576200	174.82427277471700	0.05009660444537	0.05006785858474	1.97417355371901
106.6666667	179.36459819995100	179.25924358242600	0.05136668618557	0.05133707559446	2.02479338842975
109.3333333	183.69616126683700	183.58769719220800	0.05260629930869	0.05257583615977	2.07541322314050
112	187.92846625346200	187.81692853653700	0.05381752915862	0.05378622455123	2.12603305785124
114.6666667	192.06801779481000	191.95343901142600	0.05500223426188	0.05497009834868	2.17665289256199
117.3333333	196.12064211802900	196.00305197224300	0.05616207933916	0.05612912143290	2.22727272727273

Temperature Increment (T)	Horizontal Deflection at Mid-span due to Temperature Increment for 2 Elements	Horizontal Deflection at Mid-span due to Temperature Increment for 10 Elements	Rotation at Top Hinged Joint due to Temperature Increment for 2 Elements	Rotation at Top Hinged Joint due to Temperature Increment for 10 Elements	Ratio of T/T_{cr}
120	200.09158189102100	199.97100752738200	0.05729856239961	0.05726479106392	2.27789256198347
122.6666667	203.98557471142900	203.86204098241100	0.05841303716202	0.05837846028916	2.32851239669422
125.3333333	207.80691855122600	207.68044824789000	0.05950673174991	0.05947135662781	2.37913223140496
128	211.55952670765200	211.43014075984700	0.06058076438901	0.06054459775952	2.42975206611570
130.6666667	215.24697424302900	215.11469189408800	0.06163615667365	0.06159920478333	2.48037190082645
133.3333333	218.87253746858700	218.73737642846000	0.06267384484602	0.06263611349069	2.53099173553719
136	222.43922770270400	222.30120428300800	0.06369468943995	0.06365618400402	2.58161157024794
138.6666667	225.94982028548000	225.80894951897600	0.06469948356961	0.06466020906083	2.63223140495868
141.3333333	229.40687963854000	229.26317538523800	0.06568896008849	0.06564892116887	2.68285123966942
144	232.81278100863300	232.66625605052200	0.06666379780106	0.06662299881448	2.73347107438017
146.6666667	236.16972941551100	236.02039554124000	0.06762462687583	0.06758307187270	2.78409090909091
149.3333333	239.47977623066900	239.32764431168100	0.06857203358157	0.06852972634106	2.83471074380165
152	242.74483373891200	242.58991379789700	0.06950656444737	0.06946350849738	2.88533057851240
154.6666667	245.96668797432100	245.80898924714900	0.07042872992971	0.07038492856492	2.93595041322314
157.3333333	249.14701007411300	248.98654106585100	0.07133900765608	0.07129446395435	2.98657024793388
160	252.28736635391100	252.12413488972400	0.07223784530349	0.07219256214071	3.03719008264463

Table B- 2: Properties of Hinged-Hinged Column Used for Validation of Results

L	=	1760.39	mm
A	=	5860	mm^2
I	=	4.54×10^7	mm^4
E	=	210	KN/mm^2
α	=	1.20×10^{-5}	/℃
T_{cr}	=	6030.8333	℃
P_{cr}	=	89058.5	KN

Table B- 3: Numerical Results for Hinged-Hinged Column Subjected to 1000℃ and 7500 KN with 60 Load-Steps and Eccentricity (e=0.001& convergence tolerance=0.001) for Slenderness Ratio of 50. (Data for Horizontal Mid-Span Deflections)

Temperature Increment (T)	Mechanical Load Increment (P)	Horizontal Deflection at Mid-Span due to Temperature Increment	Horizontal Deflection at Mid-Span due to Temperature Increment per Original Length	Horizontal Deflection at Mid-Span due to Mechanical Load Increment	Horizontal Deflection at Mid-Span due to Mechanical Load Increment per Original Length	Ratio of P/P_{cr}	Ratio of T/T_{cr}
0	0	0.00000000000000	0.00000000000000	0.00000000000000	0.00000000000000	0.00000000000000	0.00000000000000
16.66666667	125	0.05030006830816	0.00001143183371	0.02386886902167	0.00000542474296	0.02569750367107	0.05059735682819
33.33333333	250	0.10642216908635	0.00002418685661	0.04900517354300	0.00001113753944	0.05139500734214	0.10119471365639
50	375	0.16941225566343	0.00003850278538	0.07551438096382	0.00001716235931	0.07709251101322	0.15179207048458
66.66666667	500	0.24058198384702	0.00005467772360	0.10351400775629	0.00002352591085	0.10279001468429	0.20238942731278
83.33333333	625	0.32159875764565	0.00007309062674	0.13313539098168	0.00003025804340	0.12848751835536	0.25298678414097
100	750	0.41461504263166	0.00009423069151	0.16452578175759	0.00003739222313	0.15418502202643	0.30358414096916
116.6666667	875	0.52245847988985	0.00011874056361	0.19785083116098	0.00004496609799	0.17988252569750	0.35418149779736
133.3333333	1000	0.64891896440076	0.00014748158282	0.23329755714770	0.00005302217208	0.20558002936858	0.40477885462555
150	1125	0.79919569128121	0.00018163538438	0.27107790468167	0.00006160861470	0.23127753303965	0.45537621145375
166.6666667	1250	0.98061867815740	0.00022286788140	0.31143304224402	0.00007078023687	0.25697503671072	0.50597356828194
183.3333333	1375	1.20386343142293	0.00027360532532	0.35463857873398	0.00008059967698	0.28267254038179	0.55657092511013
200	1500	1.48510150724163	0.00033752306983	0.40101093933485	0.00009113884985	0.30837004405286	0.60716828193833
216.6666667	1625	1.85004884419731	0.00042046564641	0.45091521225320	0.00010248073006	0.33406754772394	0.65776563876652
233.3333333	1750	2.34218989027629	0.00053231588415	0.50477487804967	0.00011472156319	0.35976505139501	0.70836299559471
250	1875	3.04118787250772	0.00069117906193	0.56308397045336	0.00012797362965	0.38546255506608	0.75896035242291
266.6666667	2000	4.10968490278369	0.00093401929609	0.62642240840846	0.00014236872918	0.41116005873715	0.80955770925110
283.3333333	2125	5.93426742769740	0.00134869714266	0.69547550799237	0.00015806261545	0.43685756240822	0.86015506607930
300	2250	9.64796278586501	0.00219271881497	0.77105906694332	0.00017524069703	0.46255506607930	0.91075242290749
316.6666667	2375	18.90181370406300	0.00429586675092	0.85415197137909	0.00019412544804	0.48825256975037	0.96134977973568

Temperature Increment (T)	Mechanical Load Increment (P)	Horizontal Deflection at Mid-Span due to Temperature Increment	Horizontal Deflection at Mid-Span due to Temperature Increment per Original Length	Horizontal Deflection at Mid-Span due to Mechanical Load Increment	Horizontal Deflection at Mid-Span due to Mechanical Load Increment per Original Length	Ratio of P/P_{cr}	Ratio of T/T_{cr}
333.3333333	2500	35.48115100019710	0.00806389795459	0.94593909480939	0.00021498615791	0.51395007342144	1.01194713656388
350	2625	51.02195960078210	0.01159589990927	1.04786849349758	0.00023815193034	0.53964757709251	1.06254449339207
366.6666667	2750	63.86028785706950	0.01451370178570	1.16172876208811	0.00026402926411	0.56534508076358	1.11314185022026
383.3333333	2875	74.82849962787340	0.01700647718815	1.28975541424954	0.00029312623051	0.59104258443466	1.16373920704846
400	3000	84.50993315423140	0.01920680298960	1.43477975953904	0.00032608630899	0.61674008810573	1.21433656387665
416.6666667	3125	93.25434340489310	0.02119416895566	1.60044156179136	0.00036373671859	0.64243759177680	1.26493392070485
433.3333333	3250	101.28236654434800	0.02301871966917	1.79149977946804	0.00040715904079	0.66813509544787	1.31553127753304
450	3375	108.74169694202800	0.02471402203228	2.01429856444899	0.00045779512828	0.69383259911894	1.36612863436123
466.6666667	3500	115.73626619208600	0.02630369686184	2.27748724116165	0.00051761073663	0.71953010279002	1.41672599118943
483.3333333	3625	122.34222115526500	0.02780505026256	2.59317189440165	0.00058935724873	0.74522760646109	1.46732334801762
500	3750	128.61720405960800	0.02923118274082	2.97883392600761	0.00067700771046	0.77092511013216	1.51792070484582
516.6666667	3875	134.60617455327300	0.03059231239847	3.46068591083422	0.00078651952519	0.79662261380323	1.56851806167401
533.3333333	4000	140.34442286553400	0.03189645974217	4.07990013128282	0.00092725002984	0.82232011747430	1.61911541850220
550	4125	145.86102865804700	0.03315023378592	4.90505586660322	0.00111478542423	0.84801762114537	1.66971277533040
566.6666667	4250	151.17974321337200	0.03435903254849	6.05949418952630	0.00137715777035	0.87371512481645	1.72031013215859
583.3333333	4375	156.32038782745600	0.03552736086988	7.78959857788738	0.00177036331316	0.89941262848752	1.77090748898678
600	4500	161.29970338993100	0.03665902349771	10.66911773179790	0.00242479948450	0.92511013215859	1.82150484581498
616.6666667	4625	166.13197830418600	0.03775726779641	16.41229865822020	0.00373006787687	0.95080763582966	1.87210220264317
633.3333333	4750	170.82952153285300	0.03882489125747	33.46503684254860	0.00760569019149	0.97650513950073	1.92269955947137
650	4875	175.40302487042800	0.03986432383419	230.52819944758200	0.05239277260172	1.00220264317181	1.97329691629956
666.6666667	5000	179.86184448017700	0.04087769192731	610.14423604781500	0.13866914455632	1.02790014684288	2.02389427312775
683.3333333	5125	184.21422258643300	0.04186686876964	825.41578046889200	0.18759449556111	1.05359765051395	2.07449162995595
700	5250	188.46746412824700	0.04283351457460	978.57713147459800	0.22240389351695	1.07929515418502	2.12508898678414
716.6666667	5375	192.62807904774400	0.04377910887449	1096.95616933717000	0.24930822030390	1.10499265785609	2.17568634361233

Temperature Increment (T)	Mechanical Load Increment (P)	Horizontal Deflection at Mid-Span due to Temperature Increment	Horizontal Deflection at Mid-Span due to Temperature Increment per Original Length	Horizontal Deflection at Mid-Span due to Mechanical Load Increment	Horizontal Deflection at Mid-Span due to Mechanical Load Increment per Original Length	Ratio of P/P_{cr}	Ratio of T/T_{cr}
733.3333333	5500	196.70189802729500	0.04470497682439	1192.29729345446000	0.27097665760329	1.13069016152717	2.22628370044053
750	5625	200.69416747721000	0.04561231079028	1270.99556572172000	0.28886262857312	1.15638766519824	2.27688105726872
766.6666667	5750	204.60962813762000	0.04650218821310	1337.01603060232000	0.30386727968235	1.18208516886931	2.32747841409692
783.3333333	5875	208.45258061536900	0.04737558650349	1393.03269447815000	0.31659833965413	1.20778267254038	2.37807577092511
800	6000	212.22694041104400	0.04823339554796	1440.95035630999000	0.32748871734318	1.23348017621145	2.42867312775330
816.6666667	6125	215.93628442179400	0.04907642827768	1482.19030400369000	0.33686143272811	1.25917767988253	2.47927048458150
833.3333333	6250	219.58389047767400	0.04990542965402	1517.84153583958000	0.34496398541809	1.28487518355360	2.52986784140969
850	6375	223.17277114407500	0.05072108435093	1548.76083956005000	0.35199109990001	1.31057268722467	2.58046519823788
866.6666667	6500	226.70570277346600	0.05152402335761	1575.63554060355000	0.35809898650081	1.33627019089574	2.63106255506608
883.3333333	6625	230.18525059663900	0.05231482968105	1599.02586147613000	0.36341496851730	1.36196769456681	2.68165991189427
900	6750	233.61379049315700	0.05309404329390	1619.41407572522000	0.36804865357391	1.38766519823789	2.73225726872247
916.6666667	6875	236.99352796213500	0.05386216544594	1637.14196436267000	0.37207771917333	1.41336270190896	2.78285462555066
933.3333333	7000	240.32651472065300	0.05461966243651	1652.56171065645000	0.37558220696738	1.43906020558003	2.83345198237885
950	7125	243.61466328216700	0.05536696892777	1665.95039014452000	0.37862508866921	1.46475770925110	2.88404933920705
966.6666667	7250	246.85975980718600	0.05610449086527	1677.54471557198000	0.38126016263000	1.49045521292217	2.93464669603524
983.3333333	7375	250.06347546973700	0.05683260806130	1687.54873049682000	0.38353380238564	1.51615271659325	2.98524405286343
1000	7500	253.22737654369400	0.05755167648720	1696.13928913522000	0.38548620207619	1.54185022026432	3.03584140969163

Table B- 4: Numerical Results for Hinged-Hinged Column Subjected to 1000℃ and 7500 KN with 60 Load-Steps and Eccentricity (e=0.001& convergence tolerance=0.001) for Slenderness Ratio of 50 (Data for Rotation at Top Hinged Joint)

Temperature Increment (T)	Mechanical Load Increment (P)	Rotation at Top Hinged Joint due to Temperature Increment	Rotation at Top Hinged Joint due to Mechanical Load Increment	Ratio of P/P_{cr}	Ratio of T/T_{cr}
0	0	0.00000000000000	0.00000000000000	0.00000000000000	0.00000000000000
16.66666667	125	0.00004525022633	0.00001629315320	0.02569750367107	0.05059735682819
33.33333333	250	0.00009472431686	0.00003349057052	0.05139500734214	0.10119471365639
50	375	0.00014917013753	0.00005166782858	0.07709251101322	0.15179207048458
66.66666667	500	0.00020952528884	0.00007090914223	0.10279001468429	0.20238942731278
83.33333333	625	0.00027698139879	0.00009130863464	0.12848751835536	0.25298678414097
100	750	0.00035307645281	0.00011297183821	0.15418502202643	0.30358414096916
116.6666667	875	0.00043983053494	0.00013601747690	0.17988252569750	0.35418149779736
133.3333333	1000	0.00053995080102	0.00016057959333	0.20558002936858	0.40477885462555
150	1125	0.00065715066796	0.00018681010126	0.23127753303965	0.45537621145375
166.6666667	1250	0.00079666497680	0.00021488186600	0.25697503671072	0.50597356828194
183.3333333	1375	0.00096611725634	0.00024499244471	0.28267254038179	0.55657092511013
200	1500	0.00117705520625	0.00027736865762	0.30837004405286	0.60716828193833
216.6666667	1625	0.00144784116679	0.00031227221379	0.33406754772394	0.65776563876652
233.3333333	1750	0.00180952404634	0.00035000668668	0.35976505139501	0.70836299559471
250	1875	0.00231898397280	0.00039092623289	0.38546255506608	0.75896035242291
266.6666667	2000	0.00309234661649	0.00043544658465	0.41116005873715	0.80955770925110
283.3333333	2125	0.00440562833663	0.00048405903901	0.43685756240822	0.86015506607930
300	2250	0.00706777160785	0.00053734844244	0.46255506607930	0.91075242290749
316.6666667	2375	0.01368528094080	0.00059601656854	0.48825256975037	0.96134977973568
333.3333333	2500	0.02553118012464	0.00066091287481	0.51395007342144	1.01194713656388
350	2625	0.03663264199454	0.00073307550946	0.53964757709251	1.06254449339207
366.6666667	2750	0.04580233636996	0.00081378677226	0.56534508076358	1.11314185022026
383.3333333	2875	0.05363507233810	0.00090464938522	0.59104258443466	1.16373920704846
400	3000	0.06054763273012	0.00100769323135	0.61674008810573	1.21433656387665
416.6666667	3125	0.06678992031423	0.00112552782239	0.64243759177680	1.26493392070485
433.3333333	3250	0.07251959408069	0.00126156508755	0.66813509544787	1.31553127753304
450	3375	0.07784220137409	0.00142035347678	0.69383259911894	1.36612863436123
466.6666667	3500	0.08283202281454	0.00160809415871	0.71953010279002	1.41672599118943
483.3333333	3625	0.08754348690479	0.00183346666673	0.74522760646109	1.46732334801762
500	3750	0.09201779986938	0.00210900443584	0.77092511013216	1.51792070484582
516.6666667	3875	0.09628710484180	0.00245350083692	0.79662261380323	1.56851806167401
533.3333333	4000	0.10037663610626	0.00289647483679	0.82232011747430	1.61911541850220
550	4125	0.10430718803300	0.00348709534432	0.84801762114537	1.66971277533040

Temperature Increment (T)	Mechanical Load Increment (P)	Rotation at Top Hinged Joint due to Temperature Increment	Rotation at Top Hinged Joint due to Mechanical Load Increment	Ratio of P/P_{cr}	Ratio of T/T_{cr}
566.6666667	4250	0.10809574723457	0.00431379393339	0.87371512481645	1.72031013215859
583.3333333	4375	0.11175649129003	0.00555322088965	0.89941262848752	1.77090748898678
600	4500	0.11530139584978	0.00761674400639	0.92511013215859	1.82150484581498
616.6666667	4625	0.11874068336503	0.01173348682015	0.95080763582966	1.87210220264317
633.3333333	4750	0.12208316115537	0.02395991856618	0.97650513950073	1.92269955947137
650	4875	0.12533648032344	0.16574732703654	1.00220264317181	1.97329691629956
666.6666667	5000	0.12850733697774	0.44727688025911	1.02790014684288	2.02389427312775
683.3333333	5125	0.13160163069038	0.61753157475836	1.05359765051395	2.07449162995595
700	5250	0.13462459076891	0.74685257450518	1.07929515418502	2.12508898678414
716.6666667	5375	0.13758087796885	0.85360387890009	1.10499265785609	2.17568634361233
733.3333333	5500	0.14047466723057	0.94547718352608	1.13069016152717	2.22628370044053
750	5625	0.14330971558636	1.02656829772414	1.15638766519824	2.27688105726872
766.6666667	5750	0.14608941835602	1.09936857605723	1.18208516886931	2.32747841409692
783.3333333	5875	0.14881685600406	1.16553351572766	1.20778267254038	2.37807577092511
800	6000	0.15149483348460	1.22622725413111	1.23348017621145	2.42867312775330
816.6666667	6125	0.15412591349298	1.28231359836337	1.25917767988253	2.47927048458150
833.3333333	6250	0.15671244473752	1.33445040039224	1.28487518355360	2.52986784140969
850	6375	0.15925658611216	1.38315444862907	1.31057268722467	2.58046519823788
866.6666667	6500	0.16176032747291	1.42884080230100	1.33627019089574	2.63106255506608
883.3333333	6625	0.16422550758289	1.47184900355349	1.36196769456681	2.68165991189427
900	6750	0.16665382968302	1.51249494317406	1.38766519823789	2.73225726872247
916.6666667	6875	0.16904687506108	1.55094095068690	1.41336270190896	2.78285462555066
933.3333333	7000	0.17140611492458	1.58743165841662	1.43906020558003	2.83345198237885
950	7125	0.17373292082908	1.62214172803245	1.46475770925110	2.88404933920705
966.6666667	7250	0.17602857387124	1.65522146867254	1.49045521292217	2.93464669603524
983.3333333	7375	0.17829427282039	1.68680235639033	1.51615271659325	2.98524405286343
1000	7500	0.18053114133475	1.71700018838998	1.54185022026432	3.03584140969163

Table B- 5: Numerical Results for Hinged-Hinged Column Subjected to 6071℃ and 67234 KN with 60 Load-Steps and Eccentricity (e=0.001& convergence tolerance=0.001) for Slenderness Ratio of 20 (Data for Horizontal Mid-Span Deflections in Validation to Elastica Solution)

Temp. Increment (T)	Mechanical Load Increment (P)	Horizontal Deflection at Mid-Span due to Temperature Increment	Horizontal Deflection at Mid-Span due to Temperature Increment per Original Length	Horizontal Deflection at Mid-Span due to Mechanical Load Increment	Horizontal Deflection at Mid-Span due to Mechanical Load Increment per original length	Ratio of P/P_{cr}	Ratio of T/T_{cr}
0	0	0.00496734591098	0.00000282172892	0.01407135572685	0.00000799331316	0.00000000000000	0.00000000000000
102.891	1139.56069	0.01050210170694	0.00000596577824	0.02921262003995	0.00001659439395	0.03749999911855	0.04999992396694
205.782	2279.12138	0.01670479434965	0.00000948925286	0.04555620199697	0.00002587845806	0.07499999823710	0.09999984793388
308.673	3418.68206	0.02370111505753	0.00001346355239	0.06325732486923	0.00003593368097	0.11249999735565	0.14999977190083
411.564	4558.24275	0.03165031646368	0.00001797914118	0.08249916150507	0.00004686411504	0.14999999647421	0.19999969586777
514.455	5697.80344	0.04075721261686	0.00002315236502	0.10349942223815	0.00005879343186	0.18749999559276	0.24999961983471
617.346	6837.36413	0.05128972415618	0.00002913541774	0.12651889838002	0.00007186977541	0.22499999471131	0.29999954380165
720.237	7976.92481	0.06360520757122	0.00003613129771	0.15187267379727	0.00008627213086	0.26249999382986	0.34999946776860
823.128	9116.4855	0.07819116635441	0.00004441693405	0.17994503004972	0.00010221879151	0.29999999294841	0.39999939173554
926.019	10256.0462	0.09573042704781	0.00005438021023	0.21120954718128	0.00011997877720	0.33749999206696	0.44999931570248
1028.91	11395.6069	0.11720984120686	0.00006658171286	0.24625664344192	0.00013988747834	0.37499999118551	0.49999923966942
1131.801	12535.1676	0.14411067181202	0.00008186288175	0.28583197691293	0.00016236847023	0.41249999030407	0.54999916363636
1234.692	13674.7283	0.17876252690756	0.00010154706392	0.33089105871896	0.00018796453636	0.44999998942262	0.59999908760331
1337.583	14814.2889	0.22505212579328	0.00012784213223	0.38267866661908	0.00021738277978	0.48749998854117	0.64999901157025
1440.474	15953.8496	0.28998513668230	0.00016472769612	0.44284727479908	0.00025156189777	0.52499998765972	0.69999893553719
1543.365	17093.4103	0.38759933214312	0.00022017799164	0.51363885199484	0.00029177545337	0.56249998677827	0.74999885950413
1646.256	18232.971	0.55074035528369	0.00031285117204	0.59817347483194	0.00033979582373	0.59999998589682	0.79999878347108
1749.147	19372.5317	0.87838305140997	0.00049897045767	0.70092589792243	0.00039816491850	0.63749998501537	0.84999870743802
1852.038	20512.0924	1.86882814932438	0.00106159839432	0.82855029442844	0.00047066267837	0.67499998413392	0.89999863140496
1954.929	21651.6531	15.15841177274630	0.00861082149487	0.99139105369336	0.00056316529218	0.71249998325248	0.94999855537190

Temp. Increment (T)	Mechanical Load Increment (P)	Horizontal Deflection at Mid-Span due to Temperature Increment	Horizontal Deflection at Mid-Span due to Temperature Increment per Original Length	Horizontal Deflection at Mid-Span due to Mechanical Load Increment	Horizontal Deflection at Mid-Span due to Mechanical Load Increment per original length	Ratio of P/P_{cr}	Ratio of T/T_{cr}
2057.82	22791.2138	41.24432415527490	0.02342907148201	1.20645259483997	0.00068533221633	0.74999998237103	0.99999847933884
2160.711	23930.7744	57.27919584633170	0.03253777098792	1.50378730184023	0.00085423487741	0.78749998148958	1.04999840330579
2263.602	25070.3351	69.81324328430290	0.03965780748743	1.94198038788303	0.00110315293695	0.82499998060813	1.09999832727273
2366.493	26209.8958	80.45328150443940	0.04570194134431	2.65254632347465	0.00150679393334	0.86249997972668	1.14999825123967
2469.384	27349.4565	89.86387440571740	0.05104768183801	4.00462930456965	0.00227485231380	0.89999997884523	1.19999817520661
2572.275	28489.0172	98.39452931724870	0.05589356858253	7.58230201452787	0.00430716952053	0.93749997796378	1.24999809917355
2675.166	29628.5779	106.25567925594300	0.06035913924265	40.92236058251930	0.02324617825452	0.97499997708234	1.29999802314050
2778.057	30768.1386	113.58554498865800	0.06452291090633	253.02297379450200	0.14373113055036	1.01249997620089	1.34999794710744
2880.948	31907.6993	120.48064467080600	0.06843971125735	359.57976654791000	0.20426131901738	1.04999997531944	1.39999787107438
2983.839	33047.2599	127.01151078632800	0.07214960667190	429.91305774354700	0.24421454266056	1.08749997443799	1.44999779504132
3086.73	34186.8206	133.23153032000200	0.07568292392848	481.42317580728100	0.27347515640268	1.12499997355654	1.49999771900827
3189.621	35326.3813	139.18237092108000	0.07906333257079	521.01131428472300	0.29596342224833	1.16249997267509	1.54999764297521
3292.512	36465.942	144.89685916977800	0.08230947992328	552.27725226200800	0.31372421505619	1.19999997179364	1.59999756694215
3395.403	37605.5027	150.40203428687800	0.08543672576816	577.39684516608200	0.32799354180120	1.23749997091219	1.64999749090909
3498.294	38745.0634	155.72005078144400	0.08845765509955	597.80614047757800	0.33958715737240	1.27499997003075	1.69999741487603
3601.185	39884.6241	160.86943668908000	0.09138279287279	614.51162839997500	0.34907680421938	1.31249996914930	1.74999733884298
3704.076	41024.1848	165.86587287459700	0.09422104669179	628.24810459265300	0.35687988717008	1.34999996826785	1.79999726280992
3806.967	42163.7454	170.72276939322700	0.09698003421423	639.56930958409600	0.36331096166189	1.38749996738640	1.84999718677686
3909.858	43303.3061	175.45170011703400	0.09966633004355	648.90269957228400	0.36861284660440	1.42499996650495	1.89999711074380
4012.749	44442.8668	180.06273600467400	0.10228565504475	656.58461415557400	0.37297660160771	1.46249996562350	1.94999703471074
4115.64	45582.4275	184.56470447152300	0.10484302368104	662.88384259744500	0.37655491393235	1.49999996474205	1.99999695867769
4218.531	46721.9882	188.96539394183400	0.10734286021084	668.01797330090200	0.37947138590062	1.53749996386061	2.04999688264463
4321.422	47861.5489	193.27171710412400	0.10978909142593	672.16650642121500	0.38182798359041	1.57499996297916	2.09999680661157
4424.313	49001.1096	197.48984261953800	0.11218522146915	675.47315681736500	0.38370634503975	1.61249996209771	2.14999673057851

Temp. Increment (T)	Mechanical Load Increment (P)	Horizontal Deflection at Mid-Span due to Temperature Increment	Horizontal Deflection at Mid-Span due to Temperature Increment per Original Length	Horizontal Deflection at Mid-Span due to Mechanical Load Increment	Horizontal Deflection at Mid-Span due to Mechanical Load Increment per original length	Ratio of P/P_{cr}	Ratio of T/T_{cr}
4527.204	50140.6703	201.62530242509900	0.11453439278859	678.06242170336700	0.38517719159482	1.64999996121626	2.19999665454545
4630.095	51280.2309	205.68307993883400	0.11683943624304	680.03690638707800	0.38629880878076	1.68749996033481	2.24999657851240
4732.986	52419.7916	209.66768316204400	0.11910291262812	681.48315425890300	0.38712035805969	1.72499995945336	2.29999650247934
4835.877	53559.3523	213.58320572257900	0.12132714735227	682.47456724386700	0.38768353581005	1.76249995857191	2.34999642644628
4938.768	54698.913	217.43337820374800	0.12351425959443	683.07369903652600	0.38802387601164	1.79999995769046	2.39999635041322
5041.659	55838.4737	221.22161158322800	0.12566618697974	683.33408634394800	0.38817179049353	1.83749995680902	2.44999627438016
5144.55	56978.0344	224.95103421485400	0.12778470658729	683.30172446731900	0.38815340714658	1.87499995592757	2.49999619834711
5247.441	58117.5951	228.62452348855500	0.12987145293468	683.01626595315400	0.38799125082397	1.91249995504612	2.54999612231405
5350.332	59257.1558	232.24473307513100	0.13192793345463	682.51200145312100	0.38770480052422	1.94999995416467	2.59999604628099
5453.223	60396.7164	235.81411648554300	0.13395554187790	681.81866774152400	0.38731094839008	1.98749995328322	2.64999597024793
5556.114	61536.2771	239.33494753605500	0.13595556985867	680.96211742346600	0.38682438014000	2.02499995240177	2.69999589421487
5659.005	62675.8378	242.80933820163400	0.13792921711626	680.09319097103400	0.38633078155684	2.06249995152032	2.74999581818182
5761.896	63815.3985	246.23925425359500	0.13987760031818	678.95188788417900	0.38568245788680	2.09999995063888	2.79999574214876
5864.787	64954.9592	249.62652900844800	0.14180176089024	677.71193607186100	0.38497809625062	2.13749994975743	2.84999566611570
5967.678	66094.5199	252.97287545938000	0.14370267190789	676.38457407469800	0.38422408076483	2.17499994887598	2.89999559008264
6070.569	67234.0806	256.27989701689100	0.14558124419755	674.98320990900100	0.38342802792889	2.21249994799453	2.94999551404958

Table B- 6: Numerical Results for Hinged-Hinged Column Subjected to 6071℃ and 67234 KN with 60 Load-Steps and Eccentricity (e=0.001& convergence tolerance=0.001) for Slenderness Ratio of 20 (Data for Rotation at Top Hinged Joint in Validation to Elastica Solution)

Temp. Increment (T)	Mechanical Load Increment (P)	Rotation at Top Hinged Joint due to Temp. Increment	Rotation at Top Hinged Joint due to Mechanical Load Increment	Ratio of P/P_{cr}	Ratio of T/T_{cr}
0	0	0.00001117055075	0.00002404471353	0.00000000000000	0.00000000000000
102.891	1139.56069	0.00002337003731	0.00005004205719	0.03749999911855	0.04999992396694
205.782	2279.12138	0.00003677811512	0.00007823464266	0.07499999823710	0.09999984793388
308.673	3418.68206	0.00005161935345	0.00010890690096	0.11249999735565	0.14999977190083
411.564	4558.24275	0.00006817822111	0.00014239449617	0.14999999647421	0.19999969586777
514.455	5697.80344	0.00008682050180	0.00017909640176	0.18749999559276	0.24999961983471
617.346	6837.36413	0.00010802460546	0.00021949056185	0.22499999471131	0.29999954380165
720.237	7976.92481	0.00013242855559	0.00026415444332	0.26249999382986	0.34999946776860
823.128	9116.4855	0.00016090264261	0.00031379235865	0.29999999294841	0.39999939173554
926.019	10256.0462	0.00019466573719	0.00036927231310	0.33749999206696	0.44999931570248
1028.91	11395.6069	0.00023547928001	0.00043167648827	0.37499999118551	0.49999923966942
1131.801	12535.1676	0.00028598704550	0.00050237163687	0.41249999030407	0.54999916363636
1234.692	13674.7283	0.00035034677194	0.00058310919538	0.44999998942262	0.59999908760331
1337.583	14814.2889	0.00043549502556	0.00067617085876	0.48749998854117	0.64999901157025
1440.474	15953.8496	0.00055393445502	0.00078458567676	0.52499998765972	0.69999893553719
1543.365	17093.4103	0.00073071720407	0.00091246331220	0.56249998677827	0.74999885950413
1646.256	18232.971	0.00102445991904	0.00106552310513	0.59999998589682	0.79999878347108
1749.147	19372.5317	0.00161179320248	0.00125196768562	0.63749998501537	0.84999870743802
1852.038	20512.0924	0.00338198067717	0.00148399482813	0.67499998413392	0.89999863140496
1954.929	21651.6531	0.02709826698726	0.00178056693955	0.71249998325248	0.94999855537190
2057.82	22791.2138	0.07359722102985	0.00217285512280	0.74999998237103	0.99999847933884
2160.711	23930.7744	0.10211600426585	0.00271594914481	0.78749998148958	1.04999840330579
2263.602	25070.3351	0.12435827909250	0.00351724346143	0.82499998060813	1.09999832727273
2366.493	26209.8958	0.14319709418896	0.00481782302720	0.86249997972668	1.14999825123967
2469.384	27349.4565	0.15982164499931	0.00729439092148	0.89999997884523	1.19999817520661
2572.275	28489.0172	0.17485784031860	0.01385093750321	0.93749997796378	1.24999809917355
2675.166	29628.5779	0.18868282204294	0.07501139531330	0.97499997708234	1.29999802314050
2778.057	30768.1386	0.20154450385709	0.47549725887036	1.01249997620089	1.34999794710744
2880.948	31907.6993	0.21361613565537	0.69554174945672	1.04999997531944	1.39999787107438
2983.839	33047.2599	0.22502442150564	0.85504867357649	1.08749997443799	1.44999779504132
3086.73	34186.8206	0.23586534012686	0.98343895985194	1.12499997355654	1.49999771900827
3189.621	35326.3813	0.24621385830023	1.09200304949352	1.16249997267509	1.54999764297521
3292.512	36465.942	0.25612908891069	1.18647847896645	1.19999997179364	1.59999756694215

Temp. Increment (T)	Mechanical Load Increment (P)	Rotation at Top Hinged Joint due to Temp. Increment	Rotation at Top Hinged Joint due to Mechanical Load Increment	Ratio of P/P_{cr}	Ratio of T/T_{cr}
3395.403	37605.5027	0.26565975293783	1.27027255291277	1.23749997091219	1.64999749090909
3498.294	38745.0634	0.27484580476214	1.34561023920955	1.27499997003075	1.69999741487603
3601.185	39884.6241	0.28372068497909	1.41404582220387	1.31249996914930	1.74999733884298
3704.076	41024.1848	0.29231271780339	1.47671596527536	1.34999996826785	1.79999726280992
3806.967	42163.7454	0.30064614491122	1.53448333712391	1.38749996738640	1.84999718677686
3909.858	43303.3061	0.30874190530175	1.58802150849369	1.42499996650495	1.89999711074380
4012.749	44442.8668	0.31661823348764	1.63786857245788	1.46249996562350	1.94999703471074
4115.64	45582.4275	0.32429112519454	1.68446255427904	1.49999996474205	1.99999695867769
4218.531	46721.9882	0.33177470475533	1.72816567136409	1.53749996386061	2.04999688264463
4321.422	47861.5489	0.33908151842786	1.76929302161910	1.57499996297916	2.09999680661157
4424.313	49001.1096	0.34622277111050	1.80807599361220	1.61249996209771	2.14999673057851
4527.204	50140.6703	0.35320851925854	1.84474996660030	1.64999996121626	2.19999665454545
4630.095	51280.2309	0.36004782951695	1.87950508543879	1.68749996033481	2.24999657851240
4732.986	52419.7916	0.36674891023464	1.91250675507613	1.72499995945336	2.29999650247934
4835.877	53559.3523	0.37331922132024	1.94389995349236	1.76249995857191	2.34999642644628
4938.768	54698.913	0.37976556664598	1.97381252830954	1.79999995769046	2.39999635041322
5041.659	55838.4737	0.38609417227355	2.00235784043906	1.83749995680902	2.44999627438016
5144.55	56978.0344	0.39231075307381	2.02963690707190	1.87499995592757	2.49999619834711
5247.441	58117.5951	0.39842056977838	2.05574015532214	1.91249995504612	2.54999612231405
5350.332	59257.1558	0.40442847809137	2.08074886970290	1.94999995416467	2.59999604628099
5453.223	60396.7164	0.41033897117161	2.10473639637468	1.98749995328322	2.64999597024793
5556.114	61536.2771	0.41615621654765	2.12776915234377	2.02499995240177	2.69999589421487
5659.005	62675.8378	0.42188408833248	2.15013656662787	2.06249995152032	2.74999581818182
5761.896	63815.3985	0.42752619544939	2.17139505878123	2.09999995063888	2.79999574214876
5864.787	64954.9592	0.43308590645678	2.19187268739984	2.13749994975743	2.84999566611570
5967.678	66094.5199	0.43856637145999	2.21160957685647	2.17499994887598	2.89999559008264
6070.569	67234.0806	0.44397054151742	2.23064831660355	2.21249994799453	2.94999551404958

Table B- 7: Numerical Results for Hinged-Hinged Column for Slenderness Ratio of 50(Data for Horizontal Mid-Span Deflections; convergence tolerance=0.001)

Temperature Increment (T)	Mechanical Load Increment (P)	Horizontal Deflection at Mid-Span due to Temperature Increment	Horizontal Deflection at Mid-Span due to Temperature Increment per Original Length	Horizontal Deflection at Mid-Span due to Mechanical Load Increment	Horizontal Deflection at Mid-Span due to Mechanical Load Increment per Original Length	Ratio of P/P_{cr}	Ratio of T/T_{cr}
0	0	0.00000000000000	0.00000000000000	0.00000000000000	0.00000000000000	0.00000000000000	0.00000000000000
16.66666667	125	0.05030006830816	0.00001143183371	0.02386886902167	0.00000542474296	0.02569750367107	0.05059735682819
33.33333333	250	0.10642216908635	0.00002418685661	0.04900517354300	0.00001113753944	0.05139500734214	0.10119471365639
50	375	0.16941225566343	0.00003850278538	0.07551438096382	0.00001716235931	0.07709251101322	0.15179207048458
66.66666667	500	0.24058198384702	0.00005467772360	0.10351400775629	0.00002352591085	0.10279001468429	0.20238942731278
83.33333333	625	0.32159875764565	0.00007309062674	0.13313539098168	0.00003025804340	0.12848751835536	0.25298678414097
100	750	0.41461504263166	0.00009423069151	0.16452578175759	0.00003739222313	0.15418502202643	0.30358414096916
116.6666667	875	0.52245847988985	0.00011874056361	0.19785083116098	0.00004496609799	0.17988252569750	0.35418149779736
133.3333333	1000	0.64891896440076	0.00014748158282	0.23329755714770	0.00005302217208	0.20558002936858	0.40477885462555
150	1125	0.79919569128121	0.00018163538438	0.27107790468167	0.00006160861470	0.23127753303965	0.45537621145375
166.6666667	1250	0.98061867815740	0.00022286788140	0.31143304224402	0.00007078023687	0.25697503671072	0.50597356828194
183.3333333	1375	1.20386343142293	0.00027360532532	0.35463857873398	0.00008059967698	0.28267254038179	0.55657092511013
200	1500	1.48510150724163	0.00033752306983	0.40101093933485	0.00009113884985	0.30837004405286	0.60716828193833
216.6666667	1625	1.85004884419731	0.00042046564641	0.45091521225320	0.00010248073006	0.33406754772394	0.65776563876652
233.3333333	1750	2.34218989027629	0.00053231588415	0.50477487804967	0.00011472156319	0.35976505139501	0.70836299559471
250	1875	3.04118787250772	0.00069117906193	0.56308397045336	0.00012797362965	0.38546255506608	0.75896035242291
266.6666667	2000	4.10968490278369	0.00093401929609	0.62642240840846	0.00014236872918	0.41116005873715	0.80955770925110
283.3333333	2125	5.93426742769740	0.00134869714266	0.69547550799237	0.00015806261545	0.43685756240822	0.86015506607930
300	2250	9.64796278586501	0.00219271881497	0.77105906694332	0.00017524069703	0.46255506607930	0.91075242290749
316.6666667	2375	18.90181370406300	0.00429586675092	0.85415197137909	0.00019412544804	0.48825256975037	0.96134977973568
333.3333333	2500	35.48115100019710	0.00806389795459	0.94593909480939	0.00021498615791	0.51395007342144	1.01194713656388

Temperature Increment (T)	Mechanical Load Increment (P)	Horizontal Deflection at Mid-Span due to Temperature Increment	Horizontal Deflection at Mid-Span due to Temperature Increment per Original Length	Horizontal Deflection at Mid-Span due to Mechanical Load Increment	Horizontal Deflection at Mid-Span due to Mechanical Load Increment per Original Length	Ratio of P/P_{cr}	Ratio of T/T_{cr}
350	2625	51.02195960078210	0.01159589990927	1.04786849349758	0.00023815193034	0.53964757709251	1.06254449339207
366.6666667	2750	63.86028785706950	0.01451370178570	1.16172876208811	0.00026402926411	0.56534508076358	1.11314185022026
383.3333333	2875	74.82849962787340	0.01700647718815	1.28975541424954	0.00029312623051	0.59104258443466	1.16373920704846
400	3000	84.50993315423140	0.01920680298960	1.43477975953904	0.00032608630899	0.61674008810573	1.21433656387665
416.6666667	3125	93.25434340489310	0.02119416895566	1.60044156179136	0.00036373671859	0.64243759177680	1.26493392070485
433.3333333	3250	101.28236654434800	0.02301871966917	1.79149977946804	0.00040715904079	0.66813509544787	1.31553127753304
450	3375	108.74169694202800	0.02471402203228	2.01429856444899	0.00045779512828	0.69383259911894	1.36612863436123
466.6666667	3500	115.73626619208600	0.02630369686184	2.27748724116165	0.00051761073663	0.71953010279002	1.41672599118943
483.3333333	3625	122.34222115526500	0.02780505026256	2.59317189440165	0.00058935724873	0.74522760646109	1.46732334801762
500	3750	128.61720405960800	0.02923118274082	2.97883392600761	0.00067700771046	0.77092511013216	1.51792070484582
516.6666667	3875	134.60617455327300	0.03059231239847	3.46068591083422	0.00078651952519	0.79662261380323	1.56851806167401
533.3333333	4000	140.34442286553400	0.03189645974217	4.07990013128282	0.00092725002984	0.82232011747430	1.61911541850220
550	4125	145.86102865804700	0.03315023378592	4.90505586660322	0.00111478542423	0.84801762114537	1.66971277533040
566.6666667	4250	151.17974321337200	0.03435903254849	6.05949418952630	0.00137715777035	0.87371512481645	1.72031013215859
583.3333333	4375	156.32038782745600	0.03552736086988	7.78959857788738	0.00177036331316	0.89941262848752	1.77090748898678
600	4500	161.29970338993100	0.03665902349771	10.66911773179790	0.00242479948450	0.92511013215859	1.82150484581498
616.6666667	4625	166.13197830418600	0.03775726779641	16.41229865822020	0.00373006787687	0.95080763582966	1.87210220264317
633.3333333	4750	170.82952153285300	0.03882489125747	33.46503684254860	0.00760569019149	0.97650513950073	1.92269955947137
650	4875	175.40302487042800	0.03986432383419	230.52819944758200	0.05239277260172	1.00220264317181	1.97329691629956
666.6666667	5000	179.86184448017700	0.04087769192731	610.14423604781500	0.13866914455632	1.02790014684288	2.02389427312775
683.3333333	5125	184.21422258643300	0.04186686876964	825.41578046889200	0.18759449556111	1.05359765051395	2.07449162995595
700	5250	188.46746412824700	0.04283351457460	978.57713147459800	0.22240389351695	1.07929515418502	2.12508898678414
716.6666667	5375	192.62807904774400	0.04377910887449	1096.95616933717000	0.24930822030390	1.10499265785609	2.17568634361233
733.3333333	5500	196.70189802729500	0.04470497682439	1192.29729345446000	0.27097665760329	1.13069016152717	2.22628370044053

Temperature Increment (T)	Mechanical Load Increment (P)	Horizontal Deflection at Mid-Span due to Temperature Increment	Horizontal Deflection at Mid-Span due to Temperature Increment per Original Length	Horizontal Deflection at Mid-Span due to Mechanical Load Increment	Horizontal Deflection at Mid-Span due to Mechanical Load Increment per Original Length	Ratio of P/P_{cr}	Ratio of T/T_{cr}
750	5625	200.69416747721000	0.04561231079028	1270.99556572172000	0.28886262857312	1.15638766519824	2.27688105726872
766.6666667	5750	204.60962813762000	0.04650218821310	1337.01603060232000	0.30386727968235	1.18208516886931	2.32747841409692
783.3333333	5875	208.45258061536900	0.04737558650349	1393.03269447815000	0.31659833965413	1.20778267254038	2.37807577092511
800	6000	212.22694041104400	0.04823339554796	1440.95035630999000	0.32748871734318	1.23348017621145	2.42867312775330
816.6666667	6125	215.93628442179400	0.04907642827768	1482.19030400369000	0.33686143272811	1.25917767988253	2.47927048458150
833.3333333	6250	219.58389047767400	0.04990542965402	1517.84153583958000	0.34496398541809	1.28487518355360	2.52986784140969
850	6375	223.17277114407500	0.05072108435093	1548.76083956005000	0.35199109990001	1.31057268722467	2.58046519823788
866.6666667	6500	226.70570277346600	0.05152402335761	1575.63554060355000	0.35809898650081	1.33627019089574	2.63106255506608
883.3333333	6625	230.18525059663900	0.05231482968105	1599.02586147613000	0.36341496851730	1.36196769456681	2.68165991189427
900	6750	233.61379049315700	0.05309404329390	1619.41407572522000	0.36804865357391	1.38766519823789	2.73225726872247
916.6666667	6875	236.99352796213500	0.05386216544594	1637.14196436267000	0.37207771917333	1.41336270190896	2.78285462555066
933.3333333	7000	240.32651472065300	0.05461966243651	1652.56171065645000	0.37558220696738	1.43906020558003	2.83345198237885
950	7125	243.61466328216700	0.05536696892777	1665.95039014452000	0.37862508866921	1.46475770925110	2.88404933920705
966.6666667	7250	246.85975980718600	0.05610449086527	1677.54471557198000	0.38126016263000	1.49045521292217	2.93464669603524
983.3333333	7375	250.06347546973700	0.05683260806130	1687.54873049682000	0.38353380238564	1.51615271659325	2.98524405286343
1000	7500	253.22737654369400	0.05755167648720	1696.13928913522000	0.38548620207619	1.54185022026432	3.03584140969163

Table B- 8: Numerical Results for Hinged-Hinged Column for Slenderness Ratio of 125 (Data for Horizontal Mid-Span Deflections; convergence tolerance=0.001)

Temperature Increment (T)	Mechanical Load Increment (P)	Horizontal Deflection at Mid-Span due to Temperature Increment	Horizontal Deflection at Mid-Span due to Temperature Increment per Original Length	Horizontal Deflection at Mid-Span due to Mechanical Load Increment	Horizontal Deflection at Mid-Span due to Mechanical Load Increment per Original Length	Ratio of P/P_{cr}	Ratio of T/T_{cr}
0	0	0.00000000000000	0.00000000000000	0.00000000000000	0.00000000000000	0.00000000000000	0.00000000000000
2.666666667	43.75	0.05030006830024	0.00000457273348	0.13472078014155	0.00001224734365	0.05621328928047	0.05059735682819
5.333333333	87.5	0.10642216900018	0.00000967474264	0.28628592837200	0.00002602599349	0.11242657856094	0.10119471365639
8	131.25	0.16941225527972	0.00001540111412	0.45810966276410	0.00004164633298	0.16863986784141	0.15179207048458
10.66666667	175	0.24058198262118	0.00002187108933	0.65459686265957	0.00005950880570	0.22485315712188	0.20238942731278
13.33333333	218.75	0.32159875438505	0.00002923625040	0.88153052019918	0.00008013913820	0.28106644640235	0.25298678414097
16	262.5	0.41461503482299	0.00003769227589	1.14665646475655	0.00010424149680	0.33727973568282	0.30358414096916
18.66666667	306.25	0.52245846237017	0.00004749622385	1.46059340921464	0.00013278121902	0.39349302496329	0.35418149779736
21.33333333	350	0.64891892658265	0.00005899262969	1.83830106499278	0.00016711827864	0.44970631424376	0.40477885462555
24	393.75	0.79919561123135	0.00007265414648	2.30155103971906	0.00020923191270	0.50591960352423	0.45537621145375
26.66666667	437.5	0.98061850936884	0.00008914713722	2.88330226897226	0.00026211838809	0.56213289280470	0.50597356828194
29.33333333	481.25	1.20386307164242	0.00010944209742	3.63594607105497	0.00033054055191	0.61834618208517	0.55657092511013
32	525	1.48510071983989	0.00013500915635	4.64810371821365	0.00042255488347	0.67455947136564	0.60716828193833
34.66666667	568.75	1.85004704190341	0.00016818609472	6.08248970417573	0.00055295360947	0.73077276064611	0.65776563876652
37.33333333	612.5	2.34218546951621	0.00021292595177	8.27380554983182	0.00075216414089	0.78698604992658	0.70836299559471
40	656.25	3.04117583370159	0.00027647053034	12.03757249097690	0.00109432477191	0.84319933920705	0.75896035242291
42.66666667	700	4.10964638050749	0.00037360421641	20.01719326649680	0.00181974484241	0.89941262848752	0.80955770925110
45.33333333	743.75	5.93410739010823	0.00053946430819	48.31612721537300	0.00439237520140	0.95562591776799	0.86015506607930
48	787.5	9.64693061952886	0.00087699369268	1125.34728663827000	0.10230429878530	1.01183920704846	0.91075242290749
50.66666667	831.25	18.89109377408960	0.00171737216128	2341.25456244914000	0.21284132385901	1.06805249632893	0.96134977973568
53.33333333	875	35.43273846677640	0.00322115804243	2961.49463067558000	0.26922678460687	1.12426578560940	1.01194713656388

Temperature Increment (T)	Mechanical Load Increment (P)	Horizontal Deflection at Mid-Span due to Temperature Increment	Horizontal Deflection at Mid-Span due to Temperature Increment per Original Length	Horizontal Deflection at Mid-Span due to Mechanical Load Increment	Horizontal Deflection at Mid-Span due to Mechanical Load Increment per Original Length	Ratio of P/P_{cr}	Ratio of T/T_{cr}
56	918.75	50.93642111519450	0.00463058373774	3362.37668003644000	0.30567060727604	1.18047907488987	1.06254449339207
58.66666667	962.5	63.74470553043790	0.00579497323004	3641.25742174113000	0.33102340197647	1.23669236417034	1.11314185022026
61.33333333	1006.25	74.68671094994120	0.00678970099545	3842.03590414188000	0.34927599128563	1.29290565345081	1.16373920704846
64	1050	84.34410706734330	0.00766764609703	3989.05762361285000	0.36264160214662	1.34911894273128	1.21433656387665
66.66666667	1093.75	93.06581492918420	0.00846052862993	4097.40105162279000	0.37249100469298	1.40533223201175	1.26493392070485
69.33333333	1137.5	101.07200469288200	0.00918836406299	4177.05708409161000	0.37973246219015	1.46154552129222	1.31553127753304
72	1181.25	108.51008562212200	0.00986455323837	4234.99133700295000	0.38499921245481	1.51775881057269	1.36612863436123
74.66666667	1225	115.48380270692500	0.01049852751881	4276.20654659726000	0.38874604969066	1.57397209985316	1.41672599118943
77.33333333	1268.75	122.06917431798900	0.01109719766527	4304.39750726379000	0.39130886429671	1.63018538913363	1.46732334801762
80	1312.5	128.32375068734700	0.01166579551703	4322.34840827675000	0.39294076438880	1.68639867841410	1.51792070484582
82.66666667	1356.25	134.29242438159800	0.01220840221651	4332.19172364516000	0.39383561124047	1.74261196769457	1.56851806167401
85.33333333	1400	140.01043245762400	0.01272822113251	4335.58283101593000	0.39414389372872	1.79882525697504	1.61911541850220
88	1443.75	145.50681583584100	0.01322789234871	4333.82123248664000	0.39398374840788	1.85503854625551	1.66971277533040
90.66666667	1487.5	150.80529465827000	0.01370957224166	4327.93928459574000	0.39344902587234	1.91125183553598	1.72031013215859
93.33333333	1531.25	155.92566543497600	0.01417506049409	4318.75292337433000	0.39261390212494	1.96746512481645	1.77090748898678
96	1575	160.88464910363900	0.01462587719124	4306.92894035991000	0.39153899457817	2.02367841409692	1.82150484581498
98.66666667	1618.75	165.69651785127700	0.01506331980466	4293.00241987447000	0.39027294726132	2.07989170337739	1.87210220264317
101.3333333	1662.5	170.37356735376700	0.01548850612307	4277.40855309364000	0.38885532300851	2.13610499265786	1.92269955947137
104	1706.25	174.92647844576200	0.01590240713143	4260.50276230333000	0.38731843293667	2.19231828193833	1.97329691629956
106.6666667	1750	179.36459819995100	0.01630587256363	4242.85851247780000	0.38571441022526	2.24853157121880	2.02389427312775
109.3333333		183.69616126683700	0.01669965102426				2.07449162995595
112		187.92846625346200	0.01708440602304				2.12508898678414
114.6666667		192.06801779481000	0.01746072889044				2.17568634361234
117.3333333		196.12064211802900	0.01782914928346				2.22628370044053

Temperature Increment (T)	Mechanical Load Increment (P)	Horizontal Deflection at Mid-Span due to Temperature Increment	Horizontal Deflection at Mid-Span due to Temperature Increment per Original Length	Horizontal Deflection at Mid-Span due to Mechanical Load Increment	Horizontal Deflection at Mid-Span due to Mechanical Load Increment per Original Length	Ratio of P/P_{cr}	Ratio of T/T_{cr}
120		200.09158189102100	0.01819014380827				2.27688105726872
122.6666667		203.98557471142900	0.01854414315558				2.32747841409692
125.3333333		207.80691855122600	0.01889153805011				2.37807577092511
128		211.55952670765200	0.01923268424615				2.42867312775331
130.6666667		215.24697424302900	0.01956790674937				2.47927048458150
133.3333333		218.87253746858700	0.01989750340624				2.52986784140969
136		222.43922770270400	0.02022174797297				2.58046519823789
138.6666667		225.94982028548000	0.02054089275323				2.63106255506608
141.3333333		229.40687963854000	0.02085517087623				2.68165991189427
144		232.81278100863300	0.02116479827351				2.73225726872247
146.6666667		236.16972941551100	0.02146997540141				2.78285462555066
149.3333333		239.47977623066900	0.02177088874824				2.83345198237886
152		242.74483373891200	0.02206771215808				2.88404933920705
154.6666667		245.96668797432100	0.02236060799767				2.93464669603524
157.3333333		249.14701007411300	0.02264972818856				2.98524405286344
160		252.28736635391100	0.02293521512308				3.03584140969163

Table B- 9: Numerical Results for Hinged-Hinged Column for Slenderness Ratio of 200 (Data for Horizontal Mid-Span Deflections; convergence tolerance=0.001)

Temperature Increment (T)	Mechanical Load Increment (P)	Horizontal Deflection at Mid-Span due to Temperature Increment	Horizontal Deflection at Mid-Span due to Temperature Increment per Original Length	Horizontal Deflection at Mid-Span due to Mechanical Load Increment	Horizontal Deflection at Mid-Span due to Mechanical Load Increment per Original Length	Ratio of P/P_{cr}	Ratio of T/T_{cr}
0	0	0.00000000000000	0.00000000000000	0.00000000000000	0.00000000000000	0.00000000000000	0.00000000000000
1.083333333	10.83333333	0.05242693693829	0.00000297880324	0.13376553291499	0.00000760031437	0.03563387175722	0.05262125110132
2.166666667	21.66666667	0.11119314567821	0.00000631779237	0.27766894395261	0.00001577664454	0.07126774351444	0.10524250220264
3.25	32.5	0.17749158553006	0.00001008474918	0.43292309729918	0.00002459790326	0.10690161527166	0.15786375330397
4.333333333	43.33333333	0.25283361564704	0.00001436554634	0.60094258932799	0.00003414446530	0.14253548702888	0.21048500440529
5.416666667	54.16666667	0.33916275665479	0.00001927061117	0.78338751488602	0.00004451065425	0.17816935878610	0.26310625550661
6.5	65	0.43902096111727	0.00002494437279	0.98221914484145	0.00005580790596	0.21380323054332	0.31572750660793
7.583333333	75.83333333	0.55579800867547	0.00003157943231	1.19977147650985	0.00006816883389	0.24943710230054	0.36834875770925
8.666666667	86.66666667	0.69411687852846	0.00003943845901	1.43884419964102	0.00008175251134	0.28507097405776	0.42097000881057
9.75	97.5	0.86045014942594	0.00004888921304	1.70282494873697	0.00009675141754	0.32070484581498	0.47359125991189
10.83333333	108.3333333	1.06414671068045	0.00006046288129	1.99585220161744	0.00011340069327	0.35633871757220	0.52621251101322
11.91666667	119.1666667	1.31922652489090	0.00007495605255	2.32303551544190	0.00013199065429	0.39197258932942	0.57883376211454
13	130	1.64770711062536	0.00009361972219	2.69075811292143	0.00015288398369	0.42760646108664	0.63145501321586
14.08333333	140.8333333	2.08623200752542	0.00011853590952	3.10710013046142	0.00017653978014	0.46324033284386	0.68407626431718
15.16666667	151.6666667	2.70054951280532	0.00015344031323	3.58244266013799	0.00020354787842	0.49887420460108	0.73669751541850
16.25	162.5	3.62116952265449	0.00020574826833	4.13034959002766	0.00023467895398	0.53450807635830	0.78931876651982
17.33333333	173.3333333	5.14653086352195	0.00029241652634	4.76888866799843	0.00027095958341	0.57014194811552	0.84194001762115
18.41666667	184.1666667	8.11228845660658	0.00046092548049	5.52267012027029	0.00031378807502	0.60577581987274	0.89456126872247
19.5	195	15.39342784767660	0.00087462658225	6.42610279098981	0.00036511947676	0.64140969162996	0.94718251982379
20.58333333	205.8333333	31.30293554500600	0.00177857588324	7.52880989709006	0.00042777328961	0.67704356338718	0.99980377092511
21.66666667	216.6666667	48.06740809599720	0.00273110273273	8.90508313089393	0.00050597063244	0.71267743514440	1.05242502202643

Temperature Increment (T)	Mechanical Load Increment (P)	Horizontal Deflection at Mid-Span due to Temperature Increment	Horizontal Deflection at Mid-Span due to Temperature Increment per Original Length	Horizontal Deflection at Mid-Span due to Mechanical Load Increment	Horizontal Deflection at Mid-Span due to Mechanical Load Increment per Original Length	Ratio of P/P_{cr}	Ratio of T/T_{cr}
22.75	227.5	61.82757431150340	0.00351293035861	10.67138674033490	0.00060632879206	0.74831130690162	1.10504627312775
23.83333333	238.3333333	73.43422148157090	0.00417239894782	13.02123065378930	0.00073984265078	0.78394517865884	1.15766752422907
24.91666667	249.1666667	83.59057604916860	0.00474946454825	16.30150342885450	0.00092622178573	0.81957905041606	1.21028877533040
26	260	92.71014401776020	0.00526762181919	21.20197459649450	0.00120465764753	0.85521292217328	1.26291002643172
27.08333333	270.8333333	101.04765663795500	0.00574134412716	29.31789021074050	0.00166578921652	0.89084679393050	1.31553127753304
28.16666667	281.6666667	108.77046348235800	0.00618013997059	45.36086892990350	0.00257732209829	0.92648066568771	1.36815252863436
29.25	292.5	115.99464770286500	0.00659060498312	91.99361508612750	0.00522690994808	0.96211453744493	1.42077377973568
30.33333333	303.3333333	122.80431532601800	0.00697751791625	803.85038429632900	0.04567331728956	0.99774840920215	1.47339503083700
31.41666667	314.1666667	129.26257263919400	0.00734446435450	2779.55221971455000	0.15792910339287	1.03338228095937	1.52601628193833
32.5	325	135.41813629773200	0.00769421228964	3776.68396925703000	0.21458431643506	1.06901615271659	1.57863753303965
33.58333333	335.8333333	141.30960015607600	0.00802895455432	4452.37559749240000	0.25297588622116	1.10465002447381	1.63125878414097
34.66666667	346.6666667	146.96777303169600	0.00835044164953	4953.63169822619000	0.28145634649012	1.14028389623103	1.68388003524229
35.75	357.5	152.41824283601700	0.00866012743386	5341.81461109453000	0.30351219381219	1.17591776798825	1.73650128634361
36.83333333	368.3333333	157.68215843455800	0.00895921354742	5650.00211565206000	0.32102284748023	1.21155163974547	1.78912253744493
37.91666667	379.1666667	162.77732657148100	0.00924871173702	5898.55400455636000	0.33514511389525	1.24718551150269	1.84174378854626
39	390	167.71890434479600	0.00952948320141	6100.99588088262000	0.34664749323197	1.28281938325991	1.89436503964758
40.08333333	400.8333333	172.51991803866800	0.00980226807038	6267.00096214683000	0.35607960012198	1.31845325501713	1.94698629074890
41.16666667	411.6666667	177.19165868790900	0.01006770787999	6403.63057551129000	0.36384264633587	1.35408712677435	1.99960754185022
42.25	422.5	181.74398827040200	0.01032636296991	6516.24381313469000	0.37024112574629	1.38972099853157	2.05222879295154
43.33333333	433.3333333	186.18557996016700	0.01057872613410	6609.00064292584000	0.37551140016624	1.42535487028879	2.10485004405286
44.41666667	444.1666667	190.52410896184800	0.01082523346374	6685.18994857779000	0.37984033798737	1.46098874204601	2.15747129515419
45.5	455	194.76640577948500	0.01106627305565	6747.45136637673000	0.38337791854413	1.49662261380323	2.21009254625551
46.58333333	465.8333333	198.91858056054800	0.01130219207730	6797.93017741044000	0.38624603280741	1.53225648556045	2.26271379735683
47.66666667	476.6666667	202.98612490380300	0.01153330255135	6838.42376965607000	0.38854680509410	1.56789035731767	2.31533504845815

Temperature Increment (T)	Mechanical Load Increment (P)	Horizontal Deflection at Mid-Span due to Temperature Increment	Horizontal Deflection at Mid-Span due to Temperature Increment per Original Length	Horizontal Deflection at Mid-Span due to Mechanical Load Increment	Horizontal Deflection at Mid-Span due to Mechanical Load Increment per Original Length	Ratio of P/P_{cr}	Ratio of T/T_{cr}
48.75	487.5	206.97399592287800	0.01175988613198	6870.31035655666000	0.39035854298617	1.60352422907489	2.36795629955947
49.83333333	498.3333333	210.88668619616200	0.01198219807933	6894.86040365780000	0.39175343202601	1.63915810083211	2.42057755066079
50.91666667	509.1666667	214.72828239168700	0.01220047059044	6913.09938106924000	0.39278973756075	1.67479197258933	2.47319880176212
52	520	218.50251472594500	0.01241491560943	6925.89459099493000	0.39351673812471	1.71042584434655	2.52582005286344
53.08333333	530.8333333	222.21279894756200	0.01262572721293	6933.98405938757000	0.39397636701066	1.74605971610377	2.57844130396476
54.16666667	541.6666667	225.86227217919300	0.01283308364655	6937.99875410296000	0.39420447466494	1.78169358786099	2.63106255506608
55.25	552.5	229.45382368050500	0.01303714907276	6938.48038388401000	0.39423183999341	1.81732745961821	2.68368380616740
56.33333333	563.3333333	232.99012138348000	0.01323807507861	6935.89578969369000	0.39408498805078	1.85296133137543	2.73630505726872
57.41666667	574.1666667	236.47363488835500	0.01343600198229	6930.64867163672000	0.39378685634300	1.88859520313265	2.78892630837005
58.5	585	239.90665548014900	0.01363105997046	6923.08921273684000	0.39335734163278	1.92422907488987	2.84154755947137
59.58333333	595.8333333	243.29131362331200	0.01382337009223	6913.52202817011000	0.39281375160057	1.95986294664709	2.89416881057269
60.66666667	606.6666667	246.62959431293300	0.01401304513142	6902.21277055416000	0.39217118014512	1.99549681840431	2.94679006167401
61.75	617.5	249.92335059318200	0.01420019037461	6889.39364868768000	0.39144282094816	2.03113069016153	2.99941131277533
62.83333333	628.3333333	253.17431550464200	0.01438490429004	6875.26806187602000	0.39064023078841	2.06676456191875	3.05203256387665
63.91666667	639.1666667	256.38411267682500	0.01456727912937	6860.01450985830000	0.38977355169649	2.10239843367597	3.10465381497798
65	650	259.55426574987400	0.01474740146306	6843.78990595141000	0.38885169920179	2.13803230543319	3.15727506607930

Table B- 10: Numerical Results for Hinged-Hinged Column for Slenderness Ratio of 50 (Data for Rotation at Top Hinged Joint; convergence tolerance=0.001)

Temperature Increment (T)	Mechanical Load Increment (P)	Rotation at Top Hinged Joint due to Temperature Increment	Rotation at Top Hinged Joint due to Mechanical Load Increment	Ratio of P/P_{cr}	Ratio of T/T_{cr}
0	0	0.00000000000000	0.00000000000000	0.00000000000000	0.00000000000000
16.66666667	125	0.00004525022633	0.00001629315320	0.02569750367107	0.05059735682819
33.33333333	250	0.00009472431686	0.00003349057052	0.05139500734214	0.10119471365639
50	375	0.00014917013753	0.00005166782858	0.07709251101322	0.15179207048458
66.66666667	500	0.00020952528884	0.00007090914223	0.10279001468429	0.20238942731278
83.33333333	625	0.00027698139879	0.00009130863464	0.12848751835536	0.25298678414097
100	750	0.00035307645281	0.00011297183821	0.15418502202643	0.30358414096916
116.6666667	875	0.00043983053494	0.00013601747690	0.17988252569750	0.35418149779736
133.3333333	1000	0.00053995080102	0.00016057959333	0.20558002936858	0.40477885462555
150	1125	0.00065715066796	0.00018681010126	0.23127753303965	0.45537621145375
166.6666667	1250	0.00079666497680	0.00021488186600	0.25697503671072	0.50597356828194
183.3333333	1375	0.00096611725634	0.00024499244471	0.28267254038179	0.55657092511013
200	1500	0.00117705520625	0.00027736865762	0.30837004405286	0.60716828193833
216.6666667	1625	0.00144784116679	0.00031227221379	0.33406754772394	0.65776563876652
233.3333333	1750	0.00180952404634	0.00035000668668	0.35976505139501	0.70836299559471
250	1875	0.00231898397280	0.00039092623289	0.38546255506608	0.75896035242291
266.6666667	2000	0.00309234661649	0.00043544658465	0.41116005873715	0.80955770925110
283.3333333	2125	0.00440562833663	0.00048405903901	0.43685756240822	0.86015506607930
300	2250	0.00706777160785	0.00053734844244	0.46255506607930	0.91075242290749
316.6666667	2375	0.01368528094080	0.00059601656854	0.48825256975037	0.96134977973568
333.3333333	2500	0.02553118012464	0.00066091287481	0.51395007342144	1.01194713656388
350	2625	0.03663264199454	0.00073307550946	0.53964757709251	1.06254449339207
366.6666667	2750	0.04580233636996	0.00081378677226	0.56534508076358	1.11314185022026
383.3333333	2875	0.05363507233810	0.00090464938522	0.59104258443466	1.16373920704846
400	3000	0.06054763273012	0.00100769323135	0.61674008810573	1.21433656387665
416.6666667	3125	0.06678992031423	0.00112552782239	0.64243759177680	1.26493392070485
433.3333333	3250	0.07251959408069	0.00126156508755	0.66813509544787	1.31553127753304
450	3375	0.07784220137409	0.00142035347678	0.69383259911894	1.36612863436123
466.6666667	3500	0.08283202281454	0.00160809415871	0.71953010279002	1.41672599118943
483.3333333	3625	0.08754348690479	0.00183346666673	0.74522760646109	1.46732334801762
500	3750	0.09201779986938	0.00210900443584	0.77092511013216	1.51792070484582
516.6666667	3875	0.09628710484180	0.00245350083692	0.79662261380323	1.56851806167401
533.3333333	4000	0.10037663610626	0.00289647483679	0.82232011747430	1.61911541850220

Temperature Increment (T)	Mechanical Load Increment (P)	Rotation at Top Hinged Joint due to Temperature Increment	Rotation at Top Hinged Joint due to Mechanical Load Increment	Ratio of P/P_{cr}	Ratio of T/T_{cr}
550	4125	0.10430718803300	0.00348709534432	0.84801762114537	1.66971277533040
566.6666667	4250	0.10809574723457	0.00431379393339	0.87371512481645	1.72031013215859
583.3333333	4375	0.11175649129003	0.00555322088965	0.89941262848752	1.77090748898678
600	4500	0.11530139584978	0.00761674400639	0.92511013215859	1.82150484581498
616.6666667	4625	0.11874068336503	0.01173348682015	0.95080763582966	1.87210220264317
633.3333333	4750	0.12208316115537	0.02395991856618	0.97650513950073	1.92269955947137
650	4875	0.12533648032344	0.16574732703654	1.00220264317181	1.97329691629956
666.6666667	5000	0.12850733697774	0.44727688025911	1.02790014684288	2.02389427312775
683.3333333	5125	0.13160163069038	0.61753157475836	1.05359765051395	2.07449162995595
700	5250	0.13462459076891	0.74685257450518	1.07929515418502	2.12508898678414
716.6666667	5375	0.13758087796885	0.85360387890009	1.10499265785609	2.17568634361233
733.3333333	5500	0.14047466723057	0.94547718352608	1.13069016152717	2.22628370044053
750	5625	0.14330971558636	1.02656829772414	1.15638766519824	2.27688105726872
766.6666667	5750	0.14608941835602	1.09936857605723	1.18208516886931	2.32747841409692
783.3333333	5875	0.14881685600406	1.16553351572766	1.20778267254038	2.37807577092511
800	6000	0.15149483348460	1.22622725413111	1.23348017621145	2.42867312775330
816.6666667	6125	0.15412591349298	1.28231359836337	1.25917767988253	2.47927048458150
833.3333333	6250	0.15671244473752	1.33445040039224	1.28487518355360	2.52986784140969
850	6375	0.15925658611216	1.38315444862907	1.31057268722467	2.58046519823788
866.6666667	6500	0.16176032747291	1.42884080230100	1.33627019089574	2.63106255506608
883.3333333	6625	0.16422550758289	1.47184900355349	1.36196769456681	2.68165991189427
900	6750	0.16665382968302	1.51249494317406	1.38766519823789	2.73225726872247
916.6666667	6875	0.16904687506108	1.55094095068690	1.41336270190896	2.78285462555066
933.3333333	7000	0.17140611492458	1.58743165841662	1.43906020558003	2.83345198237885
950	7125	0.17373292082908	1.62214172803245	1.46475770925110	2.88404933920705
966.6666667	7250	0.17602857387124	1.65522146867254	1.49045521292217	2.93464669603524
983.3333333	7375	0.17829427282039	1.68680235639033	1.51615271659325	2.98524405286343
1000	7500	0.18053114133475	1.71700018838998	1.54185022026432	3.03584140969163

Table B- 11: Numerical Results for Hinged-Hinged Column for Slenderness Ratio of 125 (Data for Rotation at Top Pinned Joint; convergence tolerance=0.001)

Temperature Increment (T)	Mechanical Load Increment (P)	Rotation at Top Hinged Joint due to Temperature Increment	Rotation at Top Hinged Joint due to Mechanical Load Increment	Ratio of P/P_{cr}	Ratio of T/T_{cr}
0	0	0.00000000000000	0.00000000000000	0.00000000000000	0.00000000000000
2.666666667	43.75	0.00001810009053	0.00003682896691	0.05621328928047	0.05059735682819
5.333333333	87.5	0.00003788972674	0.00007845016048	0.11242657856094	0.10119471365639
8	131.25	0.00005966805499	0.00012583889857	0.16863986784141	0.15179207048458
10.66666667	175	0.00008381011542	0.00018025360686	0.22485315712188	0.20238942731278
13.33333333	218.75	0.00011079255915	0.00024334654741	0.28106644640235	0.25298678414097
16	262.5	0.00014123058011	0.00031733092534	0.33727973568282	0.30358414096916
18.66666667	306.25	0.00017593221141	0.00040524096861	0.39349302496329	0.35418149779736
21.33333333	350	0.00021598031430	0.00051135149711	0.44970631424376	0.40477885462555
24	393.75	0.00026286025313	0.00064188407505	0.50591960352423	0.45537621145375
26.66666667	437.5	0.00031866595887	0.00080625745673	0.56213289280470	0.50597356828194
29.33333333	481.25	0.00038644683020	0.00101944392582	0.61834618208517	0.55657092511013
32	525	0.00047082191501	0.00130676984717	0.67455947136564	0.60716828193833
34.66666667	568.75	0.00057913606351	0.00171473656618	0.73077276064611	0.65776563876652
37.33333333	612.5	0.00072380858345	0.00233899742929	0.78698604992658	0.70836299559471
40	656.25	0.00092759065143	0.00341261929710	0.84319933920705	0.75896035242291
42.66666667	700	0.00123692888646	0.00569106424350	0.89941262848752	0.80955770925110
45.33333333	743.75	0.00176220938657	0.01377674147936	0.95562591776799	0.86015506607930
48	787.5	0.00282683009507	0.32539269448424	1.01183920704846	0.91075242290749
50.66666667	831.25	0.00547117350175	0.70773250941736	1.06805249632893	0.96134977973568
53.33333333	875	0.01019945954211	0.93389105747779	1.12426578560940	1.01194713656388
56	918.75	0.01463104939318	1.10338934111080	1.18047907488987	1.06254449339207
58.66666667	962.5	0.01829267440849	1.24063091823163	1.23669236417034	1.11314185022026
61.33333333	1006.25	0.02142117586225	1.35630262697031	1.29290565345081	1.16373920704846
64	1050	0.02418270003160	1.45626817333885	1.34911894273128	1.21433656387665
66.66666667	1093.75	0.02667691141675	1.54417369389798	1.40533223201175	1.26493392070485
69.33333333	1137.5	0.02896669914660	1.62246417885777	1.46154552129222	1.31553127753304
72	1181.25	0.03109416955650	1.69289506425176	1.51775881057269	1.36612863436123
74.66666667	1225	0.03308895705078	1.75676282497642	1.57397209985316	1.41672599118943
77.33333333	1268.75	0.03497277636378	1.81506175555905	1.63018538913363	1.46732334801762
80	1312.5	0.03676206705792	1.86857344615029	1.68639867841410	1.51792070484582
82.66666667	1356.25	0.03846965305845	1.91792487630360	1.74261196769457	1.56851806167401
85.33333333	1400	0.04010560065082	1.96362756328436	1.79882525697504	1.61911541850220
88	1443.75	0.04167820582821	2.00610481539818	1.85503854625551	1.66971277533040
90.66666667	1487.5	0.04319424486556	2.04572594735277	1.91125183553598	1.72031013215859

Temperature Increment (T)	Mechanical Load Increment (P)	Rotation at Top Hinged Joint due to Temperature Increment	Rotation at Top Hinged Joint due to Mechanical Load Increment	Ratio of P/P_{cr}	Ratio of T/T_{cr}
96	1575	0.04607836793372	2.11747689411501	2.02367841409692	1.82150484581498
98.66666667	1618.75	0.04745530635204	2.15010345047447	2.07989170337739	1.87210220264317
101.3333333	1662.5	0.04879370134354	2.18082916924651	2.13610499265786	1.92269955947137
104	1706.25	0.05009660444537	2.20982134239647	2.19231828193833	1.97329691629956
106.6666667	1750	0.05136668618557	2.23730669798543	2.24853157121880	2.02389427312775
109.3333333		0.05260629930869			2.07449162995595
112		0.05381752915862			2.12508898678414
114.6666667		0.05500223426188			2.17568634361234
117.3333333		0.05616207933916			2.22628370044053
120		0.05729856239961			2.27688105726872
122.6666667		0.05841303716202			2.32747841409692
125.3333333		0.05950673174991			2.37807577092511
128		0.06058076438901			2.42867312775331
130.6666667		0.06163615667365			2.47927048458150
133.3333333		0.06267384484602			2.52986784140969
136		0.06369468943995			2.58046519823789
138.6666667		0.06469948356961			2.63106255506608
141.3333333		0.06568896008849			2.68165991189427
144		0.06666379780106			2.73225726872247
146.6666667		0.06762462687583			2.78285462555066
149.3333333		0.06857203358157			2.83345198237886
152		0.06950656444737			2.88404933920705
154.6666667		0.07042872992971			2.93464669603524
157.3333333		0.07133900765608			2.98524405286344
160		0.07223784530349			3.03584140969163

Table B- 12: Numerical Results for Hinged-Hinged Column for Slenderness Ratio of 200 (Data for Rotation at Top Hinged Joint; & convergence tolerance=0.001)

Temperature Increment (T)	Mechanical Load Increment (P)	Rotation at Top Hinged Joint due to Temperature Increment	Rotation at Top Hinged Joint due to Mechanical Load Increment	Ratio of P/P_{cr}	Ratio of T/T_{cr}
0	0	0.00000000000000	0.00000000000000	0.00000000000000	0.00000000000000
1.083333333	10.8333333	0.00001178590873	0.00002283473800	0.03563387175722	0.05262125110132
2.166666667	21.6666667	0.00002472148750	0.00004747088548	0.07126774351444	0.10524250220264
3.25	32.5	0.00003901997674	0.00007412488742	0.10690161527166	0.15786375330397
4.333333333	43.3333333	0.00005495145795	0.00010304920543	0.14253548702888	0.21048500440529
5.416666667	54.1666667	0.00007286316034	0.00013454013204	0.17816935878610	0.26310625550661
6.5	65	0.00009320914013	0.00016894773159	0.21380323054332	0.31572750660793
7.583333333	75.8333333	0.00011659479753	0.00020668861527	0.24943710230054	0.36834875770925
8.666666667	86.6666667	0.00014384566560	0.00024826253969	0.28507097405776	0.42097000881057
9.75	97.5	0.00017611743708	0.00029427423450	0.32070484581498	0.47359125991189
10.83333333	108.333333	0.00021507923126	0.00034546248717	0.35633871757220	0.52621251101322
11.91666667	119.166667	0.00026323395677	0.00040273946515	0.39197258932942	0.57883376211454
13	130	0.00032451208364	0.00046724474125	0.42760646108664	0.63145501321586
14.08333333	140.833333	0.00040545481243	0.00054042086283	0.46324033284386	0.68407626431718
15.16666667	151.666667	0.00051779849828	0.00062412120084	0.49887420460108	0.73669751541850
16.25	162.5	0.00068483930682	0.00072076739870	0.53450807635830	0.78931876651982
17.33333333	173.333333	0.00095984825465	0.00083358524281	0.57014194811552	0.84194001762115
18.41666667	184.166667	0.00149198734759	0.00096696864960	0.60577581987274	0.89456126872247
19.5	195	0.00279442529140	0.00112706103648	0.64140969162996	0.94718251982379
20.58333333	205.833333	0.00563695124085	0.00132272228431	0.67704356338718	0.99980377092511
21.66666667	216.666667	0.00863197607970	0.00156721673335	0.71267743514440	1.05242502202643
22.75	227.5	0.01109067383676	0.00188133847820	0.74831130690162	1.10504627312775
23.83333333	238.333333	0.01316493326923	0.00229963786034	0.78394517865884	1.15766752422907
24.91666667	249.166667	0.01498028897556	0.00288405053147	0.81957905041606	1.21028877533040
26	260	0.01661055618214	0.00375773281153	0.85521292217328	1.26291002643172
27.08333333	270.833333	0.01810120713388	0.00520551321032	0.89084679393050	1.31553127753304
28.16666667	281.666667	0.01948211561246	0.00806865632913	0.92648066568771	1.36815252863436
29.25	292.5	0.02077400386585	0.01639384159859	0.96211453744493	1.42077377973568
30.33333333	303.333333	0.02199188592243	0.14382002528515	0.99774840920215	1.47339503083700
31.41666667	314.166667	0.02314702715097	0.51092823212201	1.03338228095937	1.52601628193833
32.5	325	0.02424812422288	0.71396215835872	1.06901615271659	1.57863753303965
33.58333333	335.833333	0.02530206671163	0.86479596836127	1.10465002447381	1.63125878414097
34.66666667	346.666667	0.02631435468832	0.98756312275298	1.14028389623103	1.68388003524229
35.75	357.5	0.02728955600055	1.09201194207430	1.17591776798825	1.73650128634361
36.83333333	368.333333	0.02823144615119	1.18327270231359	1.21155163974547	1.78912253744493

Temperature Increment (T)	Mechanical Load Increment (P)	Rotation at Top Hinged Joint due to Temperature Increment	Rotation at Top Hinged Joint due to Mechanical Load Increment	Ratio of P/P_{cr}	Ratio of T/T_{cr}
37.91666667	379.166667	0.02914320402947	1.26445206468642	1.24718551150269	1.84174378854626
39	390	0.03002753552515	1.33757766534594	1.28281938325991	1.89436503964758
40.08333333	400.833333	0.03088676614591	1.40411338621924	1.31845325501713	1.94698629074890
41.16666667	411.666667	0.03172291163023	1.46512038028887	1.35408712677435	1.99960754185022
42.25	422.5	0.03253773260646	1.52140991708720	1.38972099853157	2.05222879295154
43.33333333	433.333333	0.03333277748106	1.57361862965351	1.42535487028879	2.10485004405286
44.41666667	444.166667	0.03410941650505	1.62225708103151	1.46098874204601	2.15747129515419
45.5	455	0.03486886913459	1.66774221894142	1.49662261380323	2.21009254625551
46.58333333	465.833333	0.03561222622817	1.71041977742919	1.53225648556045	2.26271379735683
47.66666667	476.666667	0.03634046822077	1.75060358697067	1.56789035731767	2.31533504845815
48.75	487.5	0.03705448013056	1.78848820382924	1.60352422907489	2.36795629955947
49.83333333	498.333333	0.03775506404599	1.82431496771061	1.63915810083211	2.42057755066079
50.91666667	509.166667	0.03844294959134	1.85826728083881	1.67479197258933	2.47319880176212
52	520	0.03911880275594	1.89050439485747	1.71042584434655	2.52582005286344
53.08333333	530.833333	0.03978323338898	1.92116613364182	1.74605971610377	2.57844130396476
54.16666667	541.666667	0.04043680159793	1.95037600194266	1.78169358786099	2.63106255506608
55.25	552.5	0.04108002324035	1.97824367357194	1.81732745961821	2.68368380616740
56.33333333	563.333333	0.04171337466086	2.00486701454716	1.85296133137543	2.73630505726872
57.41666667	574.166667	0.04233729679645	2.03033374314326	1.88859520313265	2.78892630837005
58.5	585	0.04295219874981	2.05472280330800	1.92422907488987	2.84154755947137
59.58333333	595.833333	0.04355846091246	2.07810550961802	1.95986294664709	2.89416881057269
60.66666667	606.666667	0.04415643770532	2.10054650851628	1.99549681840431	2.94679006167401
61.75	617.5	0.04474645999200	2.12210459058070	2.03113069016153	2.99941131277533
62.83333333	628.333333	0.04532883721169	2.14283338106574	2.06676456191875	3.05203256387665
63.91666667	639.166667	0.04590385927018	2.16278193025991	2.10239843367597	3.10465381497798
65	650	0.04647179822184	2.18199522083532	2.13803230543319	3.15727506607930

APPENDIX C: Numerical Data for Fixed-Hinged Columns

Table C- 1: Numerical Results for Fixed-Hinged Column Subjected to 325℃ with 60 Load-Steps and Eccentricity (e=0.001& convergence tolerance=0.001) for 2 & 10 Elements for Slenderness Ratio of 125

Temperature Increment (T)	Horizontal Deflection at Mid-span due to Temperature Increment for 2 Elements	Horizontal Deflection at Mid-span due to Temperature Increment for 10 Elements	Rotation at Top Hinged Joint due to Temperature Increment for 2 Elements	Rotation at Top Hinged Joint due to Temperature Increment for 10 Elements	Ratio of T/T_{cr}
0	0.00000000000000	0.00000000000000	0.00000000000000	0.00000000000000	0.00000000000000
5.416666667	0.02561907984620	0.02561907984623	0.00001823632331	0.00001823632331	0.05036018171806
10.83333333	0.05436985533578	0.05436985533506	0.00003785481986	0.00003785481986	0.10072036343612
16.25	0.08682428042141	0.08682428041568	0.00005908671324	0.00005908671324	0.15108054515419
21.66666667	0.12369950075413	0.12369950072386	0.00008222062725	0.00008222062724	0.20144072687225
27.08333333	0.16590672700307	0.16590672688085	0.00010762179047	0.00010762179043	0.25180090859031
32.5	0.21462123265483	0.21462123225027	0.00013575952806	0.00013575952791	0.30216109030837
37.91666667	0.27138494822117	0.27138494704207	0.00016724753908	0.00016724753862	0.35252127202643
43.33333333	0.33826084030863	0.33826083715538	0.00020290448334	0.00020290448209	0.40288145374449
48.75	0.41807235446048	0.41807234648000	0.00024384792648	0.00024384792328	0.45324163546256
54.16666667	0.51478810390595	0.51478808444457	0.00029164523969	0.00029164523187	0.50360181718062
59.58333333	0.63416609743303	0.63416605030971	0.00034856626637	0.00034856624744	0.55396199889868
65	0.78488754257169	0.78488742776643	0.00041802794702	0.00041802790104	0.60432218061674
70.41666667	0.98067686169564	0.98067657442156	0.00050542561971	0.00050542550505	0.65468236233480
75.83333333	1.24457716974867	1.24457641231694	0.00061980942150	0.00061980912038	0.70504254405286
81.25	1.61845429267763	1.61845211192424	0.00077761064001	0.00077760977647	0.75540272577093
86.66666667	2.18706871778355	2.18706146319992	0.00101207964550	0.00101207678322	0.80576290748899
92.08333333	3.15145609137295	3.15142519265422	0.00140205578953	0.00140204363524	0.85612308920705
97.5	5.12661154210387	5.12640089620612	0.00218867675033	0.00218859407319	0.90648327092511
102.9166667	11.07633921149280	11.07224233825350	0.00453392206691	0.00453231593796	0.95684345264317
108.3333333	33.89095113553650	33.78831710018640	0.01349063558507	0.01345042660135	1.00720363436123
113.75	58.83173588898700	58.60255288562720	0.02327901904981	0.02318934273470	1.05756381607930
119.1666667	77.50980034216890	77.19465545044660	0.03061119509533	0.03048805355640	1.10792399779736
124.5833333	92.40272648021520	92.40224722417340	0.03645894630990	0.03645942265981	1.15828417951542
130	105.54194567321800	105.54009617642500	0.04161876109906	0.04161902651404	1.20864436123348
135.4166667	117.26407317366900	117.26055081816800	0.04622270094095	0.04622267954296	1.25900454295154
140.8333333	127.94149784518300	127.93604958607200	0.05041680190949	0.05041643267884	1.30936472466960
146.25	137.80901405741600	137.80141381852900	0.05429314335222	0.05429237255133	1.35972490638766
151.6666667	147.02543896201100	147.01548090958800	0.05791401038430	0.05791278966152	1.41008508810573
157.0833333	155.70394002006700	155.69143398992100	0.06132378649798	0.06132207158880	1.46044526982379
162.5	163.92844513568700	163.91321352616900	0.06455538865621	0.06455313851707	1.51080545154185
167.9166667	171.76319624709400	171.74507181177600	0.06763401368316	0.06763118988793	1.56116563325991

Temperature Increment (T)	Horizontal Deflection at Mid-span due to Temperature Increment for 2 Elements	Horizontal Deflection at Mid-span due to Temperature Increment for 10 Elements	Rotation at Top Hinged Joint due to Temperature Increment for 2 Elements	Rotation at Top Hinged Joint due to Temperature Increment for 10 Elements	Ratio of T/T_{cr}
173.3333333	179.25883899276700	179.23777314292000	0.07057952727411	0.07057616338839	1.61152581497797
178.75	186.45538624858400	186.43109811149000	0.07340762198041	0.07340360123859	1.66188599669603
184.1666667	193.38614466101900	193.35849552625200	0.07613136392781	0.07612665687119	1.71224617841410
189.5833333	200.07849282352500	200.04734810765100	0.07876149285422	0.07875607055855	1.76260636013216
195	206.55542301472600	206.52065176512000	0.08130702819655	0.08130086217265	1.81296654185022
200.4166667	212.83646430939300	212.79793921777800	0.08377563110277	0.08376869344518	1.86332672356828
205.8333333	218.93837015160500	218.89596743713500	0.08617387407966	0.08616613752872	1.91368690528634
211.25	224.87564008351700	224.82923931842200	0.08850744560398	0.08849888356144	1.96404708700440
216.6666667	230.66092197403600	230.61040588934100	0.09078130787062	0.09077189439063	2.01440726872247
222.0833333	236.30532654290600	236.25058083316200	0.09299982014612	0.09298952991369	2.06476745044053
227.5	241.81867644960100	241.75958958558700	0.09516683646052	0.09515564476408	2.11512763215859
232.9166667	247.20970583481100	247.14616888812100	0.09728578386810	0.09727366656968	2.16548781387665
238.3333333	252.48622183985800	252.41812832079500	0.09935972579657	0.09934665930185	2.21584799559471
243.75	257.65523659217500	257.58248230097800	0.10139141381364	0.10137737504283	2.26620817731277
249.1666667	262.72307599442200	262.64555888514500	0.10338333029624	0.10336829665637	2.31656835903084
254.5833333	267.69547010908500	267.61309016523200	0.10533772388165	0.10532167324059	2.36692854074890
260	272.57762880361300	272.49028792448800	0.10725663913787	0.10723954980007	2.41728872246696
265.4166667	277.27726398748000	277.28190738596200	0.10910397264362	0.10912379224826	2.46764890418502
270.8333333	281.99108852906000	281.99230126544100	0.11095671267659	0.11097610860761	2.51800908590308
276.25	286.62789426035500	286.62546587103300	0.11277914861795	0.11279806709045	2.56836926762114
281.6666667	291.19126837039400	291.18508063375200	0.11457270133723	0.11459111160374	2.61872944933921
287.0833333	295.68460475558200	295.67454217733200	0.11633870297087	0.11635657511207	2.66908963105727
292.5	300.11104419597100	300.09699382143600	0.11807838634353	0.11809569120976	2.71944981277533
297.9166667	304.47349997533300	304.45535124429200	0.11979289502181	0.11980960418660	2.76980999449339
303.3333333	308.77468028411800	308.75232489835200	0.12148329210233	0.12149937782024	2.82017017621145
308.75	313.01710786512400	312.99043966722300	0.12315056791842	0.12316600308649	2.87053035792951
314.1666667	317.20313730530300	317.17205216742900	0.12479564682349	0.12481040494600	2.92089053964758
319.5833333	321.33497030941500	321.29936603102800	0.12641939318273	0.12643344833887	2.97125072136564
325	325.41466923593400	325.37444544951400	0.12802261668329	0.12803594349746	3.02161090308370

Table C- 2: Numerical Results for Fixed-Hinged Column for Slenderness Ratio of 50 (Data for Horizontal Mid-Span Deflections& convergence tolerance=0.001)

Temperature Increment (T)	Mechanical Load Increment (P)	Horizontal Deflection at Mid-Span due to Temperature Increment	Horizontal Deflection at Mid-Span due to Temperature Increment per Original Length	Horizontal Deflection at Mid-Span due to Mechanical Load Increment	Horizontal Deflection at Mid-Span due to Mechanical Load Increment per original length	Ratio of P/Pcr	Ratio of T/T_{cr}
0	0	0.00000000000000	0.00000000000000	0.00000000000000	0.00000000000000	0.00000000000000	0.00000000000000
25.175	371.875	0.01877273665202	0.00000426653106	0.03136716697173	0.00000712890158	0.03746053597651	0.03744938066960
50.35	743.75	0.03920453365404	0.00000891012129	0.06507063586895	0.00001478878088	0.07492107195301	0.07489876133921
75.525	1115.625	0.06151099311519	0.00001397977116	0.10139797574261	0.00002304499449	0.11238160792952	0.11234814200881
100.7	1487.5	0.08594596313155	0.00001953317344	0.14068670128693	0.00003197425029	0.14984214390602	0.14979752267841
125.875	1859.375	0.11281035439376	0.00002563871691	0.18333566198701	0.00004166719591	0.18730267988253	0.18724690334802
151.05	2231.25	0.14246350840282	0.00003237807009	0.22981970152335	0.00005223175035	0.22476321585903	0.22469628401762
176.225	2603.125	0.17533802189882	0.00003984955043	0.28070873850053	0.00006379744057	0.26222375183554	0.26214566468723
201.4	2975	0.21195931806125	0.00004817257229	0.33669290721314	0.00007652111528	0.29968428781204	0.29959504535683
226.575	3346.875	0.25297183668668	0.00005749359925	0.39861613017604	0.00009059457504	0.33714482378855	0.33704442602643
251.75	3718.75	0.29917460962161	0.00006799422946	0.46752161791236	0.00010625491316	0.37460535976505	0.37449380669604
276.925	4090.625	0.35157039255110	0.00007990236194	0.54471455198279	0.00012379876181	0.41206589574156	0.41194318736564
302.1	4462.5	0.41143478585054	0.00009350790588	0.63185003227265	0.00014360228006	0.44952643171806	0.44939256803524
327.275	4834.375	0.48041551826189	0.00010918534506	0.73105902586323	0.00016614977861	0.48698696769457	0.48684194870485
352.45	5206.25	0.56067844681035	0.00012742691973	0.84513296379308	0.00019207567359	0.52444750367107	0.52429132937445
377.625	5578.125	0.65512808730204	0.00014889274711	0.97780153065327	0.00022222762060	0.56190803964758	0.56174071004405
402.8	5950	0.76775116454711	0.00017448890103	1.13416359503497	0.00025776445342	0.59936857562408	0.59919009071366
427.975	6321.875	0.90417139240010	0.00020549349827	1.32137967287299	0.00030031356202	0.63682911160059	0.63663947138326
453.15	6693.75	1.07258415596392	0.00024376912636	1.54983215891587	0.00035223458157	0.67428964757709	0.67408885205286
478.325	7065.625	1.28541329728138	0.00029213938575	1.83516842631488	0.00041708373325	0.71175018355360	0.71153823272247
503.5	7437.5	1.56243574470040	0.00035509903289	2.20212472338383	0.00050048289168	0.74921071953010	0.74898761339207

Temperature Increment (T)	Mechanical Load Increment (P)	Horizontal Deflection at Mid-Span due to Temperature Increment	Horizontal Deflection at Mid-Span due to Temperature Increment per Original Length	Horizontal Deflection at Mid-Span due to Mechanical Load Increment	Horizontal Deflection at Mid-Span due to Mechanical Load Increment per original length	Ratio of P/Pcr	Ratio of T/T_{cr}
528.675	7809.375	1.93714917195872	0.00044026117545	2.69224934839731	0.00061187485191	0.78667125550661	0.78643699406167
553.85	8181.25	2.47110897860053	0.00056161567695	3.38111368132308	0.00076843492757	0.82413179148311	0.82388637473128
579.025	8553.125	3.29080725848295	0.00074791074056	4.42210983221510	0.00100502496187	0.86159232745962	0.86133575540088
604.2	8925	4.70198080451101	0.00106863200103	6.18135593131282	0.00140485362075	0.89905286343612	0.89878513607049
629.375	9296.875	7.65399048342755	0.00173954329169	9.80205316361520	0.00222773935537	0.93651339941263	0.93623451674009
654.55	9668.75	16.18143933956880	0.00367759984990	21.58867315682220	0.00490651662655	0.97397393538913	0.97368389740969
679.725	10040.625	36.22641240289580	0.00823327554611	341.65206220354600	0.07764819595535	1.01143447136564	1.01113327807929
704.9	10412.5	55.13380826039670	0.01253041096827	840.00202822024100	0.19090955186824	1.04889500734214	1.04858265874890
730.075	10784.375	70.17255367160370	0.01594830765264	1101.54457353553000	0.25035103943989	1.08635554331865	1.08603203941850
755.25	11156.25	82.46866720706260	0.01874287891070	1279.09994513341000	0.29070453298487	1.12381607929515	1.12348142008811
780.425	11528.125	93.48421255614860	0.02124641194458			1.16127661527166	1.16093080075771
805.6	11900	103.38948037847300	0.02349760917693			1.19873715124816	1.19838018142731
830.775	12271.875	112.45853700280800	0.02555875840973			1.23619768722467	1.23582956209692
855.95	12643.75	120.87018016574300	0.02747049549221			1.27365822320117	1.27327894276652
881.125	13015.625	128.74813775110700	0.02926094039798			1.31111875917768	1.31072832343612
906.3	13387.5	136.18201276966000	0.03095045744765			1.34857929515419	1.34817770410573
931.475	13759.375	143.23906181155700	0.03255433222990			1.38603983113069	1.38562708477533
956.65	14131.25	149.97124504610400	0.03408437387411			1.42350036710720	1.42307646544493
981.825	14503.125	156.41984967518600	0.03554996583527			1.46096090308370	1.46052584611454
1007	14875	162.61762677212400	0.03695855153912			1.49842143906021	1.49797522678414
1032.175	15246.875	168.59202873564500	0.03831637016719			1.53588197503671	1.53542460745374
1057.35	15618.75	174.36569740485300	0.03962856759201			1.57334251101322	1.57287398812335
1082.525	15990.625	179.95771274005900	0.04089948016820			1.61080304698972	1.61032336879295
1107.7	16362.5	185.38432864964500	0.04213280196583			1.64826358296623	1.64777274946255

Temperature Increment (T)	Mechanical Load Increment (P)	Horizontal Deflection at Mid-Span due to Temperature Increment	Horizontal Deflection at Mid-Span due to Temperature Increment per Original Length	Horizontal Deflection at Mid-Span due to Mechanical Load Increment	Horizontal Deflection at Mid-Span due to Mechanical Load Increment per original length	Ratio of P/Pcr	Ratio of T/T_{cr}
1132.875	16734.375	190.65952448214800	0.04333171010958			1.68572411894273	1.68522213013216
1158.05	17106.25	195.79542578487500	0.04449896040565			1.72318465491924	1.72267151080176
1183.225	17478.125	200.80263023343900	0.04563696141669			1.76064519089574	1.76012089147136
1208.4	17850	205.69046355849700	0.04674783262693			1.79810572687225	1.79757027214097
1233.575	18221.875	210.46718297695100	0.04783345067658			1.83556626284875	1.83501965281057
1258.75	18593.75	215.14014069331100	0.04889548652121			1.87302679882526	1.87246903348017
1283.925	18965.625	219.71591663565900	0.04993543559901			1.91048733480176	1.90991841414978
1309.1	19337.5	224.20042720768400	0.05095464254720			1.94794787077827	1.94736779481938
1334.275	19709.375	228.59901514201200	0.05195432162318			1.98540840675477	1.98481717548898
1359.45	20081.25	232.91652431448600	0.05293557370784			2.02286894273128	2.02226655615859
1384.625	20453.125	237.15736248196900	0.05389940056408			2.06032947870778	2.05971593682819
1409.8	20825	241.32555424103300	0.05484671687296			2.09779001468429	2.09716531749780
1434.975	21196.875	245.42478600615200	0.05577836045594			2.13525055066079	2.13461469816740
1460.15	21568.75	249.45844442815900	0.05669510100640			2.17271108663730	2.17206407883700
1485.325	21940.625	253.42964938432500	0.05759764758735			2.21017162261380	2.20951345950661
1510.5	22312.5	257.34128244815800	0.05848665510185			2.24763215859031	2.24696284017621
1535.675	22684.375	261.19601157278000	0.05936272990290			2.28509269456681	2.28441222084581
1560.85	23056.25	264.99631258523900	0.06022643467846			2.32255323054332	2.32186160151542
1586.025	23428.125	268.74448798081700	0.06107829272291			2.36001376651982	2.35931098218502
1611.2	23800	272.44268342024000	0.06191879168642			2.39747430249633	2.39676036285462
1636.375	24171.875	276.09290226365500	0.06274838687810			2.43493483847283	2.43420974352423
1661.55	24543.75	279.69701841928100	0.06356750418620			2.47239537444934	2.47165912419383
1686.725	24915.625	283.16025931445400	0.06435460438965			2.50985591042584	2.50910850486343
1711.9	25287.5	286.67616781770700	0.06515367450402			2.54731644640235	2.54655788553304

Temperature Increment (T)	Mechanical Load Increment (P)	Horizontal Deflection at Mid-Span due to Temperature Increment	Horizontal Deflection at Mid-Span due to Temperature Increment per Original Length	Horizontal Deflection at Mid-Span due to Mechanical Load Increment	Horizontal Deflection at Mid-Span due to Mechanical Load Increment per original length	Ratio of P/Pcr	Ratio of T/T_{cr}
1737.075	25659.375	290.15101042684800	0.06594341146065			2.58477698237885	2.58400726620264
1762.25	26031.25	293.58617768304800	0.06672413129160			2.62223751835536	2.62145664687224
1787.425	26403.125	296.98304383685800	0.06749614632656			2.65969805433186	2.65890602754185
1812.6	26775	300.34290620136000	0.06825975140940			2.69715859030837	2.69635540821145
1837.775	27146.875	303.66699103183300	0.06901522523451			2.73461912628488	2.73380478888105
1862.95	27518.75	306.95645884850900	0.06976283155648			2.77207966226138	2.77125416955066
1888.125	27890.625	310.21240925786000	0.07050282028588			2.80954019823789	2.80870355022026
1913.3	28262.5	313.43588532899000	0.07123542848386			2.84700073421439	2.84615293088986
1938.475	28634.375	316.62787757424100	0.07196088126687			2.88446127019090	2.88360231155947
1963.65	29006.25	319.78932757688200	0.07267939263111			2.92192180616740	2.92105169222907
1988.825	29378.125	322.92113130336100	0.07339116620531			2.95938234214391	2.95850107289867
2014	29750	326.02414213299400	0.07409639593932			2.99684287812041	2.99595045356828

Table C- 3: Numerical Results for Fixed-Hinged Column for Slenderness Ratio of 125 (Data for Horizontal Mid-Span Deflections; & convergence tolerance=0.001)

Temperature Increment (T)	Mechanical Load Increment (P)	Horizontal Deflection at Mid-Span due to Temperature Increment	Horizontal Deflection at Mid-Span due to Temperature Increment per Original Length	Horizontal Deflection at Mid-Span due to Mechanical Load Increment	Horizontal Deflection at Mid-Span due to Mechanical Load Increment per original length	Ratio of P/Pcr	Ratio of T/T_{cr}
0	0	0.00000000000000	0.00000000000000	0.00000000000000	0.00000000000000	0.00000000000000	0.00000000000000
4.0625	59.5	0.01894040805806	0.00000172185528	0.07845831395911	0.00000713257400	0.03746053597651	0.03777013628855
8.125	119	0.03957019777697	0.00000359729071	0.16284680312984	0.00001480425483	0.07492107195301	0.07554027257709
12.1875	178.5	0.06211102948675	0.00000564645723	0.25389937460719	0.00002308176133	0.11238160792952	0.11331040886564
16.25	238	0.08682428042132	0.00000789311640	0.35247810236752	0.00003204346385	0.14984214390602	0.15108054515419
20.3125	297.5	0.11402029700155	0.00001036548155	0.45960261921445	0.00004178205629	0.18730267988253	0.18885068144273
24.375	357	0.14407035443638	0.00001309730495	0.57648799821942	0.00005240799984	0.22476321585903	0.22662081773128
28.4375	416.5	0.17742229461832	0.00001612929951	0.70459413044545	0.00006405401186	0.26222375183554	0.26439095401982
32.5	476	0.21462123265529	0.00001951102115	0.84569088781074	0.00007688098980	0.29968428781204	0.30216109030837
36.5625	535.5	0.25633735708296	0.00002330339610	1.00194529168171	0.00009108593561	0.33714482378855	0.33993122659692
40.625	595	0.30340382917580	0.00002758216629	1.17603987680367	0.00010691271607	0.37460535976505	0.37770136288546
44.6875	654.5	0.35686933534702	0.00003244266685	1.37133610454734	0.00012466691860	0.41206589574156	0.41547149917401
48.75	714	0.41807235446003	0.00003800657768	1.59210418776351	0.00014473674434	0.44952643171806	0.45324163546256
52.8125	773.5	0.48874837768183	0.00004443167070	1.84385310843624	0.00016762300986	0.48698696769457	0.49101177175110
56.875	833	0.57118849292540	0.00005192622663	2.13381578687815	0.00019398325335	0.52444750367107	0.52878190803965
60.9375	892.5	0.66848051769909	0.00006077095615	2.47168174467248	0.00022469834042	0.56190803964758	0.56655204432819
65	952	0.78488754257126	0.00007135341296	2.87073825255530	0.00026097620478	0.59936857562408	0.60432218061674
69.0625	1011.5	0.92646475711507	0.00008422406883	3.34971289977276	0.00030451935452	0.63682911160059	0.64209231690529
73.125	1071	1.10210988156247	0.00010019180741	3.93587800975380	0.00035780709180	0.67428964757709	0.67986245319383

Temperature Increment (T)	Mechanical Load Increment (P)	Horizontal Deflection at Mid-Span due to Temperature Increment	Horizontal Deflection at Mid-Span due to Temperature Increment per Original Length	Horizontal Deflection at Mid-Span due to Mechanical Load Increment	Horizontal Deflection at Mid-Span due to Mechanical Load Increment per original length	Ratio of P/Pcr	Ratio of T/T_{cr}
77.1875	1130.5	1.32544949615547	0.00012049540874	4.67055500044065	0.00042459590913	0.71175018355360	0.71763258948238
81.25	1190	1.61845429267424	0.00014713220842	5.61950341590289	0.00051086394690	0.74921071953010	0.75540272577093
85.3125	1249.5	2.01895882805543	0.00018354171164	6.89412962424438	0.00062673905675	0.78667125550661	0.79317286205947
89.375	1309	2.59805426485340	0.00023618675135	8.69942216768974	0.00079085656070	0.82413179148311	0.83094299834802
93.4375	1368.5	3.50651395377998	0.00031877399580	11.45835204833930	0.00104166836803	0.86159232745962	0.86871313463656
97.5	1428	5.12661147969934	0.00046605558906	16.20655321341240	0.00147332301940	0.89905286343612	0.90648327092511
101.5625	1487.5	8.73794324228154	0.00079435847657	26.33091697821960	0.00239371972529	0.93651339941263	0.94425340721366
105.625	1547	19.83169022090590	0.00180288092917	62.95834796454900	0.00572348617860	0.97397393538913	0.98202354350220
109.6875	1606.5	40.90430915112700	0.00371857355919	1093.07586504881000	0.09937053318626	1.01143447136564	1.01979367979075
113.75	1666	58.83170965294320	0.00534833724118	2207.69732212315000	0.20069975655665	1.04889500734214	1.05756381607929
117.8125	1725.5	73.23668232771710	0.00665788021161	2828.66995798508000	0.25715181436228	1.08635554331865	1.09533395236784
121.875	1785	85.11614842552240	0.00773783167505	3256.13960453831000	0.29601269132167	1.12381607929515	1.13310408865639
125.9375	1844.5	95.84903367206900	0.00871354851564			1.16127661527166	1.17087422494493
130	1904	105.54194104388400	0.00959472191308			1.19873715124816	1.20864436123348
134.0625	1963.5	114.44299504926000	0.01040390864084			1.23619768722467	1.24641449752203
138.125	2023	122.71641432163000	0.01115603766560			1.27365822320117	1.28418463381057
142.1875	2082.5	130.47710600449800	0.01186155509132			1.31111875917768	1.32195477009912
146.25	2142	137.80901386373600	0.01252809216943			1.34857929515418	1.35972490638766
150.3125	2201.5	144.77558923526600	0.01316141720321			1.38603983113069	1.39749504267621
154.375	2261	151.42636825998400	0.01376603347818			1.42350036710720	1.43526517896476
158.4375	2320.5	157.80000937806600	0.01434545539801			1.46096090308370	1.47303531525330
162.5	2380	163.92857318669600	0.01490259756243			1.49842143906021	1.51080545154185
166.5625	2439.5	169.83819086474600	0.01543983553316			1.53588197503671	1.54857558783040
170.625	2499	175.55067700970300	0.01595915245543			1.57334251101322	1.58634572411894

Temperature Increment (T)	Mechanical Load Increment (P)	Horizontal Deflection at Mid-Span due to Temperature Increment	Horizontal Deflection at Mid-Span due to Temperature Increment per Original Length	Horizontal Deflection at Mid-Span due to Mechanical Load Increment	Horizontal Deflection at Mid-Span due to Mechanical Load Increment per original length	Ratio of P/Pcr	Ratio of T/T_{cr}
174.6875	2558.5	181.08446333795100	0.01646222393981			1.61080304698972	1.62411586040749
178.75	2618	186.45528810004600	0.01695048073637			1.64826358296623	1.66188599669603
182.8125	2677.5	191.67671523547500	0.01742515593050			1.68572411894273	1.69965613298458
186.875	2737	196.76053187440900	0.01788732107949			1.72318465491924	1.73742626927313
190.9375	2796.5	201.71705723488800	0.01833791429408			1.76064519089574	1.77519640556167
195	2856	206.55538587219300	0.01877776235202			1.79810572687225	1.81296654185022
199.0625	2915.5	211.28358153533700	0.01920759832139			1.83556626284875	1.85073667813877
203.125	2975	215.90883334104800	0.01962807575828			1.87302679882526	1.88850681442731
207.1875	3034.5	220.43758283437600	0.02003978025767			1.91048733480176	1.92627695071586
211.25	3094	224.87562829666900	0.02044323893606			1.94794787077827	1.96404708700440
215.3125	3153.5	229.22821108378900	0.02083892828034			1.98540840675477	2.00181722329295
219.375	3213	233.50008763444500	0.02122728069404			2.02286894273128	2.03958735958150
223.4375	3272.5	237.69558994882300	0.02160868999535			2.06032947870778	2.07735749587004
227.5	3332	241.81867671406500	0.02198351606492			2.09779001468429	2.11512763215859
231.5625	3391.5	245.87297678411900	0.02235208879856			2.13525055066079	2.15289776844714
235.625	3451	249.86182636491900	0.02271471148772			2.17271108663730	2.19066790473568
239.6875	3510.5	253.78830098323600	0.02307166372575			2.21017162261380	2.22843804102423
243.75	3570	257.65524310556200	0.02342320391869			2.24763215859031	2.26620817731277
247.8125	3629.5	261.46528610881800	0.02376957146444			2.28509269456681	2.30397831360132
251.875	3689	265.22087517436200	0.02411098865221			2.32255323054332	2.34174844988987
255.9375	3748.5	268.92428557442600	0.02444766232495			2.36001376651982	2.37951858617841
260	3808	272.57763873763300	0.02477978533978			2.39747430249633	2.41728872246696
264.0625	3867.5	276.08625486320300	0.02509875044211			2.43493483847283	2.45505885875551
268.125	3927	279.64400689186000	0.02542218244471			2.47239537444934	2.49282899504405

Temperature Increment (T)	Mechanical Load Increment (P)	Horizontal Deflection at Mid-Span due to Temperature Increment	Horizontal Deflection at Mid-Span due to Temperature Increment per Original Length	Horizontal Deflection at Mid-Span due to Mechanical Load Increment	Horizontal Deflection at Mid-Span due to Mechanical Load Increment per original length	Ratio of P/Pcr	Ratio of T/T_{cr}
272.1875	3986.5	283.15736569412600	0.02574157869947			2.50985591042584	2.53059913133260
276.25	4046	286.62789030933900	0.02605708093721			2.54731644640235	2.56836926762114
280.3125	4105.5	290.05711536266200	0.02636882866933			2.58477698237885	2.60613940390969
284.375	4165	293.44648616913500	0.02667695328810			2.62223751835536	2.64390954019824
288.4375	4224.5	296.79736582799500	0.02698157871164			2.65969805433186	2.68167967648678
292.5	4284	300.11104161916300	0.02728282196538			2.69715859030837	2.71944981277533
296.5625	4343.5	303.38873077411400	0.02758079370674			2.73461912628487	2.75721994906388
300.625	4403	306.63158569439400	0.02787559869949			2.77207966226138	2.79499008535242
304.6875	4462.5	309.84069868100400	0.02816733624373			2.80954019823788	2.83276022164097
308.75	4522	313.01710622948800	0.02845610056632			2.84700073421439	2.87053035792951
312.8125	4581.5	316.16179293851500	0.02874198117623			2.88446127019089	2.90830049421806
316.875	4641	319.27569507356400	0.02902506318851			2.92192180616740	2.94607063050661
320.9375	4700.5	322.35970382223000	0.02930542762020			2.95938234214391	2.98384076679515
325	4760	325.41466827306000	0.02958315166119			2.99684287812041	3.02161090308370

Table C- 4: Numerical Results for Fixed-Hinged Column for Slenderness Ratio of 200 (Data for Horizontal Mid-Span Deflections; convergence tolerance=0.001)

Temperature Increment (T)	Mechanical Load Increment (P)	Horizontal Deflection at Mid-Span due to Temperature Increment	Horizontal Deflection at Mid-Span due to Temperature Increment per Original Length	Horizontal Deflection at Mid-Span due to Mechanical Load Increment	Horizontal Deflection at Mid-Span due to Mechanical Load Increment per original length	Ratio of P/Pcr	Ratio of T/T_{cr}
0	0	0.00000000000000	0.00000000000000	0.00000000000000	0.00000000000000	0.00000000000000	0.00000000000000
1.575	23.125	0.01879217058317	0.00000106773696	0.12488489823572	0.00000709573285	0.03727165932452	0.03748656972687
3.15	46.25	0.03924690131291	0.00000222993757	0.25917352108958	0.00001472576824	0.07454331864905	0.07497313945374
4.725	69.375	0.06158049051556	0.00000349889151	0.40402377092903	0.00002295589608	0.11181497797357	0.11245970918062
6.3	92.5	0.08604765076517	0.00000488907107	0.56079469053632	0.00003186333469	0.14908663729809	0.14994627890749
7.875	115.625	0.11295037510197	0.00000641763495	0.73109233388000	0.00004153933715	0.18635829662261	0.18743284863436
9.45	138.75	0.14264937246658	0.00000810507798	0.91682880904312	0.00005209254597	0.22362995594714	0.22491941836123
11.025	161.875	0.17557898449183	0.00000997607866	1.12029913010828	0.00006365335967	0.26090161527166	0.26240598808811
12.6	185	0.21226688537406	0.00001206061849	1.34428247915483	0.00007637968632	0.29817327459618	0.29989255781498
14.175	208.125	0.25336045421454	0.00001439548035	1.59217743256345	0.00009046462685	0.33544493392071	0.33737912754185
15.75	231.25	0.29966261286275	0.00001702628482	1.86818523314683	0.00010614688825	0.37271659324523	0.37486569726872
17.325	254.375	0.35218134312103	0.00002001030359	2.17756228227774	0.00012372512967	0.40998825256975	0.41235226699560
18.9	277.5	0.41219938603206	0.00002342041966	2.52697440822792	0.00014357809138	0.44725991189427	0.44983883672247
20.475	300.625	0.48137441508907	0.00002735081904	2.92500422776421	0.00016619342203	0.48453157121880	0.48732540644934
22.05	323.75	0.56188644225101	0.00003192536604	3.38289478565993	0.00019220993100	0.52180323054332	0.52481197617621
23.625	346.875	0.65666064199074	0.00003731026375	3.91566866165476	0.00022248117396	0.55907488986784	0.56229854590308
25.2	370	0.76971478069217	0.00004373379436	4.54386405595520	0.00025817409409	0.59634654919236	0.59978511562996
26.775	393.125	0.90672084040899	0.00005151822957	5.29632487037851	0.00030092754945	0.63361820851689	0.63727168535683
28.35	416.25	1.07595239199774	0.00006113365864	6.21487539948728	0.00035311792043	0.67088986784141	0.67475825508370
29.925	439.375	1.28996636437773	0.00007329354343	7.36255323656460	0.00041832688844	0.70816152716593	0.71224482481057
31.5	462.5	1.56878058543040	0.00008913526054	8.83901931854411	0.00050221700674	0.74543318649046	0.74973139453745

Temperature Increment (T)	Mechanical Load Increment (P)	Horizontal Deflection at Mid-Span due to Temperature Increment	Horizontal Deflection at Mid-Span due to Temperature Increment per Original Length	Horizontal Deflection at Mid-Span due to Mechanical Load Increment	Horizontal Deflection at Mid-Span due to Mechanical Load Increment per original length	Ratio of P/Pcr	Ratio of T/T_{cr}
33.075	485.625	1.94636422735506	0.00011058887655	10.81168551864610	0.00061430031356	0.78270484581498	0.78721796426432
34.65	508.75	2.48529532918466	0.00014120996189	13.58509299041070	0.00077188028355	0.81997650513950	0.82470453399119
36.225	531.875	3.31461898354557	0.00018833062407	17.77750004035130	0.00101008522957	0.85724816446402	0.86219110371806
37.8	555	4.74787543781390	0.00026976564988	24.86497828813900	0.00141278285728	0.89451982378855	0.89967767344493
39.375	578.125	7.76648970690754	0.00044127782426	39.45885898093440	0.00224198062392	0.93179148311307	0.93716424317181
40.95	601.25	16.55067075266860	0.00094037902004	87.02100954823770	0.00494437554251	0.96906314243759	0.97465081289868
42.525	624.375	36.68525587715850	0.00208438953847	1376.14695273976000	0.07819016776930	1.00633480176211	1.01213738262555
44.1	647.5	55.39468098814640	0.00314742505614	3371.59224391325000	0.19156774113144	1.04360646108664	1.04962395235242
45.675	670.625	70.29199930221690	0.00399386359672	4418.75310321928000	0.25106551722837	1.08087812041116	1.08711052207930
47.25	693.75	82.48426072145990	0.00468660572281	5131.13731040441000	0.29154189263661	1.11814977973568	1.12459709180617
48.825	716.875	93.41533529711710	0.00530768950552			1.15542143906021	1.16208366153304
50.4	740	103.24749900796100	0.00586633517091			1.19269309838473	1.19957023125991
51.975	763.125	112.25061400589100	0.00637787579579			1.22996475770925	1.23705680098678
53.55	786.25	120.60108873265800	0.00685233458708			1.26723641703377	1.27454337071366
55.125	809.375	128.42118616115700	0.00729665830461			1.30450807635830	1.31202994044053
56.7	832.5	135.79955631150300	0.00771588388134			1.34177973568282	1.34951651016740
58.275	855.625	142.80280618914800	0.00811379580620			1.37905139500734	1.38700307989427
59.85	878.75	149.48268533445900	0.00849333439400			1.41632305433187	1.42448964962115
61.425	901.875	155.87939800073600	0.00885678397731			1.45359471365639	1.46197621934802
63	925	162.02619275621000	0.00920603367933			1.49086637298091	1.49946278907489
64.575	948.125	167.95008124315000	0.00954261825245			1.52813803230543	1.53694935880176
66.15	971.25	173.67355592337700	0.00986781567746			1.56540969162996	1.57443592852864
67.725	994.375	179.21557926599500	0.01018270336739			1.60268135095448	1.61192249825551
69.3	1017.5	184.59231123815200	0.01048819950217			1.63995301027900	1.64940906798238

Temperature Increment (T)	Mechanical Load Increment (P)	Horizontal Deflection at Mid-Span due to Temperature Increment	Horizontal Deflection at Mid-Span due to Temperature Increment per Original Length	Horizontal Deflection at Mid-Span due to Mechanical Load Increment	Horizontal Deflection at Mid-Span due to Mechanical Load Increment per original length	Ratio of P/Pcr	Ratio of T/T_{cr}
70.875	1040.625	189.81765523773900	0.01078509404760			1.67722466960352	1.68689563770925
72.45	1063.75	194.90367481446100	0.01107407243264			1.71449632892805	1.72438220743612
74.025	1086.875	199.86091661321600	0.01135573389848			1.75176798825257	1.76186877716300
75.6	1110	204.69866405753000	0.01163060591236			1.78903964757709	1.79935534688987
77.175	1133.125	209.42513907015100	0.01189915562899			1.82631130690162	1.83684191661674
78.75	1156.25	214.04766425420900	0.01216179910535			1.86358296622614	1.87432848634361
80.325	1179.375	218.57279459715400	0.01241890878393			1.90085462555066	1.91181505607049
81.9	1202.5	223.00642540850000	0.01267081962548			1.93812628487518	1.94930162579736
83.475	1225.625	227.35388152344000	0.01291783417747			1.97539794419971	1.98678819552423
85.05	1248.75	231.61999159473600	0.01316022679516			2.01266960352423	2.02427476525110
86.625	1271.875	235.80915040695200	0.01339824718221			2.04994126284875	2.06176133497798
88.2	1295	239.92537148867300	0.01363212338004			2.08721292217327	2.09924790470485
89.775	1318.125	243.97233180604100	0.01386206430716			2.12448458149780	2.13673447443172
91.35	1341.25	247.95340994496100	0.01408826192869			2.16175624082232	2.17422104415859
92.925	1364.375	251.87171890494000	0.01431089311960			2.19902790014684	2.21170761388546
94.5	1387.5	255.73013440393000	0.01453012127295			2.23629955947137	2.24919418361234
96.075	1410.625	259.53131942315600	0.01474609769450			2.27357121879589	2.28668075333921
97.65	1433.75	263.27774558397100	0.01495896281727			2.31084287812041	2.32416732306608
99.225	1456.875	266.97171184245000	0.01516884726378			2.34811453744493	2.36165389279295
100.8	1480	270.61536090146500	0.01537587277849			2.38538619676946	2.39914046251983
102.375	1503.125	274.11444791058800	0.01557468454037			2.42265785609398	2.43662703224670
103.95	1526.25	277.66202086030200	0.01577625118524			2.45992951541850	2.47411360197357
105.525	1549.375	281.16499283360000	0.01597528368373			2.49720117474302	2.51160017170044
107.1	1572.5	284.62493683520300	0.01617187141109			2.53447283406755	2.54908674142732

Temperature Increment (T)	Mechanical Load Increment (P)	Horizontal Deflection at Mid-Span due to Temperature Increment	Horizontal Deflection at Mid-Span due to Temperature Increment per Original Length	Horizontal Deflection at Mid-Span due to Mechanical Load Increment	Horizontal Deflection at Mid-Span due to Mechanical Load Increment per original length	Ratio of P/Pcr	Ratio of T/T_{cr}
108.675	1595.625	288.04340039721500	0.01636610229530			2.57174449339207	2.58657331115419
110.25	1618.75	291.42184059125200	0.01655805912450			2.60901615271659	2.62405988088106
111.825	1641.875	294.76163124600700	0.01674781995716			2.64628781204112	2.66154645060793
113.4	1665	298.06406945142900	0.01693545849156			2.68355947136564	2.69903302033480
114.975	1688.125	301.33038142428300	0.01712104439911			2.72083113069016	2.73651959006168
116.55	1711.25	304.56172780985800	0.01730464362556			2.75810279001468	2.77400615978855
118.125	1734.375	307.75920848485100	0.01748631866391			2.79537444933921	2.81149272951542
119.7	1757.5	310.92386691726200	0.01766612880212			2.83264610866373	2.84897929924229
121.275	1780.625	314.05669413258300	0.01784413034844			2.86991776798825	2.88646586896917
122.85	1803.75	317.15863232858200	0.01802037683685			2.90718942731278	2.92395243869604
124.425	1826.875	320.23057817618500	0.01819491921456			2.94446108663730	2.96143900842291
126	1850	323.27338583891000	0.01836780601357			2.98173274596182	2.99892557814978

Table C- 5: Numerical Results for Fixed-Hinged Column for Slenderness Ratio of 50 (Data for Rotation at Top Hinged Joint; convergence tolerance=0.001)

Temperature Increment (T)	Mechanical Load Increment (P)	Rotation at Top Hinged Joint due to Temperature Increment	Rotation at Top Hinged Joint due to Mechanical Load Increment	Ratio of P/Pcr	Ratio of T/T_{cr}
0	0	0.00000000000000	0.00000000000000	0.00000000000000	0.00000000000000
25.175	371.875	0.00003359374132	0.00002459434319	0.03746053597651	0.03744938066960
50.35	743.75	0.00006902461145	0.00005134601754	0.07492107195301	0.07489876133921
75.525	1115.625	0.00010651093240	0.00008053366909	0.11238160792952	0.11234814200881
100.7	1487.5	0.00014630886124	0.00011248507268	0.14984214390602	0.14979752267841
125.875	1859.375	0.00018872105468	0.00014758838634	0.18730267988253	0.18724690334802
151.05	2231.25	0.00023410783648	0.00018630664162	0.22476321585903	0.22469628401762
176.225	2603.125	0.00028290175466	0.00022919660940	0.26222375183554	0.26214566468723
201.4	2975	0.00033562679357	0.00027693366328	0.29968428781204	0.29959504535683
226.575	3346.875	0.00039292407617	0.00033034498851	0.33714482378855	0.33704442602643
251.75	3718.75	0.00045558676827	0.00039045459704	0.37460535976505	0.37449380669604
276.925	4090.625	0.00052460827335	0.00045854535196	0.41206589574156	0.41194318736564
302.1	4462.5	0.00060125002341	0.00053624600178	0.44952643171806	0.44939256803524
327.275	4834.375	0.00068713883842	0.00062565583480	0.48698696769457	0.48684194870485
352.45	5206.25	0.00078441007980	0.00072952739417	0.52444750367107	0.52429132937445
377.625	5578.125	0.00089592386127	0.00085154145444	0.56190803964758	0.56174071004405
402.8	5950	0.00102560184516	0.00099673361130	0.59936857562408	0.59919009071366
427.975	6321.875	0.00117897108529	0.00117217979709	0.63682911160059	0.63663947138326
453.15	6693.75	0.00136408024387	0.00138814490783	0.67428964757709	0.67408885205286
478.325	7065.625	0.00159312359528	0.00166010551232	0.71175018355360	0.71153823272247
503.5	7437.5	0.00188550376004	0.00201253564822	0.74921071953010	0.74898761339207
528.675	7809.375	0.00227407311998	0.00248655313603	0.78667125550661	0.78643699406167
553.85	8181.25	0.00281918635770	0.00315695949184	0.82413179148311	0.82388637473128
579.025	8553.125	0.00364484725054	0.00417560254276	0.86159232745962	0.86133575540088
604.2	8925	0.00505074518725	0.00590494356604	0.89905286343612	0.89878513607049
629.375	9296.875	0.00796739061449	0.00947683238582	0.93651339941263	0.93623451674009
654.55	9668.75	0.01634884536697	0.02113380859812	0.97397393538913	0.97368389740969
679.725	10040.625	0.03601463694820	0.34247079083015	1.01143447136564	1.01113327807929
704.9	10412.5	0.05455752500073	0.91196037705557	1.04889500734214	1.04858265874890
730.075	10784.375	0.06930336499580	1.32069412478338	1.08635554331865	1.08603203941850
755.25	11156.25	0.08135790042310	1.77985244665347	1.12381607929515	1.12348142008811
780.425	11528.125	0.09215387755252		1.16127661527166	1.16093080075771
805.6	11900	0.10185899795886		1.19873715124816	1.19838018142731
830.775	12271.875	0.11074216592695		1.23619768722467	1.23582956209692
855.95	12643.75	0.11897883497681		1.27365822320117	1.27327894276652

Temperature Increment (T)	Mechanical Load Increment (P)	Rotation at Top Hinged Joint due to Temperature Increment	Rotation at Top Hinged Joint due to Mechanical Load Increment	Ratio of P/Pcr	Ratio of T/T_{cr}
881.125	13015.625	0.12669043600948		1.31111875917768	1.31072832343612
906.3	13387.5	0.13396492145787		1.34857929515419	1.34817770410573
931.475	13759.375	0.14086831885193		1.38603983113069	1.38562708477533
956.65	14131.25	0.14745164656781		1.42350036710720	1.42307646544493
981.825	14503.125	0.15375545235338		1.46096090308370	1.46052584611454
1007	14875	0.15981189761855		1.49842143906021	1.49797522678414
1032.175	15246.875	0.16564795307691		1.53588197503671	1.53542460745374
1057.35	15618.75	0.17128586388508		1.57334251101322	1.57287398812335
1082.525	15990.625	0.17674437867082		1.61080304698972	1.61032336879295
1107.7	16362.5	0.18203947159978		1.64826358296623	1.64777274946255
1132.875	16734.375	0.18718488359150		1.68572411894273	1.68522213013216
1158.05	17106.25	0.19219253526531		1.72318465491924	1.72267151080176
1183.225	17478.125	0.19707284683912		1.76064519089574	1.76012089147136
1208.4	17850	0.20183498933739		1.79810572687225	1.79757027214097
1233.575	18221.875	0.20648708428466		1.83556626284875	1.83501965281057
1258.75	18593.75	0.21103636421371		1.87302679882526	1.87246903348017
1283.925	18965.625	0.21548930298010		1.91048733480176	1.90991841414978
1309.1	19337.5	0.21985172253755		1.94794787077827	1.94736779481938
1334.275	19709.375	0.22412888116395		1.98540840675477	1.98481717548898
1359.45	20081.25	0.22832554692568		2.02286894273128	2.02226655615859
1384.625	20453.125	0.23244605928746		2.06032947870778	2.05971593682819
1409.8	20825	0.23649438112242		2.09779001468429	2.09716531749780
1434.975	21196.875	0.24047414288762		2.13525055066079	2.13461469816740
1460.15	21568.75	0.24438868035941		2.17271108663730	2.17206407883700
1485.325	21940.625	0.24824106703915		2.21017162261380	2.20951345950661
1510.5	22312.5	0.25203414212057		2.24763215859031	2.24696284017621
1535.675	22684.375	0.25577053473924		2.28509269456681	2.28441222084581
1560.85	23056.25	0.25945268509039		2.32255323054332	2.32186160151542
1586.025	23428.125	0.26308286289536		2.36001376651982	2.35931098218502
1611.2	23800	0.26666318361199		2.39747430249633	2.39676036285462
1636.375	24171.875	0.27019562271706		2.43493483847283	2.43420974352423
1661.55	24543.75	0.27368202833326		2.47239537444934	2.47165912419383
1686.725	24915.625	0.27703094472669		2.50985591042584	2.50910850486343
1711.9	25287.5	0.28042931429679		2.54731644640235	2.54655788553304
1737.075	25659.375	0.28378659157781		2.58477698237885	2.58400726620264
1762.25	26031.25	0.28710417710992		2.62223751835536	2.62145664687224
1787.425	26403.125	0.29038342731808		2.65969805433186	2.65890602754185

Temperature Increment (T)	Mechanical Load Increment (P)	Rotation at Top Hinged Joint due to Temperature Increment	Rotation at Top Hinged Joint due to Mechanical Load Increment	Ratio of P/Pcr	Ratio of T/T_{cr}
1812.6	26775	0.29362562288962		2.69715859030837	2.69635540821145
1837.775	27146.875	0.29683197455898		2.73461912628488	2.73380478888105
1862.95	27518.75	0.30000362834144		2.77207966226138	2.77125416955066
1888.125	27890.625	0.30314167027423		2.80954019823789	2.80870355022026
1913.3	28262.5	0.30624713072029		2.84700073421439	2.84615293088986
1938.475	28634.375	0.30932098828322		2.88446127019090	2.88360231155947
1963.65	29006.25	0.31236417337524		2.92192180616740	2.92105169222907
1988.825	29378.125	0.31537757147529		2.95938234214391	2.95850107289867
2014	29750	0.31836202610922		2.99684287812041	2.99595045356828

Table C- 6: Numerical Results for Fixed-Hinged Column for Slenderness Ratio of 125 (Data for Rotation at Top Hinged Joint; convergence tolerance=0.001)

Temperature Increment (T)	Mechanical Load Increment (P)	Rotation at Top Hinged Joint due to Temperature Increment	Rotation at Top Hinged Joint due to Mechanical Load Increment	Ratio of P/Pcr	Ratio of T/T_{cr}
0	0	0.00000000000000	0.00000000000000	0.00000000000000	0.00000000000000
4.0625	59.5	0.00001355564812	0.00002460076629	0.03746053597651	0.03777013628855
8.125	119	0.00002785951151	0.00005137364534	0.07492107195301	0.07554027257709
12.1875	178.5	0.00004300136853	0.00008060072085	0.11238160792952	0.11331040886564
16.25	238	0.00005908671324	0.00011261408323	0.14984214390602	0.15108054515419
20.3125	297.5	0.00007624039245	0.00014780734994	0.18730267988253	0.18885068144273
24.375	357	0.00009461130502	0.00018665051793	0.22476321585903	0.22662081773128
28.4375	416.5	0.00011437854419	0.00022970932863	0.26222375183554	0.26439095401982
32.5	476	0.00013575952806	0.00027767082962	0.29968428781204	0.30216109030837
36.5625	535.5	0.00015902091238	0.00033137757555	0.33714482378855	0.33993122659692
40.625	595	0.00018449346404	0.00039187407691	0.37460535976505	0.37770136288546
44.6875	654.5	0.00021259268084	0.00046047093663	0.41206589574156	0.41547149917401
48.75	714	0.00024384792648	0.00053883506347	0.44952643171806	0.45324163546256
52.8125	773.5	0.00027894448675	0.00062911922742	0.48698696769457	0.49101177175110
56.875	833	0.00031878576603	0.00073415253931	0.52444750367107	0.52878190803965
60.9375	892.5	0.00036458785035	0.00085772811689	0.56190803964758	0.56655204432819
65	952	0.00041802794702	0.00100505115825	0.59936857562408	0.60432218061674
69.0625	1011.5	0.00048148624972	0.00118346245868	0.63682911160059	0.64209231690529
73.125	1071	0.00055845780885	0.00140365745001	0.67428964757709	0.67986245319383
77.1875	1130.5	0.00065429213236	0.00168184769598	0.71175018355360	0.71763258948238
81.25	1190	0.00077761064000	0.00204384060328	0.74921071953010	0.75540272577093
85.3125	1249.5	0.00094325493346	0.00253336804929	0.78667125550661	0.79317286205947
89.375	1309	0.00117910588362	0.00323091071074	0.82413179148311	0.83094299834802
93.4375	1368.5	0.00154428526683	0.00430255084143	0.86159232745962	0.86871313463656
97.5	1428	0.00218867672569	0.00615496804412	0.89905286343612	0.90648327092511
101.5625	1487.5	0.00361395735360	0.01011822800979	0.93651339941263	0.94425340721366
105.625	1547	0.00797280721809	0.02449017128798	0.97397393538913	0.98202354350220
109.6875	1606.5	0.01624294621008	0.43832566434364	1.01143447136564	1.01979367979075
113.75	1666	0.02327900876246	0.96016888725452	1.04889500734214	1.05756381607929
117.8125	1725.5	0.02893361486401	1.36091684719949	1.08635554331865	1.09533395236784
121.875	1785	0.03359781818114	1.83423370589139	1.12381607929515	1.13310408865639
125.9375	1844.5	0.03781224853371		1.16127661527166	1.17087422494493
130	1904	0.04161875928493		1.19873715124816	1.20864436123348
134.0625	1963.5	0.04511465331580		1.23619768722467	1.24641449752203
138.125	2023	0.04836433051211		1.27365822320117	1.28418463381057

Temperature Increment (T)	Mechanical Load Increment (P)	Rotation at Top Hinged Joint due to Temperature Increment	Rotation at Top Hinged Joint due to Mechanical Load Increment	Ratio of P/Pcr	Ratio of T/T_{cr}
142.1875	2082.5	0.05141285362616		1.31111875917768	1.32195477009912
146.25	2142	0.05429314327640		1.34857929515418	1.35972490638766
150.3125	2201.5	0.05703008400720		1.38603983113069	1.39749504267621
154.375	2261	0.05964310485081		1.42350036710720	1.43526517896476
158.4375	2320.5	0.06214736461393		1.46096090308370	1.47303531525330
162.5	2380	0.06455543961020		1.49842143906021	1.51080545154185
166.5625	2439.5	0.06687757896565		1.53588197503671	1.54857558783040
170.625	2499	0.06912233897790		1.57334251101322	1.58634572411894
174.6875	2558.5	0.07129694926375		1.61080304698972	1.62411586040749
178.75	2618	0.07340758311476		1.64826358296623	1.66188599669603
182.8125	2677.5	0.07545956108711		1.68572411894273	1.69965613298458
186.875	2737	0.07745750688613		1.72318465491924	1.73742626927313
190.9375	2796.5	0.07940546850488		1.76064519089574	1.77519640556167
195	2856	0.08130701361899		1.79810572687225	1.81296654185022
199.0625	2915.5	0.08316530561192		1.83556626284875	1.85073667813877
203.125	2975	0.08498316482284		1.87302679882526	1.88850681442731
207.1875	3034.5	0.08676311837738		1.91048733480176	1.92627695071586
211.25	3094	0.08850744109569		1.94794787077827	1.96404708700440
215.3125	3153.5	0.09021818935340		1.98540840675477	2.00181722329295
219.375	3213	0.09189722932275		2.02286894273128	2.03958735958150
223.4375	3272.5	0.09354626069224		2.06032947870778	2.07735749587004
227.5	3332	0.09516683671805		2.09779001468429	2.11512763215859
231.5625	3391.5	0.09676038127718		2.13525055066079	2.15289776844714
235.625	3451	0.09832820345177		2.17271108663730	2.19066790473568
239.6875	3510.5	0.09987151006779		2.21017162261380	2.22843804102423
243.75	3570	0.10139141652765		2.24763215859031	2.26620817731277
247.8125	3629.5	0.10288895621203		2.28509269456681	2.30397831360132
251.875	3689	0.10436508867513		2.32255323054332	2.34174844988987
255.9375	3748.5	0.10582070681710		2.36001376651982	2.37951858617841
260	3808	0.10725664318556		2.39747430249633	2.41728872246696
264.0625	3867.5	0.10863585598796		2.43493483847283	2.45505885875551
268.125	3927	0.11003421553460		2.47239537444934	2.49282899504405
272.1875	3986.5	0.11141510486050		2.50985591042584	2.53059913133260
276.25	4046	0.11277914728507		2.54731644640235	2.56836926762114
280.3125	4105.5	0.11412694514546		2.58477698237885	2.60613940390969
284.375	4165	0.11545906573771		2.62223751835536	2.64390954019824
288.4375	4224.5	0.11677604410128		2.65969805433186	2.68167967648678

Temperature Increment (T)	Mechanical Load Increment (P)	Rotation at Top Hinged Joint due to Temperature Increment	Rotation at Top Hinged Joint due to Mechanical Load Increment	Ratio of P/Pcr	Ratio of T/T_{cr}
292.5	4284	0.11807838552828		2.69715859030837	2.71944981277533
296.5625	4343.5	0.11936656782713		2.73461912628487	2.75721994906388
300.625	4403	0.12064104336978		2.77207966226138	2.79499008535242
304.6875	4462.5	0.12190224094684		2.80954019823788	2.83276022164097
308.75	4522	0.12315056745257		2.84700073421439	2.87053035792951
312.8125	4581.5	0.12438640941815		2.88446127019089	2.90830049421806
316.875	4641	0.12561013440967		2.92192180616740	2.94607063050661
320.9375	4700.5	0.12682209230523		2.95938234214391	2.98384076679515
325	4760	0.12802261646349		2.99684287812041	3.02161090308370

Table C- 7: Numerical Results for Fixed-Hinged Column for Slenderness Ratio of 200 (Data for Rotation at Top Hinged Joint; convergence tolerance=0.001)

Temperature Increment (T)	Mechanical Load Increment (P)	Rotation at Top Hinged Joint due to Temperature Increment	Rotation at Top Hinged Joint due to Mechanical Load Increment	Ratio of P/Pcr	Ratio of T/T_{cr}
0	0	0.00000000000000	0.00000000000000	0.00000000000000	0.00000000000000
1.575	23.125	0.00000840699531	0.00002447223672	0.03727165932452	0.03748656972687
3.15	46.25	0.00001727423694	0.00005109510213	0.07454331864905	0.07497313945374
4.725	69.375	0.00002665648134	0.00008014648015	0.11181497797357	0.11245970918062
6.3	92.5	0.00003661798530	0.00011195325612	0.14908663729809	0.14994627890749
7.875	115.625	0.00004723468430	0.00014690254297	0.18635829662261	0.18743284863436
9.45	138.75	0.00005859700088	0.00018545613549	0.22362995594714	0.22491941836123
11.025	161.875	0.00007081350657	0.00022816932941	0.26090161527166	0.26240598808811
12.6	185	0.00008401575651	0.00027571572375	0.29817327459618	0.29989255781498
14.175	208.125	0.00009836475969	0.00032892034893	0.33544493392071	0.33737912754185
15.75	231.25	0.00011405976936	0.00038880457311	0.37271659324523	0.37486569726872
17.325	254.375	0.00013135042624	0.00045664797852	0.40998825256975	0.41235226699560
18.9	277.5	0.00015055384805	0.00053407519016	0.44725991189427	0.44983883672247
20.475	300.625	0.00017207918740	0.00062318023956	0.48453157121880	0.48732540644934
22.05	323.75	0.00019646376481	0.00072670886008	0.52180323054332	0.52481197617621
23.625	346.875	0.00022442768358	0.00084833284268	0.55907488986784	0.56229854590308
25.2	370	0.00025695897960	0.00099307567028	0.59634654919236	0.59978511562996
26.775	393.125	0.00029545125928	0.00116799658715	0.63361820851689	0.63727168535683
28.35	416.25	0.00034193586409	0.00138333677021	0.67088986784141	0.67475825508370
29.925	439.375	0.00039949399442	0.00165453797192	0.70816152716593	0.71224482481057
31.5	462.5	0.00047303536064	0.00200602100184	0.74543318649046	0.74973139453745
33.075	485.625	0.00057088863020	0.00247881817919	0.78270484581498	0.78721796426432
34.65	508.75	0.00070839312569	0.00314758499249	0.81997650513950	0.82470453399119
36.225	531.875	0.00091717553784	0.00416390009187	0.85724816446402	0.86219110371806
37.8	555	0.00127407096438	0.00588968147813	0.89451982378855	0.89967767344493
39.375	578.125	0.00201956773122	0.00945564824833	0.93179148311307	0.93716424317181
40.95	601.25	0.00417791329161	0.02110584646999	0.96906314243759	0.97465081289868
42.525	624.375	0.00911711088841	0.34162012786096	1.00633480176211	1.01213738262555
44.1	647.5	0.01370656064325	0.90532583269729	1.04360646108664	1.04962395235242
45.675	670.625	0.01736169380500	1.30718565047250	1.08087812041116	1.08711052207930
47.25	693.75	0.02035388374849	1.74995288265602	1.11814977973568	1.12459709180617
48.825	716.875	0.02303696001661		1.15542143906021	1.16208366153304
50.4	740	0.02545070464194		1.19269309838473	1.19957023125991
51.975	763.125	0.02766125340805		1.22996475770925	1.23705680098678
53.55	786.25	0.02971183917645		1.26723641703377	1.27454337071366

Temperature Increment (T)	Mechanical Load Increment (P)	Rotation at Top Hinged Joint due to Temperature Increment	Rotation at Top Hinged Joint due to Mechanical Load Increment	Ratio of P/Pcr	Ratio of T/T_{cr}
55.125	809.375	0.03163242534267		1.30450807635830	1.31202994044053
56.7	832.5	0.03344473777621		1.34177973568282	1.34951651016740
58.275	855.625	0.03516510026668		1.37905139500734	1.38700307989427
59.85	878.75	0.03680619638574		1.41632305433187	1.42448964962115
61.425	901.875	0.03837787733546		1.45359471365639	1.46197621934802
63	925	0.03988829295036		1.49086637298091	1.49946278907489
64.575	948.125	0.04134406332372		1.52813803230543	1.53694935880176
66.15	971.25	0.04275070102708		1.56540969162996	1.57443592852864
67.725	994.375	0.04411285352646		1.60268135095448	1.61192249825551
69.3	1017.5	0.04543448146664		1.63995301027900	1.64940906798238
70.875	1040.625	0.04671899246221		1.67722466960352	1.68689563770925
72.45	1063.75	0.04796934322323		1.71449632892805	1.72438220743612
74.025	1086.875	0.04918811869924		1.75176798825257	1.76186877716300
75.6	1110	0.05037759424983		1.78903964757709	1.79935534688987
77.175	1133.125	0.05153978508088		1.82631130690162	1.83684191661674
78.75	1156.25	0.05267648599087		1.86358296622614	1.87432848634361
80.325	1179.375	0.05378930364814		1.90085462555066	1.91181505607049
81.9	1202.5	0.05487968304380		1.93812628487518	1.94930162579736
83.475	1225.625	0.05594892935340		1.97539794419971	1.98678819552423
85.05	1248.75	0.05699822614422		2.01266960352423	2.02427476525110
86.625	1271.875	0.05802865064714		2.04994126284875	2.06176133497798
88.2	1295	0.05904118665074		2.08721292217327	2.09924790470485
89.775	1318.125	0.06003673545487		2.12448458149780	2.13673447443172
91.35	1341.25	0.06101612522837		2.16175624082232	2.17422104415859
92.925	1364.375	0.06198011904621		2.19902790014684	2.21170761388546
94.5	1387.5	0.06292942182658		2.23629955947137	2.24919418361234
96.075	1410.625	0.06386468634640		2.27357121879589	2.28668075333921
97.65	1433.75	0.06478651848048		2.31084287812041	2.32416732306608
99.225	1456.875	0.06569548178332		2.34811453744493	2.36165389279295
100.8	1480	0.06659210151145		2.38538619676946	2.39914046251983
102.375	1503.125	0.06745329798505		2.42265785609398	2.43662703224670
103.95	1526.25	0.06832635600632		2.45992951541850	2.47411360197357
105.525	1549.375	0.06918846469924		2.49720117474302	2.51160017170044
107.1	1572.5	0.07004001673018		2.53447283406755	2.54908674142732
108.675	1595.625	0.07088139147685		2.57174449339207	2.58657331115419
110.25	1618.75	0.07171294614309		2.60901615271659	2.62405988088106
111.825	1641.875	0.07253501752890		2.64628781204112	2.66154645060793

Temperature Increment (T)	Mechanical Load Increment (P)	Rotation at Top Hinged Joint due to Temperature Increment	Rotation at Top Hinged Joint due to Mechanical Load Increment	Ratio of P/Pcr	Ratio of T/T_{cr}
113.4	1665	0.07334792362459		2.68355947136564	2.69903302033480
114.975	1688.125	0.07415196504843		2.72083113069016	2.73651959006168
116.55	1711.25	0.07494742634606		2.75810279001468	2.77400615978855
118.125	1734.375	0.07573457716769		2.79537444933921	2.81149272951542
119.7	1757.5	0.07651367333666		2.83264610866373	2.84897929924229
121.275	1780.625	0.07728495782160		2.86991776798825	2.88646586896917
122.85	1803.75	0.07804866162240		2.90718942731278	2.92395243869604
124.425	1826.875	0.07880500457925		2.94446108663730	2.96143900842291
126	1850	0.07955419611273		2.98173274596182	2.99892557814978

APPENDIX D: Numerical Data for Fixed-Fixed Columns

Table D- 1: Numerical Results for Fixed-Fixed Column Subjected to 630℃ with 60 Load-Steps and Eccentricity (e=0.001& convergence tolerance=0.001) for 2 & 10 Elements for Slenderness Ratio of 125

Temperature Increment (T)	Horizontal Deflection at Mid-Span due to Temperature Increment for 2 Elements	Horizontal Deflection at Mid-Span due to Temperature Increment for 10 Elements	Ratio of T/T_{cr}
0	0.00654401353121	0.00581690091628	0.00000000000000
10.5	0.00688282663103	0.00611806811737	0.04980677312775
21	0.00725911084371	0.00645254297283	0.09961354625551
31.5	0.00767945409650	0.00682618141991	0.14942031938326
42	0.00815208498686	0.00724629776743	0.19922709251101
52.5	0.00868741743336	0.00772214883007	0.24903386563877
63	0.00929882773233	0.00826562465206	0.29884063876652
73.5	0.01000378858056	0.00889225651902	0.34864741189427
84	0.01082556721240	0.00962272641447	0.39845418502203
94.5	0.01179584464804	0.01048519524723	0.44826095814978
105	0.01295889689751	0.01151901947071	0.49806773127753
115.5	0.01437854473403	0.01278092866280	0.54787450440529
126	0.01615027607453	0.01435580097138	0.59768127753304
136.5	0.01842366856004	0.01637659430145	0.64748805066079
147	0.02144700744124	0.01906400666382	0.69729482378855
157.5	0.02566479503733	0.02281315124175	0.74710159691630
168	0.03195931166981	0.02840827727785	0.79690837004405
178.5	0.04236560274593	0.03765831428601	0.84671514317181
189	0.06286749517237	0.05588222148812	0.89652191629956
199.5	0.12199852883233	0.10844318728730	0.94632868942731
210	2.08241098702981	1.85526311564390	0.99613546255507
220.5	76.50176960372400	76.35542674841350	1.04594223568282
231	109.88412920324000	109.68023868304200	1.09574900881057
241.5	135.27502765175900	135.02462487010200	1.14555578193833
252	156.60592950090400	156.31568935633700	1.19536255506608
262.5	174.97254060033000	175.03839538265000	1.24516932819383
273	191.87480977715000	191.94543233063100	1.29497610132159
283.5	207.40654470687000	207.48101480549400	1.34478287444934
294	221.85571054203500	221.93328018896300	1.39458964757709
304.5	235.42168462079900	235.50172260894400	1.44439642070485

Temperature Increment (T)	Horizontal Deflection at Mid-Span due to Temperature Increment for 2 Elements	Horizontal Deflection at Mid-Span due to Temperature Increment for 10 Elements	Ratio of T/T_{cr}
315	248.24927687995800	248.33123647104700	1.49420319383260
325.5	260.44759635275000	260.53099454391700	1.54400996696035
336	272.10163469428900	272.18615460286400	1.59381674008811
346.5	283.27780486468300	283.36290768524400	1.64362351321586
357	294.03102378542700	294.11635677576600	1.69343028634361
367.5	304.40610820330800	304.49134333863900	1.74323705947137
378	314.44048370091600	314.52531393110300	1.79304383259912
388.5	324.16578660387400	324.24992325749300	1.84285060572687
399	333.60904482938600	333.69221540091700	1.89265737885463
409.5	342.79356607409400	342.87551234790900	1.94246415198238
420	351.73961737044100	351.82009383057600	1.99227092511013
430.5	360.46495294179800	360.54372541977600	2.04207769823789
441	368.98522979443300	369.06207431427200	2.09188447136564
451.5	377.31433891391600	377.38904070039800	2.14169124449339
462	385.46467211067200	385.53702473301000	2.19149801762115
472.5	393.44733916534800	393.51714379374100	2.24130479074890
483	401.27234613920000	401.33941089593600	2.29111156387665
493.5	408.94874301464900	409.01288240477400	2.34091833700441
504	416.48474687669800	416.54578128607100	2.39072511013216
514.5	423.88784541235200	423.94560066304600	2.44053188325991
525	431.16488444023200	431.21919139493800	2.49033865638767
535.5	438.32214238228200	438.37283659099600	2.54014542951542
546	445.36539398251200	445.41231536555300	2.58995220264317
556.5	452.29996511124600	452.34295767402600	2.63975897577093
567	459.13078013353700	459.16969170888900	2.68956574889868
577.5	465.86240303875800	465.89708505339800	2.73937252202643
588	472.49907330711300	472.52938056936200	2.78917929515419
598.5	479.04473731350200	479.07052781980400	2.83898606828194
609	485.50307592924800	485.52421068721000	2.88879284140969
619.5	491.87752886944400	491.89387173569100	2.93859961453745
630	498.17131624307900	498.18273377424900	2.98840638766520

Table D- 2: Properties of Fixed-Fixed Column Used for Validation of Results

L	=	14083	mm
A	=	5860	mm^2
I	=	4.54×10^7	mm^4
E	=	210	KN/mm^2
α	=	1.20×10^{-5}	/℃
T_{cr}	=	128.614	℃
P_{cr}	=	1899.268	KN

Table D- 3: Numerical Results for Fixed-Fixed Column Subjected to (T/T_{cr}=1.1638) with 60 Load-Steps and Eccentricity (e=0.001& convergence tolerance=0.001) for Slenderness Ratio of 160 (Data for Horizontal Mid-Span Deflections and Fixed-End Moments in Validation to Elastica Solution)

Temperature Increment (T)	Horizontal Deflection at Mid-Span (Y_{max}) due to Temperature Increment	Horizontal Deflection at Mid-Span due to Temperature Increment per original length (f)	Fixed End Moment (M) due to Temperature Increment	Value of m=(ML/EI) due to Temperature Increment	Ratio of P/Pcr	Ratio of T/T_{cr}
0	0.06103362330606	0.00000433381184	70.41500000512110	0.00010401336270	0.00000000009127	0.00000000000000
2.5	0.06222866387514	0.00000441866804	71.56367711691110	0.00010571012858	0.01943798624672	0.01943801652893
5	0.06347202188539	0.00000450695510	72.75825820319230	0.00010747470141	0.03887600153792	0.03887603305785
7.5	0.06476668963633	0.00000459888552	74.00158295118430	0.00010931127583	0.05831401675172	0.05831404958678
10	0.06611591382379	0.00000469468982	75.29673246415130	0.00011122440309	0.07775203188139	0.07775206611570
12.5	0.06752322099023	0.00000479461842	76.64705339153810	0.00011321902668	0.09719004691986	0.09719008264463
15	0.06899244835546	0.00000489894379	78.05618718166210	0.00011530052557	0.11662806185879	0.11662809917355
17.5	0.07052777878397	0.00000500796293	79.52810326557760	0.00011747476318	0.13606607668936	0.13606611570248
20	0.07213378061535	0.00000512200023	81.06713685463390	0.00011974814327	0.15550409140112	0.15550413223141
22.5	0.07381545310278	0.00000524141067	82.67803204104460	0.00012212767356	0.17494210598308	0.17494214876033
25	0.07557827845505	0.00000536658354	84.36599120024810	0.00012462103873	0.19438012042239	0.19438016528926
27.5	0.07742828160104	0.00000549794663	86.13673168642690	0.00012723668415	0.21381813470476	0.21381818181818
30	0.07937209905563	0.00000563597119	87.99655118369870	0.00012998391244	0.23325614881415	0.23325619834711
32.5	0.08141705853642	0.00000578117754	89.95240325381290	0.00013287299503	0.25269416273226	0.25269421487603
35	0.08357127136379	0.00000593414164	92.01198501225640	0.00013591530170	0.27213217643836	0.27213223140496
37.5	0.08584374007632	0.00000609550273	94.18383924107660	0.00013912345141	0.29157018990894	0.29157024793388
40	0.08824448430022	0.00000626597227	96.47747383045490	0.00014251148871	0.31100820311692	0.31100826446281
42.5	0.09078468854996	0.00000644634444	98.90350202130940	0.00014609509093	0.33044621603134	0.33044628099174
45	0.09347687659380	0.00000663750852	101.47380785347000	0.00014989181254	0.34988422861661	0.34988429752066
47.5	0.09633511808896	0.00000684046355	104.20174225253400	0.00015392137485	0.36932224083144	0.36932231404959

Temperature Increment (T)	Horizontal Deflection at Mid-Span (Y_{max}) due to Temperature Increment	Horizontal Deflection at Mid-Span due to Temperature Increment per original length (f)	Fixed End Moment (M) due to Temperature Increment	Value of m=(ML/EI) due to Temperature Increment	Ratio of P/Pcr	Ratio of T/T_{cr}
50	0.09937527470702	0.00000705633582	107.10235656086000	0.00015820601091	0.38876025262813	0.38876033057851
52.5	0.10261529481417	0.00000728639979	110.19268216424500	0.00016277087860	0.40819826395051	0.40819834710744
55	0.10607556829957	0.00000753210327	113.49206718030400	0.00016764455793	0.42763627473317	0.42763636363636
57.5	0.10977935633677	0.00000779509799	117.02258425695000	0.00017285965348	0.44707428489872	0.44707438016529
60	0.11375331523622	0.00000807727672	120.80952764811100	0.00017845352860	0.46651229435565	0.46651239669422
62.5	0.11802813934646	0.00000838081897	124.88202324972500	0.00018446920654	0.48595030299453	0.48595041322314
65	0.12263935577400	0.00000870824741	129.27378270754800	0.00019095648438	0.50538831068406	0.50538842975207
67.5	0.12762831448442	0.00000906249819	134.02404290335800	0.00019797332080	0.52482631726562	0.52482644628099
70	0.13304343224181	0.00000944700922	139.17874631928700	0.00020558757964	0.54426432254597	0.54426446280992
72.5	0.13894176962888	0.00000986583221	144.79203744853400	0.00021387924031	0.56370232628764	0.56370247933884
75	0.14539105014247	0.00001032377599	150.92817868772100	0.00022294322787	0.58314032819670	0.58314049586777
77.5	0.15247227298436	0.00001082659207	157.66402958483900	0.00023289307524	0.60257832790527	0.60257851239669
80	0.16028313369003	0.00001138121752	165.09229262500300	0.00024386571769	0.62201632494845	0.62201652892562
82.5	0.16894255987137	0.00001199609702	173.32581714423600	0.00025602785036	0.64145431873157	0.64145454545455
85	0.17859681052164	0.00001268161597	182.50338687013900	0.00026958447734	0.66089230848456	0.66089256198347
87.5	0.18942780602388	0.00001345069200	192.79762417407100	0.00028479058737	0.68033029319557	0.68033057851240
90	0.20166470249754	0.00001431959678	204.42597280453200	0.00030196737703	0.69976827151404	0.69976859504132
92.5	0.21560028691803	0.00001530912022	217.66625501338500	0.00032152523083	0.71920624160498	0.71920661157025
95	0.23161471031012	0.00001644625568	232.87919167288200	0.00034399698683	0.73864420092445	0.73864462809917
97.5	0.25021069957225	0.00001776670029	250.54181432101200	0.00037008729111	0.75808214586312	0.75808264462810
100	0.27206729263131	0.00001931867044	271.29845375443600	0.00040074791549	0.77752007116299	0.77752066115703
102.5	0.29812455741062	0.00002116891751	296.04112875763000	0.00043729650356	0.79695796892266	0.79695867768595
105	0.32972235305801	0.00002341258081	326.04121484102700	0.00048161106487	0.81639582682739	0.81639669421488
107.5	0.36883813517014	0.00002619007346	363.17509453805400	0.00053646329376	0.83583362482196	0.83583471074380

Temperature Increment (T)	Horizontal Deflection at Mid-Span (Y_{max}) due to Temperature Increment	Horizontal Deflection at Mid-Span due to Temperature Increment per original length (f)	Fixed End Moment (M) due to Temperature Increment	Value of m=(ML/EI) due to Temperature Increment	Ratio of P/Pcr	Ratio of T/T_{cr}
110	0.41851741406148	0.00002971764786	410.33261368228100	0.00060612191966	0.85527132844422	0.85527272727273
112.5	0.48370735814984	0.00003434658739	472.20807686218600	0.00069752112428	0.87470887435456	0.87471074380165
115	0.57301544174942	0.00004068808260	556.96900552649300	0.00082272554401	0.89414613556365	0.89414876033058
117.5	0.70286216305364	0.00004990810311	680.19659823674000	0.00100475091211	0.91358282584497	0.91358677685950
120	0.90894373400072	0.00006454132827	875.76252834126700	0.00129363069651	0.93301818261301	0.93302479338843
122.5	1.28622621266655	0.00009133100886	1233.77885637083000	0.00182247372965	0.95244956579794	0.95246280991736
125	2.19843070632021	0.00015610387375	2099.37580537306000	0.00310108836295	0.97186211640634	0.97190082644628
127.5	7.24647071689396	0.00051454983169	6889.41214774306000	0.01017668003236	0.99091806136228	0.99133884297521
130	40.36493326959490	0.00286619106480	38314.88002657030000	0.05659674093330	0.99771873237327	1.01077685950413
132.5	63.15627687026940	0.00448453501069	59940.66754330680000	0.08854122549686	0.99824770660059	1.03021487603306
135	79.93934017019920	0.00567624925802	75865.02955999430000	0.11206386189717	0.99843906663928	1.04965289256198
137.5	93.82447571916920	0.00666219047532	89039.40027813940000	0.13152435468684	0.99854166513304	1.06909090909091
140	105.92719044613200	0.00752156741467	100522.29077297900000	0.14848628117731	0.99860639414911	1.08852892561983
142.5	116.79357803718800	0.00829315652674	110831.90650484100000	0.16371510742689	0.99865065758529	1.10796694214876
145	126.73808107024200	0.00899928542200	120266.63061909000000	0.17765158944383	0.99868248735347	1.12740495867769
147.5	135.96120068478900	0.00965419107618	129016.72600055000000	0.19057677363082	0.99870609821777	1.14684297520661
150	144.59998178126800	0.01026760463057	137212.24075374300000	0.20268276026004	0.99872394314054	1.16628099173554

Table D- 4: Numerical Results for Fixed-Fixed Column Subjected to (T/T_{cr}=1.6563) with 60 Load-Steps and Eccentricity (e=0.001& convergence tolerance=0.001) for Slenderness Ratio of 160 (Data for Horizontal Mid-Span Deflections and Fixed-End Moments in Validation to Elastica Solution)

Temperature Increment (T)	Horizontal Deflection at Mid-Span (Y_{max}) due to Temperature Increment	Horizontal Deflection at Mid-Span due to Temperature Increment per original length (f)	Fixed End Moment (M) due to Temperature Increment	Value of m=(ML/EI) due to Temperature Increment	Ratio of P/Pcr	Ratio of T/T_{cr}
0	0.06103362330606	0.00000433381184	70.41500000512110	0.00010401336270	0.00000000009127	0.00000000000000
3.55	0.06274482223187	0.00000445531887	72.05965164124550	0.00010644275626	0.02760195267807	0.02760198347107
7.1	0.06455596416200	0.00000458392255	73.79925145922910	0.00010901240231	0.05520393432293	0.05520396694215
10.65	0.06647607678652	0.00000472026390	75.64236671402290	0.00011173495596	0.08280591580052	0.08280595041322
14.2	0.06851531118337	0.00000486506373	77.59863065966040	0.00011462464696	0.11040789708972	0.11040793388430
17.75	0.07068511980517	0.00000501913523	79.67891141812530	0.00011769752911	0.13800987816604	0.13800991735537
21.3	0.07299847192378	0.00000518339933	81.89551641954100	0.00012097178233	0.16561185900078	0.16561190082645
24.85	0.07547011335979	0.00000535890306	84.26243884929530	0.00012446807660	0.19321383956034	0.19321388429752
28.4	0.07811688146621	0.00000554684201	86.79565653237420	0.00012821001354	0.22081581980500	0.22081586776860
31.95	0.08095808957679	0.00000574858755	89.51349673609450	0.00013222466523	0.24841779968775	0.24841785123967
35.5	0.08401599951929	0.00000596572043	92.43708452730850	0.00013654323652	0.27601977915211	0.27601983471074
39.05	0.08731640660646	0.00000620007229	95.59089786480140	0.00014120188497	0.30362175813062	0.30362181818182
42.6	0.09088936967665	0.00000645377753	99.00346032818260	0.00014624274412	0.33122373654131	0.33122380165289
46.15	0.09477012991706	0.00000672933850	102.70821297227200	0.00015171521136	0.35882571428420	0.35882578512397
49.7	0.09900027801648	0.00000702970844	106.74462182866400	0.00015767758384	0.38642769123640	0.38642776859504
53.25	0.10362925163596	0.00000735839777	111.15959883445200	0.00016419915743	0.41402966724525	0.41402975206612
56.8	0.10871627763892	0.00000771961201	116.00934478568700	0.00017136294902	0.44163164211957	0.44163173553719
60.35	0.11433292124935	0.00000811843278	121.36176820836500	0.00017926926953	0.46923361561711	0.46923371900826

Temperature Increment (T)	Horizontal Deflection at Mid-Span (Y_{max}) due to Temperature Increment	Horizontal Deflection at Mid-Span due to Temperature Increment per original length (f)	Fixed End Moment (M) due to Temperature Increment	Value of m=(ML/EI) due to Temperature Increment	Ratio of P/Pcr	Ratio of T/T_{cr}
63.9	0.12056647556397	0.00000856105850	127.29970161960100	0.00018804047484	0.49683558742700	0.49683570247934
67.45	0.12752453335342	0.00000905512901	133.92523964560900	0.00019782737379	0.52443755714600	0.52443768595041
71	0.13534125209202	0.00000961017041	141.36568383592800	0.00020881800959	0.55203952424232	0.55203966942149
74.55	0.14418609179891	0.00001023821556	149.78183388479800	0.00022124990716	0.57964148800365	0.57964165289256
78.1	0.15427624476420	0.00001095468662	159.37978203741100	0.00023542749521	0.60724344745871	0.60724363636364
81.65	0.16589471468597	0.00001177967881	170.42806814941000	0.00025174744679	0.63484540125464	0.63484561983471
85.2	0.17941728652646	0.00001273987548	183.28327103214200	0.00027073648151	0.66244734746237	0.66244760330579
88.75	0.19535394320995	0.00001387148897	198.42930823056100	0.00029310941712	0.69004928325498	0.69004958677686
92.3	0.21441464266958	0.00001522493123	216.53985100040300	0.00031986136562	0.71765120435483	0.71765157024793
95.85	0.23761798797903	0.00001687253016	238.58144000348400	0.00035242005043	0.74525310403900	0.74525355371901
99.4	0.26647940142552	0.00001892189129	265.99204123567000	0.00039290955988	0.77285497124834	0.77285553719008
102.95	0.30335608434383	0.00002154039232	301.00837396367100	0.00044463385891	0.80045678674056	0.80045752066116
106.5	0.35212573938608	0.00002500337709	347.30994149672700	0.00051302811777	0.82805851458101	0.82805950413223
110.05	0.41964821633139	0.00002979794268	411.40596796793200	0.00060770742258	0.85566008119191	0.85566148760331
113.6	0.51931438826124	0.00003687493423	506.00288098199900	0.00074744104501	0.88326131580757	0.88326347107438
117.15	0.68124483763053	0.00004837312262	659.68171266395000	0.00097444739392	0.91086174308090	0.91086545454545
120.7	0.99026642391837	0.00007031580498	952.93357204970600	0.00140762373434	0.93845959033592	0.93846743801653
124.25	1.81293520125443	0.00012873101115	1733.57873816102000	0.00256075202801	0.96604310064560	0.96606942148760
127.8	9.57656956818294	0.00068000305970	9100.41303291727000	0.01344265513693	0.99293647613672	0.99367140495868
131.35	53.78869610686150	0.00381937160998	51052.21414238720000	0.07541166606510	0.99808584871759	1.02127338842975
134.9	79.33445255614490	0.00563329802947	75291.09876155610000	0.11121608127799	0.99843364023129	1.04887537190083
138.45	98.59689582289680	0.00700106550250	93567.45283726680000	0.13821295758586	0.99856898263475	1.07647735537190
142	114.70208310445000	0.00814464583682	108847.59943518200000	0.16078399259433	0.99864285993048	1.10407933884298
145.55	128.82354210697700	0.00914736766333	122245.15599274500000	0.18057416385682	0.99868823355551	1.13168132231405

Temperature Increment (T)	Horizontal Deflection at Mid-Span (Y_{max}) due to Temperature Increment	Horizontal Deflection at Mid-Span due to Temperature Increment per original length (f)	Fixed End Moment (M) due to Temperature Increment	Value of m=(ML/EI) due to Temperature Increment	Ratio of P/Pcr	Ratio of T/T_{cr}
149.1	141.55050332079200	0.01005107044588	134319.25963144200000	0.19840939954508	0.99871804873280	1.15928330578512
152.65	153.22841221351200	0.01088028321579	145397.71943445100000	0.21477392212681	0.99873825302787	1.18688528925620
156.2	164.08020070231100	0.01165083569004	155692.08866212300000	0.22998022703618	0.99875202873012	1.21448727272727
159.75	173.87086402287000	0.01234604089552	164979.50564242200000	0.24369911464353	0.99876096821807	1.24208925619835
163.3	183.46770326494500	0.01302748324307	174082.73590885300000	0.25714593125076	0.99876692637735	1.26969123966942
166.85	192.58817016783700	0.01367509984060	182733.78068940200000	0.26992480306003	0.99877031503567	1.29729322314050
170.4	201.29713571561400	0.01429349697928	190994.24292272700000	0.28212672671697	0.99877079135458	1.32489520661157
173.95	209.64517122958600	0.01488626557470	198912.02790577400000	0.29382246542580	0.99877075653391	1.35249719008265
177.5	217.67405608054400	0.01545637225286	206526.83510727900000	0.30507066116964	0.99876935065045	1.38009917355372
181.05	225.41782868254100	0.01600623397792	213870.96788883700000	0.31591903078817	0.99876681554797	1.40770115702479
184.6	232.90487977183700	0.01653786668967	220971.37013358600000	0.32640737437921	0.99876333837806	1.43530314049587
188.15	240.15918306934300	0.01705297268907	227850.79415351700000	0.33656930047049	0.99875906508315	1.46290512396694
191.7	247.20120088073300	0.01755300494218	234528.66002283900000	0.34643349538201	0.99875411149230	1.49050710743802
195.25	254.04856421521600	0.01803921537329	241021.70096008600000	0.35602467655078	0.99874857093824	1.51810909090909
198.8	260.71659243328000	0.01851269176357	247344.45644180300000	0.36536432093268	0.99874251962479	1.54571107438017
202.35	267.21869638859000	0.01897438637693	253509.65476375100000	0.37447123010185	0.99873602049627	1.57331305785124
205.9	273.56669547181200	0.01942513847232	259528.51390250500000	0.38336197466777	0.99872912608153	1.60091504132232
209.45	279.77107001047500	0.01986569222591	265410.98103473200000	0.39205124808062	0.99872188062250	1.62851702479339
213	285.84116443533800	0.02029671115729	271165.92533712300000	0.40055215142528	0.99871432169040	1.65611900826446

Table D- 5: Numerical Results for Fixed-Fixed Column Subjected to (T/T_{cr}=2.4816) with 60 Load-Steps and Eccentricity (e=0.001& convergence tolerance=0.001) for Slenderness Ratio of 160 (Data for Horizontal Mid-Span Deflections and Fixed-End Moments in Validation to Elastica Solution)

Temperature Increment (T)	Horizontal Deflection at Mid-Span (Y_{max}) due to Temperature Increment	Horizontal Deflection at Mid-Span due to Temperature Increment per original length (f)	Fixed End Moment (M) due to Temperature Increment	Value of m=(ML/EI) due to Temperature Increment	Ratio of P/Pcr	Ratio of T/T_{cr}
0	0.06103362330606	0.00000433381184	70.41500000512110	0.00010401336270	0.00000000009127	0.00000000000000
5.333333333	0.06364161150846	0.00000451899715	72.92115383178020	0.00010771532233	0.04146773690437	0.04146776859504
10.66666667	0.06648536391929	0.00000472092335	75.65127870030220	0.00011174812028	0.08293550256762	0.08293553719008
16	0.06959840142640	0.00000494197067	78.63718559828870	0.00011615874610	0.12440326780459	0.12440330578512
21.33333333	0.07302091904945	0.00000518499323	81.91701859913470	0.00012100354422	0.16587103252849	0.16587107438017
26.66666667	0.07680153121108	0.00000545344299	85.53691091051530	0.00012635066021	0.20733879662903	0.20733884297521
32	0.08099959803723	0.00000575153494	89.55319225739420	0.00013228330138	0.24880655996493	0.24880661157025
37.33333333	0.08568836807682	0.00000608447023	94.03537098490960	0.00013890414185	0.29027432235202	0.29027438016529
42.66666667	0.09095929249706	0.00000645874253	99.07022773645340	0.00014634136945	0.33174208354765	0.33174214876033
48	0.09692805395709	0.00000688256612	104.76753617903200	0.00015475713611	0.37320984322594	0.37320991735537
53.33333333	0.10374316167494	0.00000736648618	111.26821874729900	0.00016435960510	0.41467760094160	0.41467768595041
58.66666667	0.11159848428643	0.00000792426873	118.75623892123500	0.00017542051766	0.45614535607302	0.45614545454546
64	0.12075199929980	0.00000857423197	127.47639233506700	0.00018830147314	0.49761310773159	0.49761322314050
69.33333333	0.13155468087634	0.00000934129752	137.76171802788800	0.00020349441941	0.53908085461089	0.53908099173554
74.66666667	0.14449655505706	0.00001026026061	150.07719964848600	0.00022168620605	0.58054859472708	0.58054876033058
80	0.16028313368833	0.00001138121752	165.09229262339200	0.00024386571768	0.62201632494845	0.62201652892562
85.33333333	0.17996849229781	0.00001277901492	183.80720003614600	0.00027151040209	0.66348404009615	0.66348429752066
90.66666667	0.20520086720149	0.00001457068907	207.78591654099600	0.00030693051055	0.70495173109950	0.70495206611570
96	0.23870997015404	0.00001695006849	239.61863494192900	0.00035395214066	0.74641938087492	0.74641983471074
101.3333333	0.28536802495303	0.00002026311496	283.92855009080200	0.00041940443457	0.78788695404675	0.78788760330579

Temperature Increment (T)	Horizontal Deflection at Mid-Span (Y_{max}) due to Temperature Increment	Horizontal Deflection at Mid-Span due to Temperature Increment per original length (f)	Fixed End Moment (M) due to Temperature Increment	Value of m=(ML/EI) due to Temperature Increment	Ratio of P/Pcr	Ratio of T/T_{cr}
106.6666667	0.35480489693961	0.00002519361592	349.85332143293900	0.00051678506586	0.82935436720188	0.82935537190083
112	0.46909040389237	0.00003330868195	458.33471836633900	0.00067702812323	0.87082138249606	0.87082314049587
117.3333333	0.69239943346704	0.00004916517652	670.26746590405300	0.00099008411608	0.91228707495334	0.91229090909091
122.6666667	1.32283453592771	0.00009393045448	1268.51721394270000	0.00187378741829	0.95374466848329	0.95375867768595
128	11.78631828085940	0.00083691059063	11197.21357729210000	0.01653993945875	0.99411319235401	0.99522644628099
133.3333333	69.18972229715350	0.00491295160826	65665.46304186600000	0.09699759460211	0.99832765869431	1.03669421487603
138.6666667	99.65332222238190	0.00707607912600	94569.76563515330000	0.13969352173527	0.99857525353338	1.07816198347107
144	122.85662311845800	0.00872367490568	116584.19285222600000	0.17221208457914	0.99867024831069	1.11962975206612
149.3333333	142.34742154707400	0.01010765718378	135075.28793927400000	0.19952616510058	0.99871947917783	1.16109752066116
154.6666667	159.48336253331100	0.01132442820168	151331.42230188600000	0.22353887829346	0.99874667160058	1.20256528925620
160	174.56391761815400	0.01239525252208	165636.92343675700000	0.24467021789546	0.99876148509223	1.24403305785124
165.3333333	188.74541896928800	0.01340223777303	179088.85085294700000	0.26454070295243	0.99876914159072	1.28550082644628
170.6666667	201.93590165068900	0.01433885380431	191600.05799553600000	0.28302160512206	0.99877172374516	1.32696859504132
176	214.31799988183300	0.01521806891601	203343.86733621000000	0.30036894731296	0.99877069879666	1.36843636363636
181.3333333	226.02435170758800	0.01604930133203	214446.15661723300000	0.31676866955583	0.99876700071915	1.40990413223141
186.6666667	237.15488228329200	0.01683964643355	225001.75973626500000	0.33236085553444	0.99876125656889	1.45137190082645
192	247.78742193908600	0.01759463071542	235084.61385916000000	0.34725472137106	0.99875260930974	1.49283966942149
197.3333333	257.98276805074100	0.01831857121429	244752.26502225800000	0.36153527106694	0.99874426074973	1.53430743801653
202.6666667	267.79119859586300	0.01901503801631	254052.52019581200000	0.37527312258328	0.99873477891853	1.57577520661157
208	277.25373520950300	0.01968694394295	263024.31293864900000	0.38852578654103	0.99872436642934	1.61724297520661
213.3333333	286.40463006636900	0.02033672113690	271700.15250732200000	0.40134128391715	0.99871318010774	1.65871074380165
218.6666667	295.27283370136700	0.02096642528752	280107.51691127100000	0.41376020379299	0.99870134144463	1.70017851239670
224	303.88307689367900	0.02157781245218	288269.87953883300000	0.42581721983259	0.99868894636896	1.74164628099174
229.3333333	312.25668433418700	0.02217239683229	296207.48128409900000	0.43754223082824	0.99867607186856	1.78311404958678

Temperature Increment (T)	Horizontal Deflection at Mid-Span (Y_{max}) due to Temperature Increment	Horizontal Deflection at Mid-Span due to Temperature Increment per original length (f)	Fixed End Moment (M) due to Temperature Increment	Value of m=(ML/EI) due to Temperature Increment	Ratio of P/Pcr	Ratio of T/T_{cr}
234.6666667	320.41219710161700	0.02275149497341	303937.92125528800000	0.44896123326401	0.99866278060300	1.82458181818182
240	328.36585612985200	0.02331626009483	311476.61557641400000	0.46009699903366	0.99864912419809	1.86604958677686
245.3333333	336.13198281390600	0.02386770911523	318837.15858084600000	0.47096960897689	0.99863514564981	1.90751735537190
250.6666667	343.72328229534000	0.02440674418804	326031.61063185800000	0.48159687803282	0.99862088111202	1.94898512396694
256	351.15108779664200	0.02493417005089	333070.73000103600000	0.49199469775872	0.99860636124680	1.99045289256198
261.3333333	358.42555943004900	0.02545070814245	339964.16154416500000	0.50217731503215	0.99859161226036	2.03192066115703
266.6666667	365.55584743651100	0.02595700819346	346720.59162180400000	0.51215756089154	0.99857665670853	2.07338842975207
272	372.55022733574300	0.02645365782340	353347.87636374800000	0.52194704000177	0.99856151412903	2.11485619834711
277.3333333	379.41621267759000	0.02694119054658	359853.14867695100000	0.53155628872069	0.99854620154469	2.15632396694215
282.6666667	386.16064977047200	0.02742009249852	366242.90814947300000	0.54099490790054	0.99853073386714	2.19779173553719
288	392.78979778766500	0.02789080812407	372523.09707770200000	0.55027167519139	0.99851512422338	2.23925950413223
293.3333333	399.30939691840600	0.02835374501659	378699.16514773200000	0.55939464058508	0.99849938422242	2.28072727272727
298.6666667	405.72472667466200	0.02880927805816	384776.12477408200000	0.56837120815873	0.99848352417491	2.32219504132231
304	412.04065603756500	0.02925775298031	390758.59869391800000	0.57720820637838	0.99846755327458	2.36366280991736
309.3333333	418.26168679728300	0.02969948944147	396650.86110149100000	0.58591194886071	0.99845147974955	2.40513057851240
314.6666667	424.39199118250600	0.03013478369889	402456.87336305100000	0.59448828712916	0.99843531098942	2.44659834710744
320	430.43544467290500	0.03056391093859	408180.31516007700000	0.60294265661717	0.99841905365260	2.48806611570248

Table D- 6: Numerical Results for Fixed-Fixed Column Subjected to (T/T_{cr}=3.6464) with 60 Load-Steps and Eccentricity (e=0.001& convergence tolerance=0.001) for Slenderness Ratio of 160 (Data for Horizontal Mid-Span Deflections and Fixed-End Moments in Validation to Elastica Solution)

Temperature Increment (T)	Horizontal Deflection at Mid-Span (Y_{max}) due to Temperature Increment	Horizontal Deflection at Mid-Span due to Temperature Increment per original length (f)	Fixed End Moment (M) due to Temperature Increment	Value of m=(ML/EI) due to Temperature Increment	Ratio of P/Pcr	Ratio of T/T_{cr}
0	0.38146014711605	0.00002708632411	440.09375129154800	0.00065008351875	0.00000000356540	0.00000000000000
7.833333333	0.40589546360379	0.00002882140157	463.56951588205400	0.00068476069289	0.06090449541424	0.06090578512397
15.66666667	0.43371945466805	0.00003079709849	490.26424766652700	0.00072419275735	0.12181009538457	0.12181157024793
23.5	0.46568981662963	0.00003306721660	520.89697916290100	0.00076944182945	0.18271565244124	0.18271735537190
31.33333333	0.50280910645824	0.00003570294440	556.41909527002000	0.00082191324528	0.24362115221222	0.24362314049587
39.16666667	0.54643145766694	0.00003880043480	598.11558927166700	0.00088350512988	0.30452657376153	0.30452892561984
47	0.59843150104703	0.00004249279962	647.76534957947200	0.00095684516434	0.36543188563317	0.36543471074380
54.83333333	0.66148102861943	0.00004696975469	707.90368260194800	0.00104567837097	0.42633703880513	0.42634049586777
62.66666667	0.73952310910325	0.00005251128531	782.27219478495800	0.00115553165550	0.48724195345295	0.48724628099174
70.5	0.83863024271201	0.00005954858125	876.63308449639300	0.00129491663663	0.54814649242790	0.54815206611570
78.33333333	0.96866607617647	0.00006878203003	1000.34592163884000	0.00147765878247	0.60905040369652	0.60905785123967
86.16666667	1.14679068534120	0.00008143011642	1169.69376411080000	0.00172781057628	0.66995318205002	0.66996363636364
94	1.40573611119710	0.00009981704304	1415.73570437103000	0.00209125088829	0.73085368904026	0.73086942148760
101.8333333	1.81664196828900	0.00012899421740	1805.97527380189000	0.00266769241173	0.79174889254743	0.79177520661157
109.6666667	2.56867783808189	0.00018239399577	2519.91305862751000	0.00372228404355	0.85262830175360	0.85268099173554
117.5	4.38522853841940	0.00031138173250	4243.95915851186000	0.00626895495586	0.91343297871931	0.91358677685950
125.3333333	14.26239609672910	0.00101272934064	13616.60794020880000	0.02011374253157	0.97286329120579	0.97449256198347
133.1666667	71.90123680667410	0.00510548800135	68308.24521596310000	0.10090137448989	0.99397032514712	1.03539834710744
141	111.98270858610400	0.00795155132842	106337.58415717500000	0.15707632903570	0.99581444130828	1.09630413223140
148.8333333	141.62312979873300	0.01005622743104	134458.22011371600000	0.19861466471646	0.99648878190704	1.15720991735537

Temperature Increment (T)	Horizontal Deflection at Mid-Span (Y_{max}) due to Temperature Increment	Horizontal Deflection at Mid-Span due to Temperature Increment per original length (f)	Fixed End Moment (M) due to Temperature Increment	Value of m=(ML/EI) due to Temperature Increment	Ratio of P/Pcr	Ratio of T/T_{cr}
156.6666667	166.17244066857000	0.01179939928252	157746.84729237900000	0.23301540923684	0.99685503573820	1.21811570247934
164.5	187.16634914669800	0.01329011283067	177661.08266789800000	0.26243167831172	0.99708264706542	1.27902148760331
172.3333333	206.35159947328900	0.01465239906795	195858.23506361300000	0.28931156203182	0.99724258420069	1.33992727272727
180.1666667	223.91283634446000	0.01589936905229	212513.67851844100000	0.31391411377382	0.99735866087298	1.40083305785124
188	240.20268628983100	0.01705606172036	227962.07123944600000	0.33673367317373	0.99744571954809	1.46173884297521
195.8333333	255.46238155117600	0.01813960623950	242432.35961434400000	0.35810842788564	0.99751240838092	1.52264462809917
203.6666667	269.86548595852700	0.01916232684904	256089.27232323200000	0.37828170651780	0.99756415220539	1.58355041322314
211.5	283.54178149002100	0.02013343897229	269055.98815145900000	0.39743546234261	0.99760454829626	1.64445619834711
219.3333333	296.59130854604700	0.02106004617359	281427.46005239400000	0.41570995490673	0.99763608833187	1.70536198347107
227.1666667	309.09342093868100	0.02194778312565	293279.11332468600000	0.43321659852451	0.99765902544210	1.76626776859504
235	321.11113443766400	0.02280112438649	304670.53301011400000	0.45004340910963	0.99767807989449	1.82717355371901
242.8333333	332.69713403678200	0.02362381095719	315651.85765540600000	0.46626444870634	0.99769229956096	1.88807933884298
250.6666667	343.89491371579600	0.02441893121286	326264.37271778400000	0.48194070203715	0.99770247978649	1.94898512396694
258.5	354.74113035221500	0.02518908804683	336542.87462136800000	0.49712356856358	0.99770924567498	2.00989090909091
266.3333333	365.26701927671200	0.02593649938485	346517.01434079300000	0.51185684715773	0.99771309405025	2.07079669421488
274.1666667	375.49945367963300	0.02666307341041	356212.30274666600000	0.52617822114612	0.99771442560051	2.13170247933884
282	385.46175201944900	0.02737046589625	365650.87683492500000	0.54012039014372	0.99771356765159	2.19260826446281
289.8333333	395.17430299494900	0.02806012458183	374852.09283984100000	0.55371194616948	0.99771079064606	2.25351404958678
297.6666667	404.65505604054400	0.02873332400187	383832.99173589900000	0.56697806126147	0.99770632029498	2.31441983471074
305.5	413.91991108812700	0.02939119316213	392608.66914661300000	0.57994103388683	0.99770034668990	2.37532561983471
313.3333333	422.98303177121700	0.03003473777912	401192.57260069200000	0.59262072803308	0.99769303123740	2.43623140495868
321.1666667	431.85709967833900	0.03066485833386	409596.74284327400000	0.60503492966046	0.99768451200750	2.49713719008264
329	440.55352267005800	0.03128236486380	417832.01155230000000	0.61719963875827	0.99767490790859	2.55804297520661
336.8333333	449.08260700994500	0.03188798918535	425908.16471267400000	0.62912931067264	0.99766432198259	2.61894876033058

Temperature Increment (T)	Horizontal Deflection at Mid-Span (Y_{max}) due to Temperature Increment	Horizontal Deflection at Mid-Span due to Temperature Increment per original length (f)	Fixed End Moment (M) due to Temperature Increment	Value of m=(ML/EI) due to Temperature Increment	Ratio of P/Pcr	Ratio of T/T_{cr}
344.6666667	457.45370070542300	0.03248239507208	433834.07866697300000	0.64083705707352	0.99765284403159	2.67985454545454
352.5	465.67531373199800	0.03306618679143	441617.83422675600000	0.65233481451396	0.99764055273135	2.74076033057851
360.3333333	473.75521953923400	0.03363991631241	449266.81301885300000	0.66363348674784	0.99762751734470	2.80166611570248
368.1666667	481.70054128046000	0.03420408942845	456787.77933275400000	0.67474306563053	0.99761379912441	2.86257190082644
376	489.51782548524400	0.03475917098870	464186.95005006900000	0.68567273441505	0.99759945246693	2.92347768595041
383.8333333	497.21310533898100	0.03530558939130	471470.05470978800000	0.69643095647735	0.99758452586963	2.98438347107438
391.6666667	504.79195530693900	0.03584374046204	478642.38735835400000	0.70702555190651	0.99756906272937	3.04528925619835
399.5	512.25953850687800	0.03637399081822	485708.85151703000000	0.71746376392821	0.99755310201332	3.10619504132231
407.3333333	519.62064797310500	0.03689668079861	492673.99935156000000	0.72775231676407	0.99753667882310	3.16710082644628
415.1666667	526.87974274744800	0.03741212702620	499542.06593144300000	0.73789746623771	0.99751982487582	3.22800661157025
423	534.04097956850900	0.03792062465835	506316.99931147900000	0.74790504420962	0.99750256891192	3.28891239669421
430.8333333	541.10824079782100	0.03842244936973	513002.48704134400000	0.75778049773571	0.99748493704549	3.34981818181818
438.6666667	548.08515911496600	0.03891785910587	519601.97960829300000	0.76752892369564	0.99746695306544	3.41072396694215
446.5	554.97513942708600	0.03940709563886	526118.71123590400000	0.77715509951569	0.99744863869450	3.47162975206611
454.3333333	561.78137836737600	0.03989038595190	532555.71839403900000	0.78666351051064	0.99743001381549	3.53253553719008
462.1666667	568.50688169914600	0.04036794347509	538915.85632100400000	0.79605837428948	0.99741109666606	3.59344132231405
470	575.15447989377800	0.04083996919158	545201.81381208500000	0.80534366260029	0.99739190401056	3.65434710743801

Table D- 7: Numerical Results for Fixed-Fixed Column Subjected to 3950℃ and 37000 KN with 60 Load-Steps and Eccentricity (e=0.001& convergence tolerance=0.001) for Slenderness Ratio of 50 (Data for Horizontal Mid-Span Deflections)

Temperature Increment (T)	Mechanical Load Increment (P)	Horizontal Deflection at Mid-Span due to Temperature Increment	Horizontal Deflection at Mid-Span due to Temperature Increment per Original Length	Horizontal Deflection at Mid-Span due to Mechanical Load Increment	Horizontal Deflection at Mid-Span due to Mechanical Load Increment per Original Length	Ratio of P/P_{cr}	Ratio of T/T_{cr}
0	0	0.00004653520732	0.00000001057618	0.00000000000000	0.00000000000000	0.00000000000000	0.00000000000000
65.83333333	616.666667	0.00004895259592	0.00000001112559	0.02959438463078	0.00000672599651	0.03169358786099	0.04996488986784
131.6666667	1233.33333	0.00005163827885	0.00000001173597	0.06110389061577	0.00001388724787	0.06338717572198	0.09992977973568
197.5	1850	0.00005463960295	0.00000001241809	0.09472680078918	0.00002152881836	0.09508076358297	0.14989466960352
263.3333333	2466.66667	0.00005801575135	0.00000001318540	0.13068978053121	0.00002970222285	0.12677435144396	0.19985955947137
329.1666667	3083.33333	0.00006184169260	0.00000001405493	0.16925314522384	0.00003846662391	0.15846793930494	0.24982444933921
395	3700	0.00006621381820	0.00000001504860	0.21071734603952	0.00004789030592	0.19016152716593	0.29978933920705
460.8333333	4316.66667	0.00007125818116	0.00000001619504	0.25543101599067	0.00005805250363	0.22185511502692	0.34975422907489
526.6666667	4933.33333	0.00007714286088	0.00000001753247	0.30380103244119	0.00006904568919	0.25354870288791	0.39971911894273
592.5	5550	0.00008409706781	0.00000001911297	0.35630521135249	0.00008097845713	0.28524229074890	0.44968400881057
658.3333333	6166.66667	0.00009244171247	0.00000002100948	0.41350847289417	0.00009397919839	0.31693587860989	0.49964889867841
724.1666667	6783.33333	0.00010264036789	0.00000002332736	0.47608363877559	0.00010820082699	0.34862946647088	0.54961378854626
790	7400	0.00011538845118	0.00000002622465	0.54483848719976	0.00012382692891	0.38032305433187	0.59957867841410
855.8333333	8016.66667	0.00013177887535	0.00000002994974	0.62075137803043	0.00014107985864	0.41201664219285	0.64954356828194
921.6666667	8633.33333	0.00015363341352	0.00000003491668	0.70501879196653	0.00016023154363	0.44371023005384	0.69950845814978
987.5	9250	0.00018423184751	0.00000004187087	0.79911970651639	0.00018161811512	0.47540381791483	0.74947334801762
1053.333333	9866.66667	0.00023013543009	0.00000005230351	0.90490420204175	0.00020566004592	0.50709740577582	0.79943823788546
1119.166667	10483.3333	0.00030665971201	0.00000006969539	1.02471764971041	0.00023289037493	0.53879099363681	0.84940312775330
1185	11100	0.00045978275446	0.00000010449608	1.16157834728610	0.00026399507893	0.57048458149780	0.89936801762115
1250.833333	11716.6667	0.00091977218497	0.00000020903913	1.31943751292375	0.00029987216203	0.60217816935879	0.94933290748899

Temperature Increment (T)	Mechanical Load Increment (P)	Horizontal Deflection at Mid-Span due to Temperature Increment	Horizontal Deflection at Mid-Span due to Temperature Increment per Original Length	Horizontal Deflection at Mid-Span due to Mechanical Load Increment	Horizontal Deflection at Mid-Span due to Mechanical Load Increment per Original Length	Ratio of P/P_{cr}	Ratio of T/T_{cr}
1316.666667	12333.3333	-0.45517017163081	0.00010344776628	1.50356991523549	0.00034172043528	0.63387175721978	0.99929779735683
1382.5	12950	79.70140007043810	0.01811395456146	1.72117871726410	0.00039117698120	0.66556534508076	1.04926268722467
1448.333333	13566.6667	112.68158842435100	0.02560945191463	1.98236536755267	0.00045053758353	0.69725893294175	1.09922757709251
1514.166667	14183.3333	138.01318671332100	0.03136663334394	2.30175032110361	0.00052312507298	0.72895252080274	1.14919246696035
1580	14800	159.38498465682400	0.03622386014928	2.70131825249140	0.00061393596648	0.76064610866373	1.19915735682819
1645.833333	15416.6667	177.82675187409600	0.04041517088048	3.21572297123275	0.00073084612983	0.79233969652472	1.24912224669603
1711.666667	16033.3333	194.83641163977600	0.04428100264540	3.90294738869539	0.00088703349743	0.82403328438571	1.29908713656388
1777.5	16650	210.48935677158000	0.04783849017536	4.86790963342631	0.00110634309851	0.85572687224670	1.34905202643172
1843.333333	17266.6667	225.06883303824300	0.05115200750869	6.32199275558540	0.00143681653536	0.88742046010769	1.39901691629956
1909.166667	17883.3333	238.77156181775600	0.05426626404949	8.76394801167341	0.00199180636629	0.91911404796867	1.44898180616740
1975	18500	251.74075418351800	0.05721380776898	13.71909107797220	0.00311797524499	0.95080763582966	1.49894669603524
2040.833333	19116.6667	264.08450542249100	0.06001920577784	29.15311248305670	0.00662570738251	0.98250122369065	1.54891158590308
2106.666667	19733.3333	275.88712193279800	0.06270161862109	269.64631925275100	0.06128325437563	1.01419481155164	1.59887647577092
2172.5	20350	287.21459267030900	0.06527604378871	676.59826514043500	0.15377233298646	1.04588839941263	1.64884136563877
2238.333333	20966.6667	298.12149218046400	0.06775488458647	900.14763152903000	0.20457900716569	1.07758198727362	1.69880625550661
2304.166667	21583.3333	308.65240471793700	0.07014827379953	1056.68172679665000	0.24015493790833	1.10927557513461	1.74877114537445
2370	22200	318.84458426639300	0.07246467824236	1175.54787861440000	0.26716997241236	1.14096916299559	1.79873603524229
2435.833333	22816.6667	328.72953786524800	0.07471125860574	1269.52381892688000	0.28852814066520	1.17266275085658	1.84870092511013
2501.666667	23433.3333	338.33419418812500	0.07689413504276	1345.62263191405000	0.30582332543501	1.20435633871757	1.89866581497797
2567.5	24050	347.68178339754400	0.07901858713581	1408.21111381790000	0.32004798041316	1.23604992657856	1.94863070484582
2633.333333	24666.6667	356.79251092651300	0.08108920702875	1460.24296982727000	0.33187340223347	1.26774351443955	1.99859559471366
2699.166667	25283.3333	365.68408125952900	0.08311001846807	1503.82174454975000	0.34177766921585	1.29943710230054	2.04856048458150
2765	25900	374.37211060432900	0.08508457059189	1540.50839191158000	0.35011554361627	1.33113069016153	2.09852537444934
2830.833333	26516.6667	382.87045596516900	0.08701601271936	1571.49617663703000	0.35715822196296	1.36282427802252	2.14849026431718

Temperature Increment (T)	Mechanical Load Increment (P)	Horizontal Deflection at Mid-Span due to Temperature Increment	Horizontal Deflection at Mid-Span due to Temperature Increment per Original Length	Horizontal Deflection at Mid-Span due to Mechanical Load Increment	Horizontal Deflection at Mid-Span due to Mechanical Load Increment per Original Length	Ratio of P/P_{cr}	Ratio of T/T_{cr}
2896.666667	27133.3333	391.19148042482000	0.08890715464200	1597.71870682984000	0.36311788791587	1.39451786588351	2.19845515418502
2962.5	27750	399.34626912513400	0.09076051571026	1619.92012470861000	0.36816366470650	1.42621145374449	2.24842004405286
3028.333333	28366.6667	407.34480670052400	0.09257836515921	1638.70261823609000	0.37243241323548	1.45790504160548	2.29838493392071
3094.166667	28983.3333	415.19612425189300	0.09436275551179	1654.56432700299000	0.37603734704613	1.48959862946647	2.34834982378855
3160	29600	422.90842201690800	0.09611555045839	1667.90298558436000	0.37906886036008	1.52129221732746	2.39831471365639
3225.833333	30216.6667	430.48917247423200	0.09783844828960	1679.06716207211000	0.38160617319821	1.55298580518845	2.44827960352423
3291.666667	30833.3333	437.94520756527100	0.09953300171938	1688.34451499365000	0.38371466249856	1.58467939304944	2.49824449339207
3357.5	31450	445.28279292453300	0.10120063475558	1695.97901511347000	0.38544977616215	1.61637298091043	2.54820938325991
3423.333333	32066.6667	452.50769140765800	0.10284265713810	1702.17889454736000	0.38685883966986	1.64806656877142	2.59817427312776
3489.166667	32683.3333	459.62521774435100	0.10446027676008	1707.12282894403000	0.38798246112364	1.67976015663240	2.64813916299560
3555	33300	466.64028578583600	0.10605461040587	1710.96486270949000	0.38885565061579	1.71145374449339	2.69810405286344
3620.833333	33916.6667	473.55744953726900	0.10762669307665	1713.83837286873000	0.38950872110653	1.74314733235438	2.74806894273128
3686.666667	34533.3333	480.38093894582400	0.10917748612405	1715.85928798385000	0.38996801999633	1.77484092021537	2.79803383259912
3752.5	35150	487.11469124095400	0.11070788437294	1717.12872340617000	0.39025652804686	1.80653450807636	2.84799872246696
3818.333333	35766.6667	493.76237848416900	0.11221872238277	1717.73515461135000	0.39039435332076	1.83822809593735	2.89796361233480
3884.166667	36383.3333	500.32743187392500	0.11371077997135	1717.75622161678000	0.39039914127654	1.86992168379834	2.94792850220265
3950	37000	506.81306326073400	0.11518478710471	1717.26023629073000	0.39028641733880	1.90161527165933	2.99789339207049

Table D- 8: Numerical Results for Fixed-Fixed Column Subjected to 630℃ and 4750 KN with 60 Load-Steps and Eccentricity (e=0.001& convergence tolerance=0.001) for Slenderness Ratio of 125 (Data for Horizontal Mid-Span Deflections)

Temperature Increment (T)	Mechanical Load Increment (P)	Horizontal Deflection at Mid-Span due to Temperature Increment	Horizontal Deflection at Mid-Span due to Temperature Increment per Original Length	Horizontal Deflection at Mid-Span due to Mechanical Load Increment	Horizontal Deflection at Mid-Span due to Mechanical Load Increment per Original Length	Ratio of P/P_{cr}	Ratio of T/T_{cr}
0	0	0.00000000000000	0.00000000000000	0.00000000000000	0.00000000000000	0.00000000000000	0.00000000000000
10.5	79.1666667	0.00654401353121	0.00000059491032	0.05903900868111	0.00000536718261	0.02542982134117	0.04980677312775
21	158.333333	0.00688282663103	0.00000062571151	0.12118763721074	0.00001101705793	0.05085964268233	0.09961354625551
31.5	237.5	0.00725911084371	0.00000065991917	0.18670205116875	0.00001697291374	0.07628946402349	0.14942031938326
42	316.666667	0.00767945409650	0.00000069813219	0.25586738004017	0.00002326067091	0.10171928536466	0.19922709251101
52.5	395.833333	0.00815208498686	0.00000074109864	0.32900192998909	0.00002990926636	0.12714910670583	0.24903386563877
63	475	0.00868741743336	0.00000078976522	0.40646215458522	0.00003695110496	0.15257892804699	0.29884063876652
73.5	554.166667	0.00929882773233	0.00000084534798	0.48864854652507	0.00004442259514	0.17800874938816	0.34864741189427
84	633.333333	0.01000378858056	0.00000090943533	0.57601265617419	0.00005236478692	0.20343857072932	0.39845418502203
94.5	712.5	0.01082556721240	0.00000098414247	0.66906549656756	0.00006082413605	0.22886839207049	0.44826095814978
105	791.666667	0.01179584464804	0.00000107234951	0.76838766529066	0.00006985342412	0.25429821341165	0.49806773127753
115.5	870.833333	0.01295889689751	0.00000117808154	0.87464160679084	0.00007951287334	0.27972803475281	0.54787450440529
126	950	0.01437854473403	0.00000130714043	0.98858656250757	0.00008987150568	0.30515785609398	0.59768127753304
136.5	1029.16667	0.01615027607453	0.00000146820692	1.11109692220814	0.00010100881111	0.33058767743514	0.64748805066079
147	1108.33333	0.01842366856004	0.00000167487896	1.24318491486096	0.00011301681044	0.35601749877631	0.69729482378855
157.5	1187.5	0.02144700744124	0.00000194972795	1.38602888535909	0.00012600262594	0.38144732011747	0.74710159691630
168	1266.66667	0.02566479503733	0.00000233316319	1.54100882999509	0.00014009171182	0.40687714145864	0.79690837004405
178.5	1345.83333	0.03195931166981	0.00000290539197	1.70975146174703	0.00015543195107	0.43230696279980	0.84671514317181
189	1425	0.04236560274593	0.00000385141843	1.89418792650263	0.00017219890241	0.45773678414097	0.89652191629956
199.5	1504.16667	0.06286749517237	0.00000571522683	2.09662851694099	0.00019060259245	0.48316660548213	0.94632868942731
210	1583.33333	0.12199852883233	0.00001109077535	2.31986052561850	0.00021089641142	0.50859642682330	0.99613546255507

Temperature Increment (T)	Mechanical Load Increment (P)	Horizontal Deflection at Mid-Span due to Temperature Increment	Horizontal Deflection at Mid-Span due to Temperature Increment per Original Length	Horizontal Deflection at Mid-Span due to Mechanical Load Increment	Horizontal Deflection at Mid-Span due to Mechanical Load Increment per Original Length	Ratio of P/P_{cr}	Ratio of T/T_{cr}
220.5	1662.5	2.08241098702981	0.00018931008973	2.56727805309607	0.00023338891392	0.53402624816446	1.04594223568282
231	1741.66667	76.50176960372400	0.00695470632761	2.84305664615844	0.00025845969511	0.55945606950563	1.09574900881057
241.5	1820.83333	109.88412920324000	0.00998946629120	3.15239193206463	0.00028658108473	0.58488589084679	1.14555578193833
252	1900	135.27502765175900	0.01229772978652	3.50183143299227	0.00031834831209	0.61031571218796	1.19536255506608
262.5	1979.16667	156.60592950090400	0.01423690268190	3.89974467865934	0.00035452224351	0.63574553352912	1.24516932819383
273	2058.33333	174.97254060033000	0.01590659460003	4.35700465530589	0.00039609133230	0.66117535487029	1.29497610132159
283.5	2137.5	191.87480977715000	0.01744316452520	4.88799927491955	0.00044436357045	0.68660517621145	1.34478287444934
294	2216.66667	207.40654470687000	0.01885514042790	5.51217664849253	0.00050110696804	0.71203499755262	1.39458964757709
304.5	2295.83333	221.85571054203500	0.02016870095837	6.25648408721844	0.00056877128066	0.73746481889378	1.44439642070485
315	2375	235.42168462079900	0.02140197132916	7.15936828063278	0.00065085166188	0.76289464023495	1.49420319383260
325.5	2454.16667	248.24927687995800	0.02256811608000	8.27764167683165	0.00075251287971	0.78832446157611	1.54400996696035
336	2533.33333	260.44759635275000	0.02367705421389	9.69893583897124	0.00088172143991	0.81375428291728	1.59381674008811
346.5	2612.5	272.10163469428900	0.02473651224494	11.56587705977680	0.00105144336907	0.83918410425844	1.64362351321586
357	2691.66667	283.27780486468300	0.02575252771497	14.12725103300640	0.00128429554846	0.86461392559961	1.69343028634361
367.5	2770.83333	294.03102378542700	0.02673009307140	17.85933554928900	0.00162357595903	0.89004374694077	1.74323705947137
378	2850	304.40610820330800	0.02767328256394	23.80287837377760	0.00216389803398	0.91547356828194	1.79304383259912
388.5	2929.16667	314.44048370091600	0.02858549851827	34.75044019524540	0.00315913092684	0.94090338962310	1.84285060572687
399	3008.33333	324.16578660387400	0.02946961696399	61.58878938682550	0.00559898085335	0.96633321096427	1.89265737885463
409.5	3087.5	333.60904482938600	0.03032809498449	220.32488331963800	0.02002953484724	0.99176303230543	1.94246415198238
420	3166.66667	342.79356607409400	0.03116305146128	1252.66080650937000	0.11387825513722	1.01719285364660	1.99227092511013
430.5	3245.83333	351.73961737044100	0.03197632885186	1886.44021805466000	0.17149456527770	1.04262267498776	2.04207769823789
441	3325	360.46495294179800	0.03276954117653	2313.38061080881000	0.21030732825535	1.06805249632893	2.09188447136564
451.5	3404.16667	368.98522979443300	0.03354411179949	2636.23915612001000	0.23965810510182	1.09348231767009	2.14169124449339
462	3483.33333	377.31433891391600	0.03430130353763	2893.28102666837000	0.26302554787894	1.11891213901126	2.19149801762115

Temperature Increment (T)	Mechanical Load Increment (P)	Horizontal Deflection at Mid-Span due to Temperature Increment	Horizontal Deflection at Mid-Span due to Temperature Increment per Original Length	Horizontal Deflection at Mid-Span due to Mechanical Load Increment	Horizontal Deflection at Mid-Span due to Mechanical Load Increment per Original Length	Ratio of P/P_{cr}	Ratio of T/T_{cr}
472.5	3562.5	385.46467211067200	0.03504224291915	3103.99752282248000	0.28218159298386	1.14434196035242	2.24130479074890
483	3641.66667	393.44733916534800	0.03576793992412	3280.00755905306000	0.29818250536846	1.16977178169359	2.29111156387665
493.5	3720.83333	401.27234613920000	0.03647930419447	3428.89221397923000	0.31171747399811	1.19520160303475	2.34091833700441
504	3800	408.94874301464900	0.03717715845588	3556.02372886185000	0.32327488444199	1.22063142437592	2.39072511013216
514.5	3879.16667	416.48474687669800	0.03786224971606	3665.31208557623000	0.33321018959784	1.24606124571708	2.44053188325991
525	3958.33333	423.88784541235200	0.03853525867385	3759.73267476003000	0.34179387952364	1.27149106705825	2.49033865638767
535.5	4037.5	431.16488444023200	0.03919680767638	3841.60780766658000	0.34923707342424	1.29692088839941	2.54014542951542
546	4116.66667	438.32214238228200	0.03984746748930	3912.78862535699000	0.35570805685064	1.32235070974058	2.58995220264317
556.5	4195.83333	445.36539398251200	0.04048776308932	3974.77617945364000	0.36134328904124	1.34778053108174	2.63975897577093
567	4275	452.29996511124600	0.04111817864648	4028.80498752360000	0.36625499886578	1.37321035242291	2.68956574889868
577.5	4354.16667	459.13078013353700	0.04173916183032	4075.93007266499000	0.37053909751500	1.39864017376407	2.73937252202643
588	4433.33333	465.86240303875800	0.04235112754898	4116.95249160384000	0.37426840832762	1.42406999510524	2.78917929515419
598.5	4512.5	472.49907330711300	0.04295446120974	4152.64168020170000	0.37751288001834	1.44949981644640	2.83898606828194
609	4591.66667	479.04473731350200	0.04354952157395	4183.62327101565000	0.38032938827415	1.47492963778757	2.88879284140969
619.5	4670.83333	485.50307592924800	0.04413664326630	4210.58294346942000	0.38278026758813	1.50035945912873	2.93859961453745
630	4750	491.87752886944400	0.04471613898813	4233.67990643148000	0.38487999149377	1.52578928046990	2.98840638766520

Table D- 9: Numerical Results for Fixed-Fixed Column Subjected to 245℃ and 2250 KN with 60 Load-Steps and Eccentricity (e=0.001& convergence tolerance=0.001) for Slenderness Ratio of 200 (Data for Horizontal Mid-Span Deflections)

Temperature Increment (T)	Mechanical Load Increment (P)	Horizontal Deflection at Mid-Span due to Temperature Increment	Horizontal Deflection at Mid-Span due to Temperature Increment per Original Length	Horizontal Deflection at Mid-Span due to Mechanical Load Increment	Horizontal Deflection at Mid-Span due to Mechanical Load Increment per Original Length	Ratio of P/P_{cr}	Ratio of T/T_{cr}
0	0	0.03573903922957	0.00000203062723	0.00000000000000	0.00000000000000	0.00000000000000	0.00000000000000
4.083333333	37.5	0.03758075732708	0.00000213527030	0.11518741906951	0.00000654473972	0.03083700440529	0.04958540969163
8.166666667	75	0.03962515596034	0.00000225142932	0.23784057920114	0.00001351366927	0.06167400881057	0.09917081938326
12.25	112.5	0.04190768263896	0.00000238111833	0.36871964299688	0.00002094997972	0.09251101321586	0.14875622907489
16.33333333	150	0.04447256422808	0.00000252685024	0.50869171835922	0.00002890293854	0.12334801762115	0.19834163876652
20.41666667	187.5	0.04737570377301	0.00000269180135	0.65875035357002	0.00003742899736	0.15418502202643	0.24792704845815
24.5	225	0.05068880605641	0.00000288004580	0.82003945827933	0.00004659315104	0.18502202643172	0.29751245814978
28.58333333	262.5	0.05450538540149	0.00000309689690	0.99388286878177	0.00005647061754	0.21585903083700	0.34709786784141
32.66666667	300	0.05894974004411	0.00000334941705	1.18182117495104	0.00006714893039	0.24669603524229	0.39668327753304
36.75	337.5	0.06419075531606	0.00000364720201	1.38565797848685	0.00007873056696	0.27753303964758	0.44626868722467
40.83333333	375	0.07046386556495	0.00000400362873	1.60751852598773	0.00009133627989	0.30837004405286	0.49585409691630
44.91666667	412.5	0.07810741569410	0.00000443792135	1.84992475932585	0.00010510936133	0.33920704845815	0.54543950660793
49	450	0.08762578861920	0.00000497873799	2.11589240880621	0.00012022115959	0.37004405286344	0.59502491629956
53.08333333	487.5	0.09980549922602	0.00000567076700	2.40905807104095	0.00013687829949	0.40088105726872	0.64461032599119
57.16666667	525	0.11594453181847	0.00000658775749	2.73384766101925	0.00015533225347	0.43171806167401	0.69419573568282
61.25	562.5	0.13834881298045	0.00000786072801	3.09570285590578	0.00017589220772	0.46255506607930	0.74378114537445
65.33333333	600	0.17154629470767	0.00000974694856	3.50139024002720	0.00019894262727	0.49339207048458	0.79336655506608
69.41666667	637.5	0.22581278688601	0.00001283027198	3.95943067274698	0.00022496765186	0.52422907488987	0.84295196475771
73.5	675	0.33053216686936	0.00001878023675	4.48070720484602	0.00025458563664	0.55506607929515	0.89253737444934
77.58333333	712.5	0.61718454849019	0.00003506730389	5.07934461596805	0.00028859912591	0.58590308370044	0.94212278414097
81.66666667	750	4.59705496091886	0.00026119630460	5.77401355337731	0.00032806895190	0.61674008810573	0.99170819383260

Temperature Increment (T)	Mechanical Load Increment (P)	Horizontal Deflection at Mid-Span due to Temperature Increment	Horizontal Deflection at Mid-Span due to Temperature Increment per Original Length	Horizontal Deflection at Mid-Span due to Mechanical Load Increment	Horizontal Deflection at Mid-Span due to Mechanical Load Increment per Original Length	Ratio of P/P_{cr}	Ratio of T/T_{cr}
85.75	787.5	72.88462361688250	0.00414117179641	6.58991933657721	0.00037442723503	0.64757709251101	1.04129360352423
89.83333333	825	107.14095851403100	0.00608755446102	7.56193498840565	0.00042965539707	0.67841409691630	1.09087901321586
93.91666667	862.5	132.88322662291000	0.00755018333085	8.73972796924045	0.00049657545280	0.70925110132159	1.14046442290749
98	900	154.40270654848800	0.00877288105389	10.19653633200030	0.00057934865523	0.74008810572687	1.19004983259912
102.0833333	937.5	172.88868585927500	0.00982322078746	12.04503296386620	0.00068437687295	0.77092511013216	1.23963524229075
106.1666667	975	189.86379728965000	0.01078771575509	14.46799533510360	0.00082204518949	0.80176211453745	1.28922065198238
110.25	1012.5	205.44313663989500	0.01167290549090	17.78286924978070	0.00101039029828	0.83259911894273	1.33880606167401
114.3333333	1050	219.92314645891800	0.01249563332153	22.59378755535220	0.00128373792928	0.86343612334802	1.38839147136564
118.4166667	1087.5	233.50821225918800	0.01326751206018	30.20951269677290	0.00171644958504	0.89427312775330	1.43797688105727
122.5	1125	246.34630778729800	0.01399694930610	44.09291407256700	0.00250527920867	0.92511013215859	1.48756229074890
126.5833333	1162.5	258.54864595720200	0.01469026397484	77.37929347703370	0.00439655076574	0.95594713656388	1.53714770044053
130.6666667	1200	270.20168521208100	0.01535236847796	260.51952629412400	0.01480224581217	0.98678414096916	1.58673311013216
134.75	1237.5	281.37285874109400	0.01598709424665	2093.62763265635000	0.11895611549184	1.01762114537445	1.63631851982379
138.8333333	1275	292.11786422304500	0.01659760592176	3238.05987218078000	0.18398067455573	1.04845814977974	1.68590392951542
142.9166667	1312.5	302.48209528725300	0.01718648268678	3979.21781313010000	0.22609192120057	1.07929515418502	1.73548933920705
147	1350	312.50342034726100	0.01775587615609	4525.22194020420000	0.25711488296615	1.11013215859031	1.78507474889868
151.0833333	1387.5	322.21382149656200	0.01830760349412	4950.08634948634000	0.28125490622082	1.14096916299559	1.83466015859031
155.1666667	1425	331.64060065925200	0.01884321594655	5290.86228099562000	0.30061717505657	1.17180616740088	1.88424556828194
159.25	1462.5	340.80728552528000	0.01936405031394	5569.43316912722000	0.31644506642768	1.20264317180617	1.93383097797357
163.3333333	1500	349.73432181661700	0.01987126828504	5800.01111955501000	0.32954608633835	1.23348017621145	1.98341638766520
167.4166667	1537.5	358.43961041281200	0.02036588695527	5992.57104505700000	0.34048699119642	1.26431718061674	2.03300179735683
171.5	1575	366.93892981711700	0.02084880283052	6154.34678159246000	0.34967879440866	1.29515418502203	2.08258720704846
175.5833333	1612.5	375.24627252541000	0.02132081093894	6290.80060283442000	0.35743185243377	1.32599118942731	2.13217261674009
179.6666667	1650	383.37411581634600	0.02178262021684	6406.16449728472000	0.36398661916391	1.35682819383260	2.18175802643172

Temperature Increment (T)	Mechanical Load Increment (P)	Horizontal Deflection at Mid-Span due to Temperature Increment	Horizontal Deflection at Mid-Span due to Temperature Increment per Original Length	Horizontal Deflection at Mid-Span due to Mechanical Load Increment	Horizontal Deflection at Mid-Span due to Mechanical Load Increment per Original Length	Ratio of P/P_{cr}	Ratio of T/T_{cr}
183.75	1687.5	391.33364194115800	0.02223486601938	6503.78541094623000	0.36953326198558	1.38766519823789	2.23134343612335
187.8333333	1725	399.13491881000700	0.02267812038693	6586.35492109008000	0.37422471142557	1.41850220264317	2.28092884581498
191.9166667	1762.5	406.78704950558300	0.02311290054009	6656.06761854556000	0.37818566014463	1.44933920704846	2.33051425550661
196	1800	414.29829695457900	0.02353967596333	6714.76993038165000	0.38152101877169	1.48017621145374	2.38009966519824
200.0833333	1837.5	421.67618862301000	0.02395887435358	6763.88659332936000	0.38431173825735	1.51101321585903	2.42968507488987
204.1666667	1875	428.92760501309400	0.02437088664847	6804.73408736311000	0.38663261860018	1.54185022026432	2.47927048458150
208.25	1912.5	436.05885492300100	0.02477607130244	6838.59689751334000	0.38855664190417	1.57268722466960	2.52885589427313
212.3333333	1950	443.07573981211800	0.02517475794387	6865.93946331904000	0.39011019677949	1.60352422907489	2.57844130396476
216.4166667	1987.5	449.98360913909500	0.02556725051927	6887.77939407954000	0.39135110193634	1.63436123348018	2.62802671365639
220.5	2025	456.78740817359900	0.02595383000986	6904.78882930981000	0.39231754711988	1.66519823788546	2.67761212334802
224.5833333	2062.5	463.49171949610100	0.02633475678955	6917.55031398850000	0.39304263147662	1.69603524229075	2.72719753303965
228.6666667	2100	470.10079917525700	0.02671027268041	6926.56947268689000	0.39355508367539	1.72687224669604	2.77678294273128
232.75	2137.5	476.61860843412100	0.02708060275194	6932.28701437722000	0.39387994399871	1.75770925110132	2.82636835242291
236.8333333	2175	483.04884147400200	0.02744595690193	6935.08835288248000	0.39403911095923	1.78854625550661	2.87595376211454
240.9166667	2212.5	489.39495001116700	0.02780653125063	6935.31157186418000	0.39405179385592	1.81938325991189	2.92553917180617
245	2250	495.66016498883300	0.02816250937437	6933.25406284132000	0.39393488993417	1.85022026431718	2.97512458149780

VITA

Graduate School

Southern Illinois University Carbondale

Bikash Khanal

khanalbikash@siu.edu

Tribhuwan University Kathmandu, Nepal

Bachelor of Science in Civil Engineering, May, 2009

Thesis Title:

Post-Buckling of Non-Sway Axially Restrained Columns under Thermal (Fire) Loads.

Major Professor: Dr. Aslam Kassimali, Ph.D.